REPUBLIQUE ALGERIENNE DEMOCRATIQUE ET POPULAIRE
MINISTERE DE L'ENSEIGNEMENT SUPERIEUR ET DE LA RECHERCHE
SCIENTIFIQUE
UNIVERSITE M'HAMED BOUGARA-BOUMERDES

Faculté Sciences de l'Ingénieur
Département de **Génie Mécanique**
Laboratoire Energétique -Mécanique **& I**ngénieries (**LEMI**)

Thèse de Doctorat LMD

Présenté par :
BOUDAOUD Salah

En vue de l'obtention du diplôme de **DOCTORAT LMD 3**^{ème} **Cycle** en :
Filière : Génie Mécanique
Option : Modélisation et Simulation en Mécanique

Modélisation et simulation des performances d'une centrale hybride solaire-gaz à tour

Devant le jury composé de :

Mr Bouali	Elahmoun	Professeur	UMBB	Président
Mr Khellaf	Abdallah	Dir. de recherche	CDER	Dir. de thèse
Mr Mohammedi	Kamal	Professeur	UMBB	Co-Dir. thèse
Mme Boudries	Rafika	Maitre de Rech A	CDER	Examinatrice
Mr Balistrou	Mourad	Maitre Conf .A	UMBB	Examinateur

Année Universitaire .2015./.2016.

Abstract

Renewable energy sources continue to be the best alternative for the future electricity generation plant as the demand on electricity increases, with the increasing need to reduce greenhouses gas affecting negatively the climate and the biodiversity all over the world.

In the present study, a technical and economic feasibility for the implementation of hybrid molten salt cavity receiver power plant in Algeria, under various weather conditions (costal, highland and Sahara region) has been carried out. For this end, we have investigated the effect of solar radiation intensity, plant capacity factor and hybridization on the thermal plant efficiency and the levelized electricity cost.

Two scenarios namely solar only mode and hybrid fossil backup mode has been considered in the present analysis. Taking into account various factor, a method has been applied to optimize the solar multiple, plant capacity factor and the fossil fuel fraction, to get a trade-off between the incremental investment costs of the heliostat field and thermal energy storage.

The analysis has shown that the use of higher fossil fuel fraction significantly reduces the levelized electricity cost and sensibly increases the plant capacity factor. Therefore, hybrid molten salt central receiver power systems are the attractive solution for fast deployment of CSP technology in Algeria.

Key Word: Solar Multiple, Capacity Factor, Levelized Electricity Cost, Thermal Energy Storage, Fossil Fuel Fraction.

Résumé

Les Sources d'énergie renouvelables continuent à être la meilleure alternative pour la production d'électricité dans le future, en vue de faire face à la demande croissante en cette énergie, et la nécessité incontestable de réduire les gaz à effet de serres affectant négativement le climat et la biodiversité partout dans le monde.

Dans notre travail, une étude de faisabilité technico-économique pour la mise en œuvre de la centrale hybride solaire-gaz à cavité centrale fonctionnant au sel fondu en Algérie, sous diverses conditions météorologiques (le nord, les hauts plateaux et la région sud) a été réalisée. Pour cela, nous avons étudié l'effet de l'intensité du rayonnement solaire, le facteur capacité thermique et l'hybridation sur le rendement global de la centrale ainsi que le coût moyen actualisé de l'électricité.

Deux scénarios ont a été pris en compte dans la présente analyse, à savoir mode solaire seul et le mode hybride avec une source fossile. En tenant en compte divers facteurs, une méthode a été appliquée pour optimiser le facteur de multiple solaire (surdimensionnement du champ solaire), le facteur de capacité thermique et la fraction de du combustible fossile, ainsi pour obtenir un meilleur compromis entre l'augmentation des coûts d'investissement du champ d'héliostats et le stockage de l'énergie thermique.

L'analyse a montré que l'augmentation de la fraction du combustible fossile réduit considérablement le coût moyen actualisé de l'électricité et augmente le facteur de capacité de la centrale électrique. Par conséquent, les centrales solaires hybrides avec un récepteur central fonctionnant au sel fondu sont la solution la plus attractive pour le déploiement rapide de ce type de technologie à haute concentration en Algérie..

Mots Clés : Multiple Solaire, Facteur de Capacité, Coût de l'électricité, Stockage thermique, fraction fossile

الملخص

تعد مصادر الطاقة المتجددة أفضل بديل لإنتاج الكهرباء في المستقبل من أجل تلبية الطلب المتزايد على هذه الطاقة، والحاجة التي لا يمكن إنكارها للحد من انبعاثات ثاني أكسيد الكربون التي تؤثر سلبا على المناخ والتنوع البيولوجي في جميع أنحاء العالم.

في بحثنا، قمنا بدراسة الإمكانيات التقنية والاقتصادية لإنجاز محطة توليد الكهرباء الهجينة ذات الطاقة الشمسية والغاز ،المجهزة بنظام هندسي ذات تجويف المغذى بالملح المصهور المركزي لا نتاج الحرارة في الجزائر، في مختلف الظروف الجوية (الشمال، المرتفعات والمنطقة الجنوبية). لهذا، قمنا بدراسة تأثير شدة الإشعاع الشمسي، عامل السعة الحراريةتو نسبة التهجين على الأداء العام للمحطة وتكلفة الوحدة الكهربائية.

واعتبرت سينار يوهين في هذا التحليل، وهي وضع الطاقة الشمسية فقط ووضع هجين مع مصدر الأحفوري. مع الأخذ بعين الاعتبار عوامل مختلفة، تم تطبيق طريقة لتحسين عامل التضخيم الشمسي، عامل السعة الحرارية للمحطة ونسبة الوقود الأحفوري للحصول على تسوية أفضل بين زيادة التكاليف الاستثمارية للمجال المستقبلات الشمسية وتخزين الطاقة الحرارية.

وأظهر التحليل أن زيادة نسبة الوقود الأحفوري يقلل بشكل كبير من تكلفة الوحدة الكهربائية ويزيد من عامل قدرة محطة توليد الكهرباء. وبالتالي محطات الطاقة الشمسية الهجينة مع جهاز استقبال المركزي العاملة بالملح المنصهر هي الحل الأكثر جذبا لانتشار السريع لهذه التكنولوجيا ذات

تركيز شمسي عال في الجزائر .

الكلمات المفتاحية: عامل التضخيم الشمسي ، السعة الحرارية ، تكلفة الكهرباء، تخزين الطاقة الحرارية، جزء الوقود الأحفوري.

Acknowledgments

Table of Contents

List of figures

List of table

Nomenclature

A	Inlet surface of the receiver, [m²]
A_h	Heliostat area,[m²]
A_v	Specific surface, [m²/m³]
CF	Capacity factor, [%]
C_{invst}	Total investment of the plant, [$]
C_{insur}	Annual insurance rate, [%]
C_{fuel}	Annual fuel cost, [$]
C_{om}	Annual operating and maintenance costs, [$]
C_{htf}	Heat capacity of the molten salt fluid, [kJ/kg.K]
C	Stefan Boltzmann constant, [W/m².K⁴]
C_p	Isobaric specific heat of the air, [J/mol.K]
k_d	Real debt interest rate, [%]
d	Annual discount rate, [$]
DNI	Direct normal irradiance, [kWh/m²]
D_{ot}	Outer diameter of the tube, [m]
D_{it}	Inner diameter of the tube, [m]
L_t	Length of the tube, [m]
E	Thermal power at design point, [MW]
E_t	Yearly energy output, [kW]
E_{net}	Annual generated electricity, [kWh]
E_{gp}	Actual generated energy at part load, [kW$_e$]
E_{gf}	Generated energy at full load, [kW$_e$]
FFF	Fossil fuel fraction, [%]
F_t	Net cash flow in a period t, [$]
f_{cr}	Cost reference factor, [-]
GHI	Global horizontal irradiance, [kWh/m²]
k_t	Thermal conductivity of the receiver tube, [W/m.K]

H_h	Height of the heliostat mirror, [m]
h_{htf}	Convection heat transfer of the molten salt, [W/m².K]
h_{conv}	Convective heat losses from each receiver tube, [W/m².K]
I_d	Direct irradiation flux received by the heliostat field, [kWh/m²]
I_0	Irradiative flux density, [W/m²]
k	Thermal conductivity of the air, [W/m².K]
K	Permeability, [m²]
LEC	Levelized energy cost, [\$/kWh]
m_{htf}	Molten salt flow rate, [kg/s]
M	Air molar mass, [g/mol]
n	Depreciation period,[year]
N_h	Total number of the heliostat field, [-]
N_t	Total number of the receiver tube, [-]
NPV	Net present value, [\$]
Nu	Nusselt number, [-]
P_{cycle}	Power cycle at design gross output, [kW]
P	Pressure, [Pa]
q_{conv}	Energy loss by convection heat transfer from the receiver tube, [W]
q_{htf}	Energy absorbed by molten salt heat transfer fluid, [W]
q_{rad}	Energy loss by radiation from the receiver tube, [W]
q_{ec}	Total incident radiation that is received by the cavity receiver, [W]
q_{ref}	Energy loss by reflection from the surface of the receiver tube, [W]
q_{sf}	Thermal power produced by the solar field, [kW$_{th}$]
q_{pb}	Thermal power required by the power block at nominal conditions , [kW$_{th}$]
q_0	Solid/fluid heat exchange, [W/m^3]
R_{cond}	Heat transfer resistance by conduction,[K/W]
R_{conv}	Heat transfer resistance by convection, [K/W]

R	Ideal gas constant, [J/mol.K]
SM	Solar Multiple, [-]
SEG	Solar electricity generation,[kWh/m²]
t	Analysis period, [year]
TES	Thermal energy storage, [hours]
TMY	Typical meteorological year, [-]
TRY	Test reference year, [-]
$T_{htf, x}$	Inlet temperature of the molten salt at x position, [K]
$T_{htf, x+dx}$	Outlet temperature of the molten salt at x+dx position,[K]
T_{st}	Receiver temperature at the surface, [K]
T_w	Receiver temperature at shaded surface side, [K]
$T_{ic, air}$	Temperature of the air in the inner cavity, [K]
T	Air temperature, [K]
T_2	Solid temperature, [K]
US_i	Heat transfer conductance coefficient, [W/K]
u	Air velocity, [m/s]
W_h	Width of the heliostat, [m]
ΔR	Radial distance between heliostats, [m]
$ΔA_z$	Azimuthal distance between heliostats, [m]
C_{hf}	Cost of 1 m² of reflective surface relative to the same cost of the reference zone, [-]
C_{hel}	Relative heliostat structure cost, [$/m²]
C_{land}	Relative land cost, [$/m²]
C_{wire}	Relative wire cost, [$/m²]
C_{-z}	Cost of a compound related to each zone Z, [$]
C_{-R}	Cost of a compound related to reference zone,[$]
z	Coordinate along the flow direction, [m]

Greek letters

α	Coefficient of dynamical viscosity, [kg/m.s]
α_h	Heliostat azimuth angle in degree, [°]
β	Optical concentration ratio ,[-]
θ	Receiver elevation angle from heliostat, [°]
μ	Convective heat transfer coefficient, [W/m².K]
ε	Surface emissivity, [-]
δ	Characteristic length of the pore structure, [m]
σ	Stefan Boltzmann constant, 5.67×10^{-8}[W/m².K^4]
λ	Radiation wavelength [μm]
ρ	Density, [kg/m^3]
ξ	Extinction coefficient of the radiation, [m^{-1}]
ϵ	Porosity,[-]
φ	Inlet angle of the radiation flow, [°]
η_{opt}	Optical efficiency of the heliostat field,[-]
η_{yf}	Yearly average field efficiency related to each zone,[-]
η_{cos}	Cosine efficiency = 1 – cosine loss,[-]
η_{shad}	Shadowing efficiency = 1 – shadowing loss,[-]
η_{block}	Blocking efficiency = 1– blocking loss,[-]
η_{atm}	Atmospheric transmittance = 1 – atmospheric attenuation,[-]
η_{int}	Receiver intercept factor = 1 – spillage,[-]
η	Efficiency, [%]

Indices

v	Volumetric
p	Pressure
0	Located at the irradiated front surface
aAmb	Ambient
in	Inlet value
out	Outlet value

Abbreviation

CRS	Central Receiver System
CSP	Concentrated Solar Power
DLR	DeutschesZentrumfürLuft- und Raumfahrte.V.
HTF	Heat Transfer Fluid
MENA	Middle East North Africa
PS	Planta Solar
SAM	System Advisor Model

In the context of the population growth over the world, year by year the proliferation of big urban cities induces new method of life and human behavior. The appearance of big industrial factory that satisfies the different needs expressed by the population has led to greater energy consumption. Mainly, this demand on energy has been covered in some countries by fossil fuel energy sources where available, and by Carbone coal in other ones. In the two situations, due to economic consideration (low energy price), the huge demand on theses fossil sources has led to the greenhouse effect growth in the atmosphere and severe climatic change.

Knowing the climatic threats to be faced in the coming eras and the continuous depletion of the world's most valued fossil energy resources, concentrating solar power could be the best alternative technology to sustainable development of energy resources for global energy problems. It is also capable of substantially reducing carbon dioxide emission in the atmosphere.

The development of renewable energies in Algeria was perceived since 1962 date of the independence.

In Algeria, the consumption of energy at the national level is increasing yearly due to demographic and urban growth, in addition to the economic expansion in constant progression. As far as the resources are concerned, based essentially on oil and natural gas, they are not limitless and are gradually being exhausted.

The important economic changes perceived in the last years all over the world, led Algerian stakeholders to embark on big structural reforms. In this perspective, the Algerian state intends to promote and accelerate more attractive programs to diversify the energy source production infrastructures. This new policy required a legal framework that the government has adopted on the different sectors and the different levels [01, 02].

This readiness to promote these energies resulted in the setting of specialized agencies to promote research and development in this field.

In July 2002, a joint venture named NEAL was created by the association of (Sonatrach 45%, Sonelgaz 45% and SIM 10%) [03]. New Energy Algeria has as main objectives the development of alternative energy sources including solar, wind and biomass.

For this, NEAL has joined the Solarpace program and incorporated renewable energy targets in the national context for public and private shareholders.

Due to its geographic location, Algeria has several advantages for the deployment of solar electricity generating systems. It is situated between the 35° and 38° of latitude north and 8° and 12° longitude east. It has an area of 2.381.741 km² [04, 05]. The climatic characteristics for Algeria are given in table 1. According to a study carried out by the German Aerospace Agency (DLR), Algeria has, with a useful area of 1.787.000 km², the largest land potential in the Mediterranean region. Its CSP technology implementation potential is in the order of 169.440 TWh/year [06].

TABLE 1: RADIOMETRIC AND METEOROLOGICAL CHARACTERISTICS IN ALGERIA.

Element Description	Costal region	Highland	Sahara
Surface (%)	4	10	86
Area (km²)	95.27	238.74	2.048.297
Mean daily sunshine duration (h)	7.26	8.22	9.59
Average duration of sunshine (h/year)	2650	3000	3500
Received average energy (kWh/m²/year)	1700	1900	2650
Relative humidity (%)	40.16	40.33	27.66
Mean annual temperature (°C)	19	25	29.50
Mean annual wind velocity (m/s)	2.1	3.8	4.1
Solar daily energy density (kWh/m²)	4.66	5.21	7.26
Potential daily energy (Twh)	443.96	1240.89	14.870.63
Mean annual precipitation (mm)	500	350	150

The climate is transitional between maritime in the north and semi-arid to arid when getting to the south via the highland regions. The average annual temperature measured is about 24.5°C.

Sunshine duration on almost all the country is over 2000 h/year and can reach 3940 h/year in the highland and Sahara regions.

The daily energy obtained on a horizontal plane is about 1700 kWh/m²/year for the north and 2263 kWh/m²/year for the south.

However, the knowledge of the solar potential of each region is fundamental for the sizing and implementation of the different type of solar electricity generating systems (SEGS).

In order for renewable energy systems to be promoted in the country, the Electricity Law of 5th of February 2002 was promulgated. This law states mainly that renewable electricity can be financed either through feed-in tariffs or directly by the state.

Moreover, the Feed-in tariff Decree of 25th of March 2004 has defined "premium" levels for power generated from solar energy and especially for CSP Plants, as described below:

• 300% of market price for electricity production from 100% solar source,

• 200% of market price if more that 25% of the power is produced by solar–gas hybrid system,

• 100–180% of market price in the case that the percentage of the produced power by solar–gas hybrid with solar is less than 25%.

Algerian authorities have set as target the solar energy and/or co-generation applications to reach 5% of the energy mix by 2015 and increase the share of RES in electricity production to 10% by 2027 [05, 06, 07].

Important ways of achieving these targets using various RES have been described in a recent paper. In order to help in these efforts a review of legislation is currently underway. Significant boost is also expected after the construction of the PV manufacturing plant in Rouiba province area. This plant is expected to have a capacity of 50 MW/year. This plant is within the strategic plan of the SONELGAZ Company and its affiliated subsidiary [07, 08].

As an example of first deployment of SEGS,the "HassiR'mel"Integrated Solar Combined Cycle (ISCC) plant of 150 MW is currently in full operation in northern Algeria. This area is close togas pipelines and high voltage grid. This project is being promotedby solar power plant one (SPP1), an Abener and NEAL joint ventureformed for this purpose, which will operate and exploit the plantfor a period of 25 years. The plant construction started on the 7th ofnovember 2007 and has finished by November 2010 [05, 07].

The plant consists of a conventional combined cycle and a solar field with a nominal thermal power of 95 MW_{th}. The 25 MW solar field of parabolic trough technology provides complementarythermal energy to the combined cycle.

The solar field is composed of 216 solar collectors in 54 loops with an inlet heat transfer fluid temperature of 290°C and an outlet temperature of 390°C. The working HTF is a synthetic oil of composition ……

The "HassiR'mel" plant uses the heat generated in the same steam turbine that makes use of the waste heat from the gas turbine for electricity generation. This configuration is double effective, since not only it minimizes the investment cost but also reduces the CO_2

emissions associated with the conventional plant 131400 (ton/year). The 20% of the project cost (63 million D) is financed by the shareholders, and the rest 80% (252 million D) is financed by local banks (BEA – 54.72%, CPA – 20.03% & BNA – 25.25%) [07].

Project assets and cash flow are the only security to lenders, while the project cash flow is used to service the debt and distribute dividends. Finally, 15 years of repayment "soft loan" of 3.75% interest rate has been received to reduce the impact of financing charges on tariffs.

Objectives and methodology

The problem statement here is the following: what are the set-ups of a large solar tower thermal power plant that satisfy both energy and economic objectives, at a given location, with a given conversion cycle, and under given material safety constraints.

Thus the objectives of this thesis are:

- The performance assessment of the power plant with molten salt cavity receiver;
- The development of a method to optimize the plant solar multiple, capacity factor and levelized electricity cost;
- The comparison between the actual simulated results to the experimental results reported for the solar plant PS20 for validation purpose;
- The definition of parameters affecting the performance of the solar power plant in hybrid mode: fossil fuel fraction, LEC and the capacity factor.
- The definition of parameters affecting the location of solar power plant for future deployment purpose: DNI and land constraints;
- The analysis of the HITREC air receiver thermal performance as unit stand of the central receiver power plant using CAD and CFD tools.

The methodology adopted in the thesis is the combination of the thermal and economic parameters for the evaluation of the solar central receiver power plant using two scenarios (solar only mode and hybrid fossil fuel mode). This analysis have been carried out using at the same time SAM advisor aided design tool, validated by experimental results taken from real plant installation (PS20) in Spain. The determination of the levelized electricity cost, the net cost of electricity by kW_e produced, the capacity factor and the efficiency of the thermodynamic cycle are the main factors determined in this work.

Scope of the thesis

First, electricity generation technology based on concentrated solar power plant is described. The radiation source which is the most important factor for the deployment and the implementation of utility scale solar electricity generation plant in the MENA region (Sun Belt region) is defined.

Though, a review and a history of the development and promotion of such technology since 1860 are carried out. The specification of the different type of the concentrated solar power technology (parabolic trough, linear Fresnel, central receiver and dish engine) has been undertaken. However, in the present work, emphases on the central receiver power tower plant is given with a detailed state of the art for the development over the centuries in the world, principally in Spain, united states and china. An assessment between the different types of each CSP technology is given in table II.1. The different application for utility scale and grid connection (based on power purchase agreement, PPA escalation rate), advantages, drawbacks and dispatch ability of the plant configuration (solar only, hybrid fossil fuel, with or without storage) and ability to respond to pick hours demand is stated.

The main technical and economic design parameters for CSP technology have been described. The factors affecting the performance and costs of such technologies are: optical concentration ratio, direct normal irradiance and geographic site selection (situation).

Instantaneous performance evaluation at design point and name plate capacity of 20 MW_e of a molten salt cavity receiver have been carried out. Nonetheless, a daily solar field performance analysis is plotted. At the end of the present chapter, a review of main software used as an aided design and decision making to evaluate and optimize the performance and costs of such solar power plant is listed.

Second, a detailed methodology for central receiver system design and optimization is defined under different aspects.

The first facet deals with the modeling of the solar heat exchanger geometry called cavity receiver. Using balance energy model over the discretized element (volume) of the receiver tubes, the different losses (natural, forced convective heat transfer and reflective radiation heat transfer) are assessed. Experimental physical correlation based on dimensionless number such as Nusselt, Grashof, Reynolds and Prandtl have been assumed in

the present study. This in fact, to evaluate the different regime and behavior of the cavity receiver (thermal to fluid flow interaction through tubes), and in the same time the estimation of the reflective radiation losses from the internal cavity considered as no gray black body surface based on the view factor radiation model.

The following analysis deals with the heliostat field layout optimization using DELSOL-3 algorithm. For this end, a Hermit polynomial expansion-convolution method is used to predict flux images from the heliostats field. As main result, a staggered layout for north field solar central cavity receiver configuration is considered in the present work.

This choice of the power plant model is motivated by the following aims:

➔ Based on the state of the art for this type of technology configuration, we assume that it gives the minimum optical losses (cosine effect, shadowing and blocking effect, atmospheric attenuation effect, spillage and canting effect, mirror reflectivity …);

➔ For medium power plant capacity utility scale, a northern configuration is wondered than the circular large scale power plant;

➔ For technical and economic consideration for the deployment of such technology in Algeria subject of the present thesis work, medium risks and lower costs are the main reasons and the first objective for an eventual future implementation than the circular high risks configuration.

Heat transfer fluid system is described, given his physical and chemical characteristics.

A storage option with tow tank model and dispatch control strategy conducted using SAM advisor model are described. Technical and economic parameters affecting the operating conditions of solar central receiver power plant, either in solar only mode or hybrid fossil fuel mode has been given (solar multiple, capacity factor, solar electricity generation, thermal energy storage, fossil fuel fraction, levelized electricity cost, weighted average capital cost, net present value).

Third, a small description of general hybrid solar power plant model is given. Integration of fossil duel fired boiler into solar power plant cycle needs to be over sized to accommodate the steam production by the solar field.

brief report about fossil back up methodology under SAM advisor simulation tool is described. It consists mainly on how to manage the time in the day (24 hours) to achieve rated capacity for base load plant.

However, hybrid concept integration of solar power tower plant is considered. The best approach adopted based on literature survey to hybridizing such electricity generation plant to a base load fossil plant is the power booster mode. Finally, the environmental indicator for climate change context represented by the CO_2 avoidance is stated.

Fourthly, parametric study was conducted to determine the interaction between the different technical and economic indicator namely, CF, SM, TES, LEC, SEGS, DNI and FFF affecting the working conditions of the solar central receiver power plant. Indeed, not only these parameters could give information or decision for the technical and economic feasibility for the implementation of such power plant. Other consideration for real decision making is to be foreseen. Existing installation power plant (PS20) model is given with some indicator for validation purpose. This to compare the effectiveness of the present study carried out under SAM advisor simulation tool.

However, further analysis about the air flow and heat transfer inside the continuum homogenous model of the open volumetric air receiver are assumed in the present work. The main objective is to investigate all parameters such as the radiation model applied at the surface of the absorber, the Brinkman model applied to the fluid flow through the porous structure affecting the physical model.

Finally, the general conclusion which we could take from this thorough investigation on the hybrid molten salt cavity receiver solar power plant, under Algerian climate is that the analysis has pointed out to the fact that there is a strong relation between the capacity factor, solar multiple, and the TES factors. However, the larger the storage capacity, the larger the solar multiple and the lower is the LEC since the storage system has the lowest investment costs. The two scenarios considered in the present work have showed that in solar only mode, the higher the DNI the higher the storage capacity, thus the higher the plant capacity factor considering the same solar multiple. This is the case of Tamanrasset that has the highest solar radiation intensity compared with Batna and Algiers. The hybridization is an attractive option that enhances the efficiency and increase the capacity factor. It decrease the LEC compared with the solar only mode.

Chapter I. Concentrated Solar Power, State of the Art and Background

I.1. Solar energy: it's use

Solar energy has a high exergy value since it originates from processes occurring at the sun's surface at a black-body equivalent temperature of approximately 5777 K. Because of this high exergetic value, more than 93% of the energy may be theoretically converted to mechanical work by using thermodynamic cycles [08]

According to thermodynamics and Planck´s equation, the conversion of solar heat to mechanical work or Gibbs free energy is limited by the Carnot efficiency, and therefore to achieve maximum conversion rates, the energy should be transferred to a thermal fluid or reactants at temperatures close to that of the sun [08, 09].

Even though solar radiation is a source of high temperature and exergy at origin, with a high radiosity of 63 MW/m^2, sun-to-earth geometrical constraints lead to a dramatic dilution of flux and to irradiance available for terrestrial use; only slightly higher than1 kW/m^2 with a consequent supply of low temperatures to the thermal fluid.

It is therefore an essential requisite for solar thermal power plants and high temperature solar chemistry applications to make use of optical concentration devices that enable the thermal conversion to be carried out at high solar fluxes and with relatively low heat losses.

The use of solar energy for electricity production promises to be one of the most viable options to substitute fossil fuel solar electricity generation system.

Solar Energy (SE) is accepted as a key resource for the future of the world. The utilization of SE could cover a significant part of the energy demand in the countries.

Solar energy technologies have a long history. Between 1860 and the First World War, a range of technologies were developed to generate steam, by capturing the sun's heat.

The years immediately following the oil-shock in the seventies saw much interest in the development and commercialization of solar energy technologies. However, this emerging solar energy industry of the 1970s and early 80s collapsed due to the sharp decline in oil prices and a lack of sustained policy support[09, 10].

Solar energy markets have regained momentum since early 2000, revealing phenomenal growth recently. The total installed capacity of solar based electricity generation capacity has increased to more than 40 GW by the end of 2010 from almost negligible capacity in the early nineties.

Chapter I. Concentrated Solar Power, State of the Art and Background

I.2.Introduction to CSP technologies

Concentrating solar power (CSP) plants use mirrors to concentrate sunlight onto a receiver, which collects and transfers the solar energy to a heat transfer fluid that can be used to supply heat for end-use applications or to generate electricity through conventional steam turbines.

Large CSP plants can be equipped with a heat storage system to allow for heat supply or electricity generation at night or when the sky is cloudy.

There are four CSP plant variants which are today represented at pilot and commercial scale, parabolic trough collectors (PTC), linear Fresnel reflector systems (LFR), power towers or central receiver systems (CRS), and dish/engine systems (DE). They vary depending on the design, configuration of mirrors and receivers, heat transfer fluid used and whether or not heat storage is involved.

The first three types are used mostly for power plants in centralized electricity generation, with the parabolic trough system being the most commercially mature technology. Solar dishes are more suitable for distributed generation.

All the existing pilot plants mimic (imitate) parabolic geometries with large mirror areas and work under real operating conditions. PTC and LFR are 2-D concentrating systems in which the incoming solar radiation is concentrated onto a focal line by one axis tracking mirrors. They are able to concentrate the solar radiation flux 30 to 80 times, heating the thermal fluid up to 450ºC,with power conversion unit sizes of 30 to 80MW, and therefore, they are well suited for centralized power generation at dispatchable markets with a Ranking steam turbine/generator cycle.

CRS optics is more complex, since the solar receiver is mounted on top of a tower and sunlight is concentrated by means of a large parabolic that is discretized into a field of heliostats.

This 3Dconcentrator is therefore off-axis and heliostats require two-axis tracking. Concentration factors are between 200 and 1000 and unit sizes are between 10 and 200MW, and they are therefore well suited for dispatchable markets and integration into advanced thermodynamic cycles.

A wide variety of thermal fluids, like saturated steam, superheated steam, molten salts, atmospheric air or pressurized air, can be used, and temperatures vary between 300ºC and 1000 ºC. Finally, DE systems are small modular unit with autonomous generation of electricity by Sterling engines or Brayton mini-turbines located at the focal point.

Chapter I. Concentrated Solar Power, State of the Art and Background

Dishes are parabolic 3Dconcentrators with high concentration ratios (1000 to 3000 suns) and a unit size of 5-25 kW. Their current market niche is in both distributed on-grid and remote/off-grid power applications.

Parabolic troughs, by far the most mature technology, have been demonstrated commercially.

Those for linear Fresnel, dish and tower systems are, in general, projections based on component and early commercial projects and the assumption of mature development of current technology. With current investment costs, all STE technologies are generally thought to require a public financial support strategy for market deployment. At present direct capital costs of STE and power generation costs are estimated to be2-3 times those of fossil-fueled power plants, however industry roadmaps advance 60% cost reduction before 2025 [10]. In fact governments at some countries like Spain are already accelerating the process of drastic tariff reduction with the goal of STE, PV and wind energy becoming tariff-equivalent in less than one decade.

Every square meter of STE field can produce up to 1200 kWh thermal energy per year or up to 500 kWh of electricity per year.

That means a cumulative savings of up to 12 tons of carbon dioxide and 2.5 tons of fossil fuel per square meter of CSP system over its25-year lifetime will be achieved [11].

After two decades of frozen or failed projects, approval in the past few years for specific financial incentives in Europe, the US, India, Australia and elsewhere, is now paving the way for launching of the first commercial ventures.

Spain with 2400 MW connected to the grid in 2013 is taking the lead on current commercial developments, together with USA where a target of 4500 MW for the same year has been fixed. Other relevant programs such as the "Solar Mission" in India have been recently approved for 22 GW-solar, with a large fraction being thermal [12].

CSP plants require high direct solar irradiance to work and are therefore a very interesting option for installation in the Sun Belt region (between 40 degrees north and south of the equator). This region includes the Middle East, North Africa, South Africa, India, and Southwest of the United States, Mexico, Peru, Chile, Western China, Australia, southern Europe and Turkey. The technical potential of CSP-based electricity generation in most of these regions is typically many times higher than their electricity demand, resulting in opportunities for electricity export through high-voltage lines

Chapter I. Concentrated Solar Power, State of the Art and Background

However, the deployment of CSP is still at an early stage with approximately 2 GW of installed capacity worldwide up to 2012, although an additional 12 GW of capacity is planned for installation by 2015. Today's installed capacity of CSP is very small when compared with approximately 70 GW of solar photovoltaic (PV) plants already in operation, and the 30 GW of new PV installations completed in2011. The total installation cost for CSP plants without storage is generally higher than for PV. However, it is expected that these costs will fall by around 15% by 2015owing to technology learning, economies of scale, and improvements in manufacturing and performance, thus reducing the levelized electricity costs (LEC) from CSP plants to around USD 0.15-0.24/kWh.

By 2020, expectations are that capital costs investment will decline even further by between 30% and 50%. Like PV, an advantage of CSP plants is that their output, when no thermal storage is used, follows closely the electricity and heat demand profile during the day in Sun Belt regions.

The significant advantage of CSP over PV is that it can integrate low-cost thermal energy storage to provide intermediate and base-load electricity. This can increase significantly the capacity factor of CSP plants and the dispatchability of the generated electricity, thus improving grid integration and economic competitiveness of such power plants.

However, there is a trade-of between the capacity of heat storage required and capital cost of the plant. Another advantage offered by CSP technology is the ease of integration into existing fossil fuel-based power plants that use conventional steam turbines to produce electricity, whereby the part of the steam produced by the combustion of fossil fuels is substituted by heat from the CSP plant.

Similar to conventional power plants, most CSP installations need water to cool and condense the steam cycle. Since water is often scarce in the Sun Belt regions, CSP plants based on dry cooling systems are the preferred option with regards to efficient and sustainable use of water.

As indicated in appendices table 1, a review the main advantage and drawbacks of each type of CSP technology have been carried out and dispatchability of the plant configuration is stated.

However, such plants are typically about 10% more expensive than water-cooled ones. Compared with PV, CSP is still a relatively capital-intensive technology with a small market.

However, CSP plants could become economically competitive as a result of the significant potential for capital cost reductions.

In addition to renewable heat and power generation concentrating solar plants has other economically viable and sustainable applications, such as co-generation for domestic and industrial heat use, water desalination and enhanced oil recovery in mature and heavy oil fields.

CSP technology deployment also has the potential for substantial local value addition through localization of production of components, services and operation and maintenance, thus creating local development and job opportunities.

I.2.1. Definition of the concentration

Concentrating Solar Power (CSP) plants use mirrors to concentrate the sun's ray sand produce heat for electricity generation via a conventional thermodynamic cycle.

Unlike solar photovoltaic (PV), CSP uses only the direct component of sunlight (DNI) and can provide carbon-free heat and power only in regions with high DNI (i.e. Sun Belt regions).

Sunlight consists of direct and indirect (diffused) components. The direct component (i.e. DNI or Direct Normal Irradiance) represents up to 90% of the total sunlight during sunny days but is negligible on cloudy days. Direct sunlight can be concentrated using mirrors or other optical devices (e.g. lenses).

CSP plant scan provide cost-effective energy in regions with DNI> 2000 kWh/m²/year, typically arid and semi-arid regions at latitudes between 15° and 40° north or south of the equator.

Note that equatorial regions are usually too cloudy. High DNIs can also be available at high altitudes where scattering is low. In the best regions (DNI>2800 kWh/m²/year), the CSP generation potential is 100 to 130 GWh$_e$/km²/year.

This is approximately the same electricity generated annually by a 20 MW coal-fired power plant with a75% capacity factor (CF).

The capacity factor is the number of hours per year that the plant can produce electricity while dispatch ability is the ability of the plant to provide electricity on the operator's demand.

The solar multiple (SM) is the ratio of the actual size of the solar field to the solar field size needed to feed the turbine at nominal design capacity with maximum solar irradiance (~ 1 kW/m²).

To cope with thermal losses, plants with no storage have a solar multiple between 1.1 to 1.5 (up to 2.0 for LFR) while plants with thermal storage may have solar multiples of 3 to 5.

I.2.2. Type of concentration technology

As stated before, The CSP technology includes four variants type of concentration; namely, parabolic trough collector (PTC),linear Fresnel reflector (LFR), central receiver solar tower (CRS) and dish engine solar system (DE).

In PTC and LFR plants, mirrors concentrate the sun's rays on a focal line, with concentration factors on the order of 60 to 80 and maximum achievable temperatures of about 550°C.

In CRS and DE plants, mirrors concentrate the sunlight on a single focal point with higher concentration factors 600 to 1000and operating temperatures 800 to 1000°C.

I.2.2.1. Parabolic trough collector (PTC)

PTC is the most mature CSP technology, accounting for more than 90% of the currently installed CSP capacity over the world. See figure 1.1.
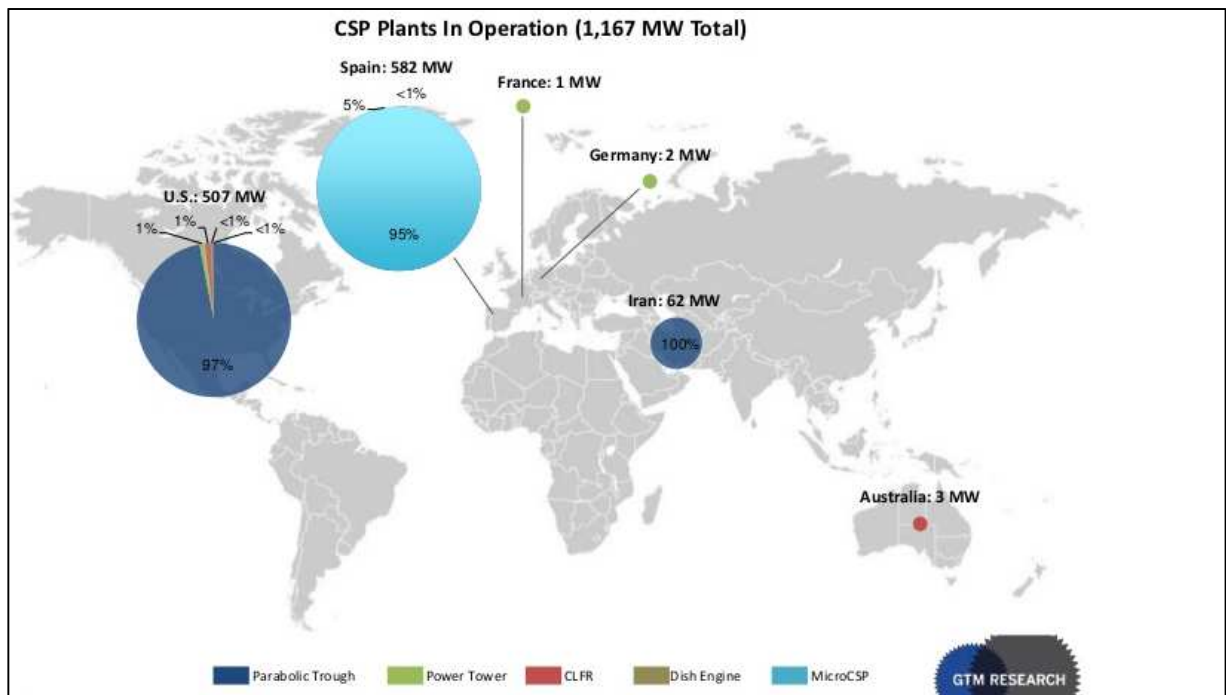
FIGURE 1.1: PARABOLIC TROUGH COLLECTOR DEPLOYMENT OVER THE WORLD. [13].

Chapter I. Concentrated Solar Power, State of the Art and Background

As illustrated in figure1.2, it is based on parabolic mirrors that concentrate the sun's rays on heat receivers (i.e. steel tubes) placed on the focal line.

Receivers have a special coating to maximize energy absorption and minimize infrared re-irradiation and work in an evacuated glass envelope to avoid convection heat losses. The solar heat is removed by a heat transfer fluid (e.g. synthetic oil, molten salt)flowing in the receiver tube and transferred to a steam generator to produce the superheated steam that runs the turbine. Mirrors and receivers (i.e. the solar collectors) track the sun's path along a single axis (usually east to west).An array of mirrors can be up to 100 meters long with a curved aperture of 5 to 6 meters.

Most PTC plants currently in operation have capacities between 14 to 80 MW_e, efficiencies of around 14 to 16% (i.e. the ratio of solar irradiance power to net electric output) and maximum operating temperatures of 390°C, which is limited by the degradation of synthetic oil used for heat transfer.

The use of molten salt at550°C for either heat transfer or storage purposes is under demonstration. High temperature molten salt may increase both plant efficiency (e.g. 15% to 17%) and thermal storage capacity.

In addition to the solar electricity generating systems (SEGS) project (i.e. nine units with a total capacity of 354 MW in operation since the 1980, major and more recent PTC projects in operation include two 70MW units in the United States (i.e. Nevada Solar One and MNGSEC Florida), about thirty 50-MW units in Spain and smaller units in a number of other countries [03].

The three 50 MW Andasol units by ACS/Cobra Group and Marquesado Solar SL and the two 50MW (Valle I and II) plants by Torresol Energy in Spain are particularly interesting, as they use synthetic oil as the heat transfer fluid and molten salt as the thermal storage fluid.

They have a thermal storage capacity of around 7.5 hours[11, 12, 13], which can raise the capacity factor up to 40%.

In Italy, a 5 MW demonstration plant (ENEL, ENEA) with eight hours of thermal storage started operation in June 2010 to test the use of molten salt as either heat transfer or storage fluid, which can significantly improve the storage performance and the capacity factor (by up to 50%) because the higher operation temperature and thermal capacity of molten salt enable more storage capacity with reduced storage volume and costs [12].

Large PTC plants under construction include the Mojave project (a 250 MW plant in California due to start operation in 2013), the 280 MW Solana project in Arizona due in 2013, the Shams 1 100MW project in the United Arab Emirates due in 2012/2013), the Godawari project (India, 50 MW, 2013) and a further fifteen 50-MW plants in Spain.

FIGURE 1.2: PARABOLIC TROUGH PLANT INSTALLATION IN SPAIN [14].

I.2.2.2. Linear Fresnel reflectors (LFR)

LFR plants showed in figure I.3 are similar to PTC plants but use a series of ground-based, flat or slightly curved mirrors placed at different angles to concentrate the sunlight onto a fixed receiver located several meters above the mirror field.

Each line of mirrors is equipped with a single axis tracking system to concentrate the sunlight onto the fixed receiver. The receiver consists of a long, selectively-coated tube where flowing water is converted into saturated steam (DSG or Direct Steam Generation). Since the focal line in the LFR plant can be distorted by astigmatism, a secondary mirror is placed above the receiver to refocus the sun's rays.

As an alternative, multi-tube receivers can be used to capture sunlight with no secondary mirror. The main advantages of LFR compared to PTC systems are the lower cost of ground-based mirrors and solar collectors (including structural, supports and assembly).

While the optical efficiency of the LFR system is lower than that of the PTC systems (i.e. higher optical losses), the relative simplicity of the plant translates into lower manufacturing and installation costs compared to PTC plants.

However, it is not clear whether LFR electricity is cheaper than that from PTC plants. In addition, as LFR systems use direct steam generation, thermal energy storage is likely to be more challenging and expensive.

LFR is the most recent CSP technology with only a few plants in operation (e.g.1.4 MW in Spain, 5 MW in Australia and a new 30MW power plant, the Puerto Errado 2, in Spain, which started operation in September 2012).

Further LFR plants are currently under construction (e.g. Kogan Creek, Australia 44 MW, 2013) or in consideration.

FIGURE 1.3: LINEAR FRESNEL COLLECTOR PLANT [15]

I.2.2.3. Central receiver solar towers (CRS)

In the CRS plants shown in figure1.4, a large number of computer assisted mirrors (heliostats) track the sun individually over two axes and concentrate the solar irradiation onto a single receiver mounted on top of a central tower where the solar heat drives a thermodynamic cycle and generates electricity.

In principle, CRS plants can achieve higher temperatures than PTC and LFR systems because they have higher concentration factors. The CRS plants can use water-steam (DSG),

synthetic oil or molten salt as the primary heat transfer fluid. The use of high-temperature gas is also being considered.

Direct steam generation (DSG) in the receiver eliminates the need for a heat exchanger between the primary heat transfer fluid (e.g. molten salt) and the steam cycle, but makes thermal storage more difficult. Depending on the primary heat transfer fluid and the receiver design, maximum operating temperatures may range from 250 to 300°C (using water-steam) to 390°C (using synthetic oil) and up to 565°C (using molten salt). Temperatures above800°C can be obtained using gases.

The temperature level of the primary heat transfer fluid determines the operating conditions (i.e. subcritical, supercritical or ultra-supercritical) of the steam cycle in the conventional part of the power plant.

CRS plants can be equipped with thermal storage systems whose operating temperatures also depend on the primary heat transfer fluid. Today's best performance is obtained using molten salt at 565°C for either heat transfer or storage purposes. This enables efficient and cheap heat storage and the use of efficient supercritical steam cycles. High-temperature CRS plants offer potential advantages over other CSP technologies in terms of efficiency, heat storage, performance, capacity factor sand costs.

In the long run, they could provide the cheapest CSP electricity, but more commercial experience is needed to confirm these expectations.
Current installed capacity includes the PS10 and PS20 demonstration projects (i.e. Spain) with capacities of 11 MW and 20 MW, respectively. Both plants are equipped with a 30-60 minute steam-based thermal storage to ensure power production despite varying solar radiation.

The PS10 consists of 624 heliostats over 75000 m². Its receiver converts 92% of solar energy into saturated steam at 250°C and generates 24.3 GWh a year (i.e. 25% capacity factor), with17% efficiency. In Spain, a 19-MW molten salt-based CRS plant (i.e. Gemasolar) with a 15-hours molten salt storage system started operation in the second half of 2011.

It is expected to run for almost 6500 operation hours per year, reaching a 74% capacity factor and producing fully dispatchable electricity.

Larger CRS plants are under construction (e.g. the 370 MW Ivanpah project in California with water-steam at 565°C and 29% efficiency and the 50 MW Supcon project in China) or under development (e.g. eight units with a total capacity of 1.5 GW in the southwestern United States). Large plants have expansive solar fields with a high number of

heliostats and a greater distance between them and the central receiver. This results in more optical losses, atmospheric absorption and angular deviation due to mirror and sun-tracking imperfections.

FIGURE 1.4: PS10 AND PS20 LARGE CAVITY CENTRAL RECEIVER POWER PLANT. SPAIN [16]

I.2.2.4. Dishes solar engine (DE)

The DE system represented in figure1.5 consists of a parabolic dish shaped concentrator (like a satellite dish) that reflects sunlight into a receiver placed at the focal point of the dish. The receiver may be a Sterling engine (i.e. kinematic and free-piston variants) or a micro-turbine.

DE systems require two-axis sun tracking systems and offer very high concentration factors and operating temperatures. However, they have yet to be deployed on any significant commercial scale. Research currently focuses on combined sterling engines and generators to produce electricity.

The main advantages of DE systems include high efficiency (i.e. up to 30%) and modularity (i.e. 5 to 50 kW), which is suitable for distributed generation.

Unlike other CSP options, DE systems do not need cooling systems for the exhaust heat. This makes DE suitable for use in water-constrained regions, though at relatively high electricity generation costs compared to other CSP options. The DE technology is still under demonstration and investment costs are still high. Several DE prototypes have successfully operated over the last ten years with capacities ranging from 10 to 100 kW (e.g. Big Dish,

Australian National University). The Big Dish technology uses an ammonia based thermo chemical storage system.

FIGURE 1.5: MODULATED DISH-STERLING POWER PLANT INSTALLATION. [17]

Thermal storage systems for DE are still under development. Multi-megawatt DE projects (i.e. up to 100 MW) have been proposed and are under consideration in Australia and the United States.

At present, more than 90% of the installed CSP capacity consists of PTC plants; CRS plants total about 70 MW and LFR plants about 40 MW. A comparison of CSP technology performance is shown in table 1.2.

TABLE 1.1:CHARACTERISTICS OF SOLAR THERMAL ELECTRICITY SYSTEM [18].

	Parabolic troughs	Central Receiver	Dish-Stirling
Power Unit	30-80 MW*	10-200 MW*	5-25 kW
Temperature operation	390 ºC	565 ºC	750 ºC
Annual capacity factor	23-50 %*	20-77 %*	0,25
Peak efficiency	20%	23%	29.4 %
Net anual efficiency	11 -16 %*	7-20 %*	12-25 %
Commercial status	Mature	Early projects	Prototypes demonstration
Technology risk	Low	Medium	High
Thermal storage	Limited	Yes	Batteries
Hybrid schemes	Yes	Yes	Yes
Cost W installed	-----------------------------	-----------------------------	-----------------------------
$/W	3.49-2.34*	3,83-2,16*	11 .00-1 .14*
$/Wpeak**	3.49-1.13*	2,09-0,78*	11 .00-0.96*

* Data interval for the period 2010-2025
** Without thermal storage.

I.2.3. Design of CSP

The design of a solar power plant involves an interactive process in which the level of detail is refined in each construction phases. These design phases include site selection, the calculation of the concentration ratio of the solar electricity generation system selected, carrying–on direct normal irradiance measurements. This leads to the establishment of a feasibility study for the implementation of the solar power plant to the dedicated site. The design phases are not successive steps and there is a high degree of information exchange among the various design phases.

I.2.3.1.Theoretical concentration ratio calculation

Solar concentrating systems are characterized by the use of devices, such as mirrors or lenses, which are able to redirect the incident solar radiation received onto a particular surface, collector surface A_c, and concentrate it onto a smaller surface, absorber surface A_{abs}.

The quotient of areas is called the geometric concentration ratio,

$C_{onc} = A_{abs}/A_c$……………………………………………………………………. (1.1)

See figure 1.6

We will determine the theoretical maximum concentration ratio of the focal spot or the focal line in parabolic systems. The Sun image in the focal plane is an ambiguous spot whose total size and form depend on the aperture of the mirror and on the range of the rim angle β.

a =r.α …………………………………………………………………………. (1.2)

b= r.α/cosβ …………………………………………………………………. (1.3)

Considering all points at the distance from the focal point, the Sun image in the focal plane has acircular form with the diameter

d=b= r.α/cosβ …………………………………………………...…….. (1.4)

The Sun image covers the following area:

$A_{abs}= \pi.r^2.\alpha^2/cos^2 \beta$ ……………………………………………………….. (1.5)

The diameter d of the parabolic mirror is related to the maximal value of ρand to βas follows:

d = 2 ρ sin β …………………………………………………………………. (1.6)

and the aperture area amounts to:

$A_c=\pi.r^2 sin^2\beta$ …………………………………………………………………. (1.7)

The concentration ratio C_{onc} is

$C_{onc} = A_{abs}/A_c$…………………………………………………………………. (1.8)

$C_{onc}=4/\alpha^2. sin^2\beta. cos^2\beta$ ……………………………………………………………… (1.9)

I.3. State of the art of CSP

CSP uses renewable solar resource to generate electricity while producing very low levels of greenhouse-gas emissions. Thus, it has strong potential to be a key technology for mitigating climate change. In addition, the flexibility of CSP plants enhances energy security.

Unlike solar photovoltaic (PV) technologies, CSP has an inherent capacity to store heat energy for short periods of time for later conversion to electricity.
When combined with thermal storage capacity, CSP plants can continue to produce electricity even when clouds block the sun or after sun down. CSP plants can also be equipped with backup power from fossil fuels.

I.3.1. Central Receiver System

Central receiver system with large heliostat fields and solar cavity receivers located on top of a tower are now in a position for deployment of the first generation of grid-connected commercial plants. The first one began operating in California in 1980 spurred by federal and state tax incentives and mandatory long term power purchase contracts. From 1990 to 2000, a drop in fossil fuel prices pushed the governments to repeal the policy framework that has supported the development of CSP. In the last decade, the market re-emerged again especially in Spain, the USA and Algeria in response to government incentive measures such as feed-in tariffs [19, 23].

Falcone et al. have reported the experiments of the Solar One plant of 10 MW_e. They have tested two HTF systems. In the first test, the water/steam has been used as a working fluid. The results have shown a receiver outlet steam temperature of about 510°C at 10.3 MPa [25]. In the second experiment, the molten salt HTF which is a mixture of 60% sodium nitrate and 40% of potassium nitrate was tested. A receiver outlet temperature of 565 °C has been reached.

The Solar One power plant is equipped with a thermal energy storage system that increases the capacity factor to about 30%. The largest demonstration molten salt power tower is the 10MW Solar Two plant that is located near Barstow, in California (USA). The plant has begun operating in June 1996, and has successfully demonstrated the potential of nitrate salt technology. A 13.5 % overall efficiency has been reached [23, 25].

The 17 MW Solar Tres power plant erected in Spain, is the first commercial molten salt power tower. It has the same concept as Solar One power plant and Solar Two power plant.

Known also as Gemasolar, Solar Tres power plant has an annual capacity factor of about 64%. Moreover, this ratio can reach 71% in hybrid mode. The LEC is estimated to be about 0.16 $/kWh[18].

Recently, there are many central receiver power plants that are underway or in the planning stage. The Ivanpah power plant, which is made up of 3 units of 392 MW each, is under construction in San Bernardino County, California, USA [21].

In 2006, the 11 MW_e CRS power plant PS10 was built by Abengoa Solar in Seville Spain. It has been followed by the20 MW_e power tower plants PS20 in the same location, the5 MW Sierra Sun Tower (in Lancaster, USA) and the 1.5 MW in Julich Germany in 2009 [20,21].

Since 2011, the Gemasolar power plant, built in Spain as large as the PS 20 power plant, but with surrounded heliostat field and15 h storage capacity, has been operating and delivering power for grid utility. After the three pioneer CSP countries, i.e., the USA, Germany and Spain, China have entered the CSP market by implementing, in 2010, the Beijing Yanqing solar power plant. It has been then followed by Beijing Badaling Solar Tower in 2012 [18.21].

The most important central receiver power plants in operation or under erection throughout the world are reported in table1.3 below:

Table 1.2: State of the art of central receiver power plant

Project acronym	Plant status	Country built-in	Plant rate	HTF	Surface of mirrors	Land area	Receiver type	Year start production	Storage	Receiver Tout
SSPS	Experimental	Spain	0.5	Liquid Sodium	?	?	?	1981	?	?
EURELIOS	Experimental	Italy	1	Water/Steam	?	?	?	1981	?	?
SUNSHINE	Experimental	Japan	1	Water/Steam	?	?	?	1981	?	?
Solar one	Commercial	California, USA	10 MW	Molten salt	72650 m²	51 hectare	15	1982	?	?
CESA-1	Experimental	Spain	1	Water/Steam	?	?	?	1983	?	?
MSEE/CAT B	Experimental	USA	1	Molten salt	?	?	?	1984	?	?
THEMIS	Experimental	France	2.5	Molten salt	?	?	?	1984	?	?
SPP-5	Experimental	Russia	5	Water/Steam	?	?	?	1986	?	?
TSA	Experimental	Spain	1	Air	?	?	?	1993	?	?
Solar two	Commercial	California, USA	20 MW	Molten salt	81400 m²	?	?	1996	?	?
Solar tres	Commercial	Seville, Spain	15 MW	Water/Steam	268000 m²	?	?	?	?	?
Solar 50/cuatro	Commercial	Sotheme, Spain	50 MW	Molten salt	971000 m²	?	?	?	?	?
Solar 100	Commercial	Souwth estern, USA	100 MW	Molten salt	1466000 m²	?	?	?	?	?
CSIRO Solargas	Experimental	Australia	0.5 MW	Water/Steam	?	?	Cavity	2005	?	?
PS 10	Commercial	Seville, Spain	11 MW	Water/Steam	75000 m²	55 hectare	Cavity	2007	Other	300
Jülich	Experimental	Germany	1.5 MW	Air	17650 m²	17 hectare	Cavity	2008	1.5 h	680
Acme	Experimental	India	2.5 MW	Water/Steam	16022 m²	12 acres		2011	None	440
Gemasolar	Commercial	Seville, Spain	19.9 MW	Molten salt	304750 m²	195 hectare	External	2011	15 h	565
Consolar	Experimental	Israel	0.5 MW	Air	?	?	Pressurized air	2001	Hybrid	?
Solgate	Experimental	Spain	0.3 MW	Air			Pressurized air	2002	Hybrid	?
Eureka	Experimental	Spain	2 MW	Water/Steam	?	?	Pressurized H2O	2009	?	?
Yanqing	Experimental	China, yanqing	1 MW	?	10000 m²	?	Cavity	2011	?	?

Table 1.3: State of the art of central receiver power plant.

Project acronym	Plant status	Country built-in	Plant rate	HTF	Surface of mirrors	Land area	Receiver type	Year start production	Storage	Receiver Tout
Lake Cargelligo	Experimental	Australia	3 MW	Water/Steam	6080 m²	?	?	2011	Other	500
CSIRO Brayton	Experimental	Australia	1 MW	Air	?	?	Cavity	2011	?	?
PS 20	Commercial	Seville, Spain	20 MW	Water/Steam	1618 m²	210 acres	Cavity	2012	1	300
Greenway	Experimental	Turkey	1,4 MW	Water/Steam	?	?	Cavity	2012	?	?
Beijing Badaling	Experimental	China	1.0 MW	?	10000 m²	13 acres	Cavity	2012	1 h	?
Delingha	Commercial	China	50 MW		?	?		2013	?	?
E-cube 1	Experimental	China	1 MW	?	?			2013	?	?
Sierra sun tower	Commercial	California, USA	5.0 MW	Water/Steam	27670 m²	?	Cavity/external	2014	None	440
Ivanpah (3 units)	Commercial	California, USA	377 MW	Water/Steam	2600000 m²	3500 acres	External	2014	Other	570
Khi Solar one	Commercial	South Africa	50 MW	Water/Steam	576800 m²	?	?	2014	2 h	?
Jemalong solar	Experimental	Australia	1.1 MW	Liquid sodium	15000 m²	10 hectare	?	2014	3 h	560
BrightSource Coyote 1	Experimental	Nevada, USA	200 MW	Water/Steam	?	?	?	2014	?	?
Crescent dunes	Commercial	Nevada, USA	110 MW	Molten salt	1071361 m²	1600 acres	External	2015	10 h	565
BrightSource Coyote 2	Commercial	Nevada, USA	200 MW	Water/Steam	?	?	?	2015	?	?
Supcon Solar	Commercial	China	50 MW	Molten salt	434880 m²	330 hectare	Cavity	2016	2,5	?
Rice Solar energy	Commercial	California, USA	150 MW	Molten salt	1071361 m²	1410 acres	External	2016	Other	560
Palen solar	Commercial	California, USA	500 MW	?	?	1337 hectare	?	2016	None	?
BrightSource PG&E 5	Commercial	California, USA	200 MW	Water/Steam	?	?	?	2016	?	?
BrightSource PG&E 6	Commercial	California, USA	200 MW	Water/Steam	?	?	?	2016	?	?
Ashalim TSPS	Commercial	Israel	121 MW					2017	None	?
Noor III	Commercial	Morocco	150 MW	Molten salt	?	?	?	2017	8	?
BrightSource PG&E 7	Commercial	California, USA	200 MW	Water/Steam	?	?	?	2017	?	?
Atacama-1	Commercial	Chile	110 MW	Molten salt	1484000 m²	700 hectare	70	2018	17,5	550
Red stone	Commercial	South Africa	100 MW	Molten salt	?	?	?	2018	12	566

Nowadays many power tower projects are underway worldwide and most of them will be operational in 2013. In Spain, about 700 MW of CSP-plants are being commissioned. For the USA, a total of 1.2 GW CSP power installations are underway and should be in operation in 2013. Near San Bernardino County, California, the largest plant Ivanpah has reached around 75% completion more than 10.135 GW CSP power installations are announced mainly by the USA and Spain but also by China [19, 20].

Projects in the field are also under consideration in the Sun Belt countries such as Algeria, Morocco, Saudi Arabia and India [19, 21]. Saudi Arabia has recently announced an enormous deployment of CSP technology in over the next 20 years, with a target of 25 GW by2032 [20, 21]. In the USA, a large part of the projects are for the 200–500 MW CRS power plants.

The Palen project includes two 250 MW adjacent power plants similar to Ivanpah technology. Each plant is designed with about85000 heliostats for sunlight reflection to the receiver located on the top of a 228 m tower. Expected to be operational by June2016, this project insight is projected to start by the end of 2013[21, 24].

Likewise, Bright Source is developing another two 500 MW projects named Rio Mesa and Hidden Hills. These two projects are still in the certification process. On the other hand, in Arizona, Crossroads Solar Energy Project that includes a 150 MW tower technology and a 65 MW solar photovoltaic (PV) technology is being developed by Solar Reserve's [18, 21].

I.3.2. Design procedure

In power towers or central receiver systems, incident sunrays are tracked by large mirrored collectors (heliostats), which concentrate the energy flux onto radiative /convective heat exchangers called solar receivers, where energy is transferred to a thermal fluid, mounted on top of a tower.

It is constituted of the main element:

- Collector system, or heliostat field, created with a large number of two-axis tracking units distributed in rows;
- Solar receiver, where the concentrated flux is absorbed. It is the key element of the plant and serves as the interface between the solar portion of the plant and the more conventional power block;
- Heat exchanger system, where a heat transfer fluid may be used to carry the thermal energy from the receiver to the turbine;

- Heat storage system, with which system dispatch ability is ensured during events like cloud passages, and can adapt to demand;
- Fossil fuel backup for hybrid systems with a more stable output;
- Power block, including steam generator and turbine-alternator;
- Master control, UPS, and heat rejection systems

I.3.2.1. Available solar radiation source information

There are two reliable sources that provide information on the two of the most basic meteorological parameters: monthly mean temperature and solar radiation. These sources are the NASA website [28] and TUTIEMPO [29]. NASA has produced a grid map of the longitude. The solar radiation data are an estimation that has been produced from satellite-based scans of terrestrial cloud cover. Note that NASA does not provide the mean-daily maximum and minimum temperature.

TUTIEMPO on the other hand provides daily mean, maximum and minimum temperature data for any given location. The data are based on measurements carried out by a wide network of meteorological stations and hence these latter data are very reliable. Note that the NASA data are available on a mean-monthly basis, whereas TUTIEMPO are downloadable on a day-by-day basis. It is important to remember that NASA data are based on satellite observations that represent inferred values of irradiation; in contrast, TUTIEMPO provides ground measured data for temperature.

Hence, if reliable regressions are available between irradiation and mean temperature, then the latter data may be used to obtain more realistic estimates of irradiation.

I.3.3.2. Description and review of used software

In this section, a description and a review of software and codes that have been used in the literature for concentrating solar power (CSP) analysis and simulation is given[27].

The software and codes are described according to specific CSP technologies: power tower systems, linear concentrator systems, and dish/engine systems.

In the present review, a description of probabilistic methods for uncertainty and sensitivity analyses of concentrating solar power technologies is also provided.

I.3.3.3. Optical design and performance of heliostat fields

Chapter I. Concentrated Solar Power, State of the Art and Background

Central receiver power towers consist of a field of large, nearly-flat mirror (heliostats) that track the sun and focus the sunlight onto a receiver on top of a tower. In a typical configuration, a heat-transfer fluid such as water/steam or molten-nitrate salt is heated in the receiver and used to power a conventional steam-turbine power cycle to generate electricity.

Excess thermal energy can be stored during daylight hours to allow operation of the steam turbine during night. An advantage of power tower systems over linear concentrator systems is that higher temperatures can be achieved in the working fluid. Higher temperatures can lead to a lower-cost storage system.

➔ **ASAP**

ASAP is commercial ray-tracing software that performs optical simulations of various geometries and systems. It renders system geometry, ray traces, and light sources, and it models visible, ultraviolet, and infrared radiation. It can optimize optical systems with an optimization interface, and it can import geometry data from Solid Works via an IGES (Initial Graphics Exchange Specification) translator. The flux distribution reflected from solar collectors can only be projected on planar surfaces currently, but the next version will allow conformal mapping of the flux distribution on non-planar surfaces

➔ **DELSOL**

DELSOL is a performance and design code that includes optical and economic analyses. An analytical Hermite polynomial expansion/convolution-of-moments method is used to predict flux images from the heliostats in a computationally efficient manner. The code accounts for variations in insolation, cosine for shortening, shadowing and blocking, and spillage, along with atmospheric attenuation, mirror and receiver reflectivity, receiver radiation and convection, and piping losses. The code can be used to evaluate the system levelized energy cost and optimize the field layout, receiver dimensions, and tower height based on these costs. The code is written in FORTRAN77, and input to the code is entered via user-specified text files [26].

➔ **HELIOS**

HELIOS uses cone optics to evaluate the solar flux density from fields ranging from 1 to 559 individual heliostats (or cells with multiple heliostats). Parabolic dish and other collector shapes can also be evaluated with HELIOS. The code accounts for shadowing, blocking, declination of the sun, earth orbit eccentricity, molecular and aerosol scattering, atmospheric refraction, angular distribution of incoming solar rays, reflectivity, shapes of

focused facets, and error distributions in the surface curvature, aiming, facet orientation, and shadowing and blocking.

➔ **MIRVAL**

MIRVAL is a Monte Carlo ray-tracing program that calculates field efficiencies and flux maps for individual heliostats and central receiver systems. Monte Carlo ray tracing methodology consists of following stochastic paths of a large number of rays as they interact with the surfaces. Each ray has a specific direction and carries a certain amount of energy.

The irradiance of a surface is proportional to the number of impacting rays, and the reflection of the rays depends on the emissive, reflective, and absorptive behavior in the surface.

It accounts for shadowing, blocking, heliostat tracking, angular distribution of incoming solar rays, scattering, attenuation between the heliostats and receiver, reflectivity, aiming strategies, and random errors in heliostat tracking and conformation of the reflective surface.

Three partial receiver configurations and four heliostat types are included in the program. Input to the code is entered via user-specified text files.

➔ **SOLTRACE**

SolTrace is an optical simulation tool designed to model optical systems used in concentrating solar power (CSP) applications. The code was first written in early 2003, but has seen significant modifications and changes since its inception, including conversion from a Pascal-based software development platform to C++. SolTrace is unique in that it can model virtually any optical system utilizing the sun as the source. It has been made available for free and as such is in use worldwide by industry, universities, and research laboratories.

The fundamental design of the code is discussed, including enhancements and improvements over the earlier version. Comparisons are made with other optical modeling tools, both non-commercial and commercial in nature. Finally, modeled results are shown for some typical CSP systems and, in one case, compared to measured optical data.

➔ **Tonatiuh**

The Tonatiuhis an open source code configuration, cutting-edge, accurate, and easy to use Monte Carlo ray tracer for the optical simulation of solar concentrating systems. It intends to advance the state-of-the-art of the simulation tools available for the design and analysis of

solar concentrating systems, and to make those tools freely available to anyone interested in using and improving them. Some of the most relevant design goals of Tonatiuh are:

- To develop a robust theoretical foundation that will facilitate the optical simulation of almost any type of solar concentrating systems.
- To exhibit a clean and flexible software architecture, that will allow the user to adapt, expand, increase, and modify its functionalities with ease.

➔ HFLCAL

Development of HFLCAL started in the early 80's by Michael Kiera and was developed for two main tasks; the calculation of the annual plant output at a given configuration and the layout and optimization of a total system. Today it continues to be used and developed by the DLR, who uses it for the layout and optimization of heliostat fields. The software uses a simplified mathematical model of concentrator optics, modeling the reflected image of each heliostat by a circular normal distribution. Although ray tracing techniques have the advantage of reproducing real interactions between reflective surfaces, each ray has to be modeled, which requires large computation times compared to simpler mathematical models.

Few of the codes reviewed employed Monte Carlo methods for field optimization. HFLCAL features include: automatic multi aiming, secondary concentrator optics, tower reflector systems, various receiver models and the ability of least-cost optimization.

➔ STRAL

STRAL is a completely new ray tracing software which generates rays on the surface of the heliostat, as opposed to generating the rays in a plane above the heliostats. As no rays ever miss the target, it is computationally more efficient than other tools. STRAL enables the setup of heliostat field models in great detail using highly resolved heliostat mirror surface and geometry data as well as real sun shapes and blocking and shading.

➔ TieSol

The TieSol suite uses the parallel processing power of Graphic Processing Units (GPU) to implement extremely fast Monte Carlo ray tracing, well beyond the currently available capabilities of other software.

The software suite allows for the design, analysis and optimization of CRS systems. This is achieved by analyzing the effects of different optical and mechanical errors on the field, receiver flux map computation, as well as efficiency and annual performance

computation. Tietronix has developed an advanced visualization tool for TieSol capable of displaying the heliostat tracking in real time

➔ **HFLD**

HFLD is a MATLAB code for field layout design based on the edge ray principal of non-imaging optics. The edge ray principal simply states that if the limiting rays (rays coming from the edges of the source) are transferred to the receiver, this will ensure that all rays coming from the inner points in the source will end upon the receiver.

The accuracy and feasibility of the HFLD code has been confirmed by comparing with published data from the PS10 field. When compared with other codes, such as DELSOL, HFLD has a shorter computational time during design and optimization of the heliostat field.

The code also calculates the annual sunshine and duration on the land surface between heliostats, to evaluate the feasibility of crop growth

I.3.3.4.Heat transfer fluid (HTF) transport, exchange, and storage power cycle

➔ **RADSOLVER**

Radsolver calculates the radiation energy transfer within arbitrarily shaped solar cavity receivers. It accounts for non-gray surfaces and accommodates wavelength-dependent radiative properties for emission and reflection using an arbitrary number of wavelength bands. RADSOLVER includes thermal emission and reflection and absorption of thermal and solar radiation within zones defined for the cavity. Convection of air within the cavity is neglected. Input to the code is entered via user-specified text files.

➔ **SAM advisor**

SAM includes high-level models for piping heat loss and thermal storage, but these components are treated as "lumped" systems. Explicit models of spatial and temporal processes within these subsystem components are not included

➔ **SOLERGY**

Solergy performs an energy balance on the entire system and accounts for heat losses in each component, including piping and storage thermal losses

➔ **TRNSYS**

TRYNSYS is a software platform that enables the user to model different transient systems using modular components. Each component represents a physical process or feature

in the system, and components can be developed and added, as needed, to a system model. A component reads in a text-based input file and provides output through the solution of

algebraic or differential equations. Components include solar thermal collectors (parabolic concentrating solar collector, flat plate solar collector), heat exchangers (counter-flow, cross-flow, parallel flow, shell-andtube, waste heat recover, etc.), thermal storage tanks (stratified, variable volume, etc.), hydraulics (pumps, pipes, values, etc.), controllers, and more. Specific processes can be modeled for subcomponents of the total system, and total-system performance analyses can also be performed. The software contains a GUI that allows drag-and-drop arrangement and editing of component icons.

➔ **GATECYCLE**

GATECYCLE is commercial software that models the performance of Rankine, gas-turbine, and combined power cycles via mass and energy balances in each component. It includes component-level processes such as fouling, pressure losses, boiler operations, and cooling tower operations. Design and off-design performance can be simulated to evaluate potential system modifications. A graphical user interface is used to construct the power cycles and enter data

➔ **IPSEPRO**

IPSEPRO is commercial software that contains a set of modules for simulating heat and mass balances in power plants and heating systems. The software can be used to predict design and off-design performance and estimate costs during conceptual design. IPSEPRO also allows the user to create new component models or new model libraries. A graphical user interface is used to build models and enter data.

➔ **STEAMPRO**

STEAMPRO is commercial software that solves mass and energy balances to simulate the performance for Rankine-cycle steam power plants. Design criteria and inputs for system components are prescribed by the user. Similar to GATECYCLE, the user constructs a model by connecting appropriate building blocks via a graphical user interface.

I.3.3.4.Probabilistic modeling

All of the codes evaluated implement deterministic evaluations of the system or component performance, which yield a single value for the simulated output (e.g., LEC).

Input parameters are typically entered as specific values rather than distributions of values that integrate the inherent uncertainty in many of the system features and processes. As a result, the confidence of the result and uncertainty associated with the results are not reported.

The confidence and likelihood of the simulated metric (e.g., levelized energy cost) being above or below a particular value or range can be readily assessed and presented using these probabilistic methods.

In addition, sensitivity analyses can be used with probabilistic analyses to determine the most important components, features, and/or processes that impact the simulated performance.

This information can be used to guide and prioritize future research and characterization activities that are truly important to the relevant performance metrics.

Uncertainty analyses were performed by Kolb et al. (1994) to evaluate the impact of uncertainties in input parameters on central receiver performance models of levelized energy cost. A screening analysis was first conducted to determine a subset [32] of the hundreds of input parameters that would be assigned uncertainty distributions as opposed to deterministic point values. A stepwise regression analysis was then performed to determine the input parameters that were most correlated to the variability of the simulated performance metric (levelized energy cost).

I.3.3.5.Code selection procedure

Garcia et al, suggested a strategy of code selection for industrial projects, to first determine the general layout of the plant in terms of tower height, heliostat position [28].Then perform a detailed study including a closer description of the heliostat flux and field performance. This latter task can be performed with any of the Monte Carlo ray tracers, while the layout can be performed with the HFLCAL or HFLD codes. The authors then suggest that the system is modeled with tools such as TRYNSYS, which can model the transient behavior of thermal systems [28], or the Solar Advisor Model (SAM), which supports industry calculations of the cost of energy [29]. For a researcher, there is no standard tool.

Chapter II. Central Receiver System Design and Optimization

The cavity of a solar central receiver plant intercepts and absorbs sunlight from thousand concentrating heliostats. Its basic function is the concentration of the direct solar radiation flux, and converts it to thermal energy.

II.1. Geometry modeling for the cavity receiver

The sizing procedure of the receiver from optic and geometric consideration is carried out in this section.

The geometry of the cavity is designed such that it maximizes the absorption of the entering radiation, minimizes the heat loss by convection and radiation to the ambient.

For the design of the receiver, the active tube panels form the absorbing surface inside of a shielded cavity.

The radiation is focused on the aperture of the cavity such that the solar is distributed over the four adjacent panels that form the semi-cylindrical interior absorbing surface. Figure 2.1
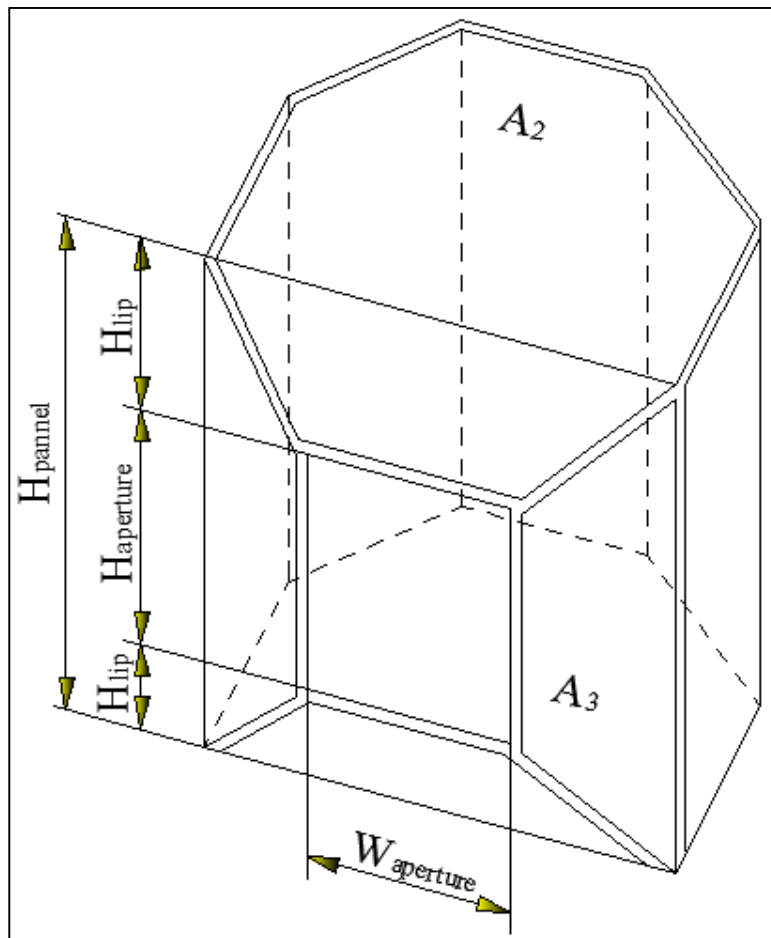
FIGURE 2.1: 3D VIEW OF THE CAVITY RECEIVER GEOMETRY

The temperature of the absorber panels varies with vertical position in a manner dependent on the incident solar flux and flow direction of the HTF. In this case, the HTF is assumed to enter at the bottom of each receiver panel (at its lowest temperature) and flow vertically through tubing to an outlet header located at the top of the panel (Figure 2.2).
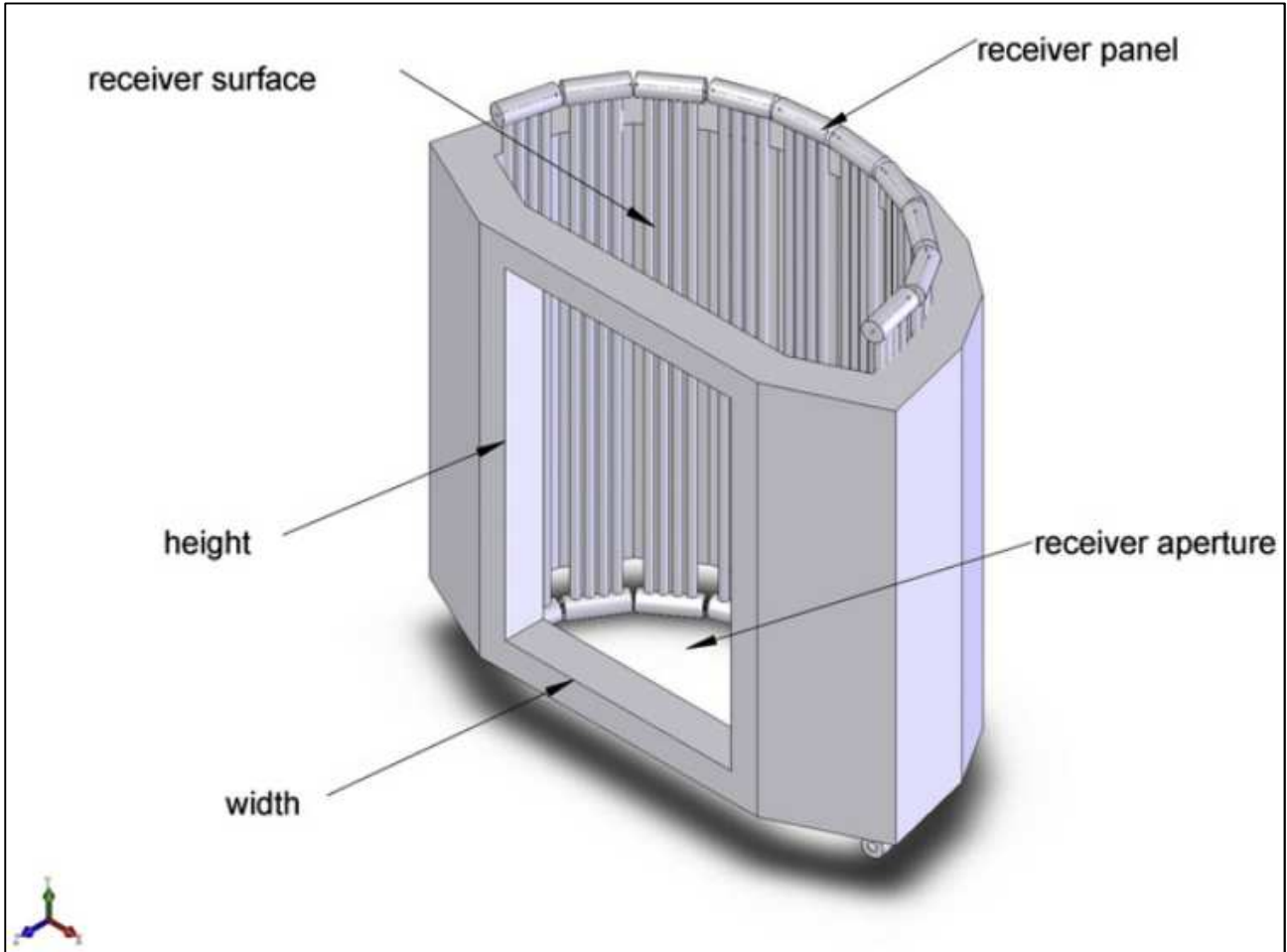
FIGURE2.2: TUBULAR CONFIGURATION OF THE CAVITY RECEIVER PANEL.[31]

In the present work, the dimensions of the cavity receiver are chosen through optimization functions in SAM to provide a name plate electric power of 20 MW$_e$. The resulting dimensions are given in table 2.1 below.

Table 2.1: Selected geometric dimensions of the cavity receiver and predicated performance parameter. **[47]**

H panel [m]	15.74
H lip [m]	1.60
H aperture [m]	14.31
W aperture [m]	14.00
Tube outer diameter [mm]	60
required HTF outlet temperature [°C]	574
Maximum allowable flux density [kW/m²]	800
Maw flow rate to receiver [kg/s]	622.16
Receiver design thermal power [kW]	91.76

II.2.Energy balance model applied in the present study

As represented in figure 2.3, the global steady state energy balance components of the cavity receiver within the control volume dx is given in equation2.1.
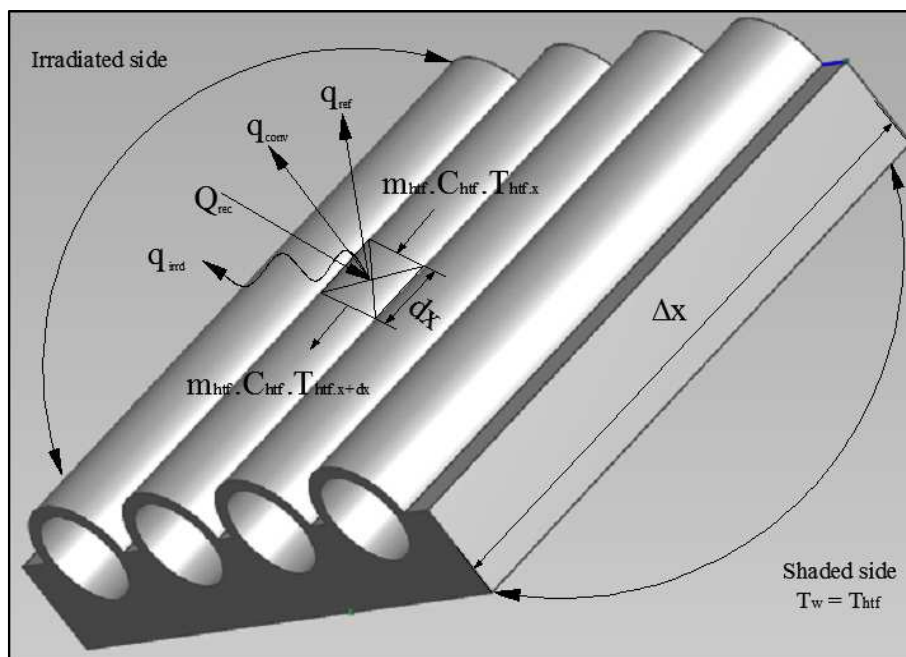
FIGURE 2.3: THE ENERGY BALANCE MODEL FOR SINGLE RECEIVER TUBE.

$$\boldsymbol{Q_{rec}} = q_{ref} + q_{conv} + q_{irrd} + \dot{m}_{htf}.C_{htf}.\Delta T_{htf} \dots\dots\dots\dots\dots\dots\dots\dots \text{(2.1)}$$

The receiver energy balance is founded by two terms (energy losses terms and energy gain terms). Therefore, the result of an energy balance applied to a single tube at position x on

panel N can be scaled by the number of tubes in that panel. Since each tube is then essentially the same of its neighbor, tube-to-tube conduction and radiation exchange is neglected. Axial conduction is also neglected since the much larger internal convection due to salt flowing in the tubes dominates over the relatively large resistance to conduction

II.3.Energy losses terms modeling

The energy losses from the cavity receiver are modeled on three terms:

- The reflective radiation losses represented by the first component in the equation 2.1;
- The convective heat losses represented by the second term;
- The radiation losses represented by the third term.

In a cavity receiver, convective losses can be reduced because the absorbing surfaces are protected from direct wind influence and the heated air inside the cavity is inhibited from escaping to the environment by the ceiling construction.

The radiation losses from the active surfaces are partly absorbed by inactive surfaces on the side walls, which reheat the air inside the cavity. Consequently, the air inside the cavity is assumed to be at higher temperatures than the ambient air. Convection losses can be separated into natural convection due to buoyancy and forced convection driven by ambient winds.

II.3.1.The reflective radiation losses

The proportion of the radiation incident on the receiver surface that is reflected depends on the absorptivity of the receiver surface coating and on the incidence angle of the radiation intersecting the surface.

The energy that is initially reflected from the tower is represented by the q_{ref} term. The receiver model assumes a constant, spectrally independent, hemispherical absorptivity (α) for the receiver surface elements. [02]

$$q_{ref,x} = (1 - \alpha).D_t.n_t.\varphi_{field}.dx \dots\dots\dots\dots\dots\dots\dots\dots\dots\dots\dots\dots\dots\dots \text{(2.2)}$$

II.3.2.The convective heat losses

Convection losses can be separated into natural convection due to buoyancy and forced convection driven by ambient winds.

The geometry of cavity-type receivers offers the potential to reduce long-wave radiation losses as well as convective heat losses compared to the external receiver type.

A review of the literature shows a number of investigations on natural convection losses cavity receivers; however, it is imprecise whether these correlations can be applied for the significantly higher wall temperatures and larger Rayleigh numbers that are present at central receivers system.[32]

$$q_{conv} = \bar{h}.A_{rcv}.(T_w - T_0) \ldots\ldots\ldots\ldots\ldots\ldots\ldots\ldots\ldots\ldots\ldots\ldots\ldots\ldots\ldots\ldots\ldots\ldots\ldots \text{(2.3)}$$

$$\bar{h} = h_{nat} + h_{fcd} \ldots\ldots\ldots\ldots\ldots\ldots\ldots\ldots\ldots\ldots\ldots\ldots\ldots\ldots\ldots\ldots\ldots\ldots\ldots\ldots \text{(2.4)}$$

$\bar{h}$: Global convective heat transfer coefficient [W/m².K];

h_{fcd}: Forced convection heat transfer coefficient [W/m².K];

h_{nat}: Natural convection heat transfer coefficient [W/m².K];

A_{rcv}: Cavity aperture area [m²]

T_w: Internal cavity wall temperature [°K]

T_0: Ambient air temperature [°K]

II.3.2.1.The forced convection heat losses

As stated in earlier studies [32, 33], forced convection heat losses have been investigated experimentally. No correlations are available for predicting forced or mixed convection from cavity receivers. Few experimental investigations have been performed in this area, with the results being somewhat contradictory. It has been suggested that as first approximation, forced convection from a flat plate with the size of the aperture at the receiver average temperature could be used [32]. Later experiments showed that inertia effects on convection become significant and the natural convection correlations may not be representative anymore at Richardson numbers lower than 0.2 [32, 33].

The ratio of the Grashof number to the square of the Reynolds number is a use ful indicator of the driving forces of the flow and therefore what kind of convection mechanism has to be considered in transfer model. This ratio is also called Richardson number.

$$Ri = \frac{Gr}{Re^2}$$ ....…………………………………………..……………………………………… (2.5)

Nellis, G. and Klein, S.A, have determined that for wind velocities below 5 m/s, natural convection is the dominant mechanism of convective heat transfer; forced convection is an insignificant influence. With increasing velocity forced convection becomes an increasingly significant mechanism of convective heat transfer.

For wind velocities between 6-20 m/s, a mixed convection heat transfer regime has to be considered. For wind velocities higher than 25 m/s, forced convection are dominant.

The cavity receiver is mounted at the top of the solar tower. To account for the increasing wind velocity with increased elevation the correlation in equation (2.6) from (Duffie, J. A., Beckman, W.A.,2006) is used

$$\frac{u_1}{u_2} = \left(\frac{z_1}{z_2}\right)^{0.14}$$ …………………………………………………………………………….. (2.6)
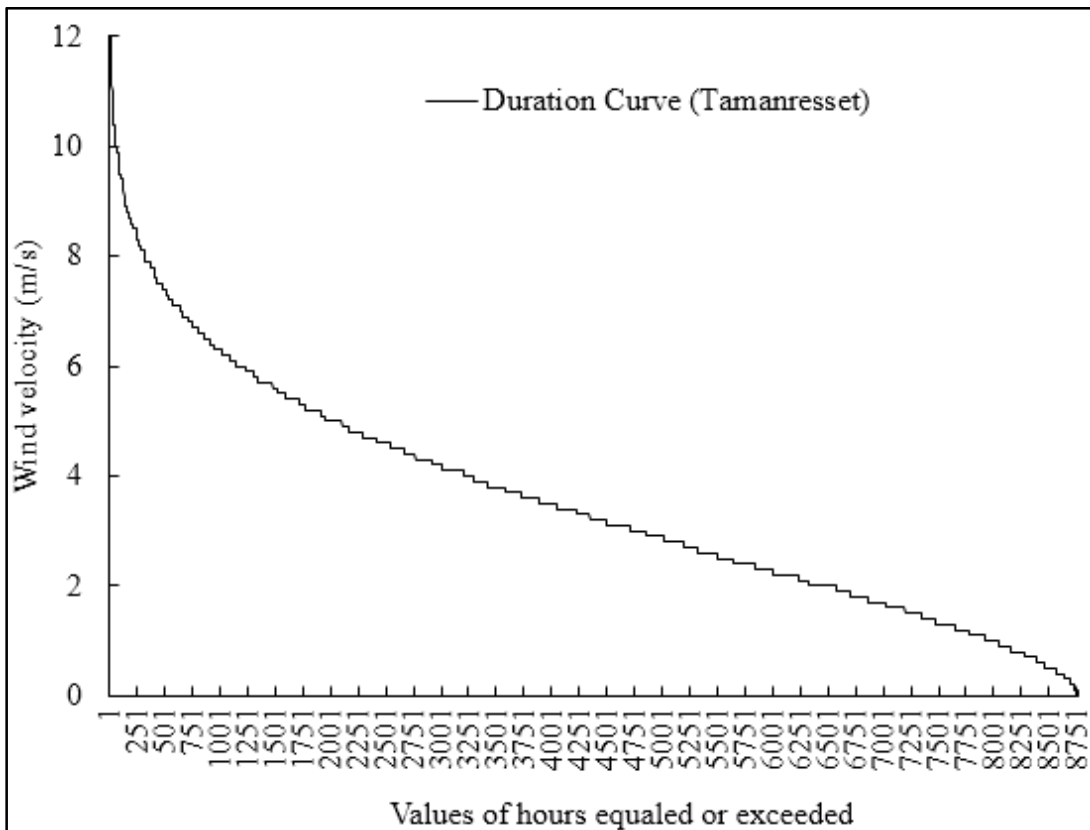
FIGURE 2.4: WIND VELOCITY PROFILE FOR MEASUREMENTS OVER HOURS (MEAN VALUE).

Figure 2.4 shows that a significant time of the year the wind velocity is low enough so that forced convection is not expected to have a dominating influence on the convection heat loss mechanism inside the cavity. The majority of the year wind velocities are of a magnitude that forced convection needs to be considered in from of a mixed convection regime. The wind never exceeds wind velocities of 12 m/s, natural convection is a significant convection mechanism over the full range of observed wind speeds.

II.3.2.2. The natural convection heat losses

In earlier research works, an equation that solves for the heat losses through the aperture due to natural convection was reported [32, 33]. The Nusselt number correlation reported same works is derived from experimental work on cubical cavities.

$$Nu = 0.088. Gr^{\frac{1}{3}}.\left(\frac{T_w}{T_0}\right)^{0.18} \dots\dots\dots\dots\dots\dots\dots\dots\dots\dots\dots\dots\dots\dots (2.7)$$

The correlation is applicable for Grashof numbers in the range: $10^5 \leq Gr \leq 10^{12}$. All properties in the dimensionless numbers are evaluated at ambient temperature [02, 03 and 04].

The wall temperature is the average of all internal cavity surface temperatures. The Grashof number is defined as [02]:

$$Gr = \frac{g.\beta.(T_w-T_0)}{v^2} \dots\dots\dots\dots\dots\dots\dots\dots\dots\dots\dots\dots\dots\dots\dots (2.8)$$

The Nusselt number provides the heat loss coefficient.

$$h_{nat} = \frac{Nu.k}{L} \dots\dots\dots\dots\dots\dots\dots\dots\dots\dots\dots\dots\dots\dots\dots\dots (2.9)$$

The influence of an upper and lower lip as well as the receiver tilt angle is correlated with equation [02] :

$$h_{nat} = h_{nat.0}.\left(\frac{A_1}{A_2}\right).\left(\frac{A_3}{A_1}\right)^{0.63} \dots\dots\dots\dots\dots\dots\dots\dots\dots\dots\dots\dots (2.10)$$

Figure II.1, illustrates the area definitions A_1, A_2 and A_3.

A_2 is the complete interior surface area A_1 minus the lower lip area. A_3 is the wall area below the horizontal plane passing through the bottom edge of the upper lip.

II.3.3. The radiation heat losses

In order to calculate the heat losses by radiation, the SAM advisor code model assumes that the loss is not a function of time or operation mode of the cavity receiver. This allows the setup of some parameters: operation of wall temperature in the range of 480°C, emissivity ε=0.90, average wind speed $u_0 = 7.2$ m/s and ambient air temperature $T_0 = 20$°C. [32, 33].

The thermal radiation heat losses are expressed as a function of the receiver aperture area in the following equation:

$$q_{irrd} = \varepsilon\sigma A T_w^4 \dots\dots\dots\dots\dots\dots\dots\dots\dots\dots\dots\dots\dots\dots\dots\dots\dots\dots (2.11)$$

Where σ is the Stefan-Boltzmann constant and A is the receiver aperture area.

II.4. Heliostat field optimization algorithm

Using DELSOL 3 algorithm shown in figure 2.5, the heliostat field optimization is defined by the iterative calculation of the zone by zone annual average and design point optical performance for each tower height and receiver size. The results which are scaled are the descriptions of heliostat images on the receiver for each zone.

The cosine, shadowing and blocking, and atmospheric attenuation losses used in the system optimization is described in this Section figure 2.6.

- Cosine losses: If the heliostat surface is not orthogonal to the incident radiation, the effective reflecting area is smaller than the complete heliostat surface.
- Shading and blocking effects: Surrounding heliostats shield parts of the incoming radiation or block the reflected radiation.
- Atmospheric scatter: Particles in the air absorb or reflect part of the radiation on its way to the receiver.
- Spillage: A fraction of the reflected heliostat image does not the target surface due to multiple sources (tracking inaccuracies, influence of the tower, shape of the sun, etc.)

The overall heliostat field efficiency utilized by the cavity receiver model is defined as the incident radiative power on the receiver, which is the product of the average solar flux $\dot{q}_{inc}$ and the active receiver surface A_{rec}, divided by the total radiation on the heliostat field.

$$\eta_{field} = \frac{\dot{q}_{rec}.A_{rec}}{DNI.A_{hel}.N_{hel}} \dots\dots\dots\dots\dots\dots\dots\dots\dots\dots\dots\dots\dots\dots\dots\dots\dots (2.12)$$

$$\dot{q}_{rec}.A_{rec} = \dot{q}_{hel.total}. -\dot{q}_{loss.field} \dots\dots\dots\dots\dots\dots\dots\dots\dots\dots\dots\dots\dots\dots (2.13)$$
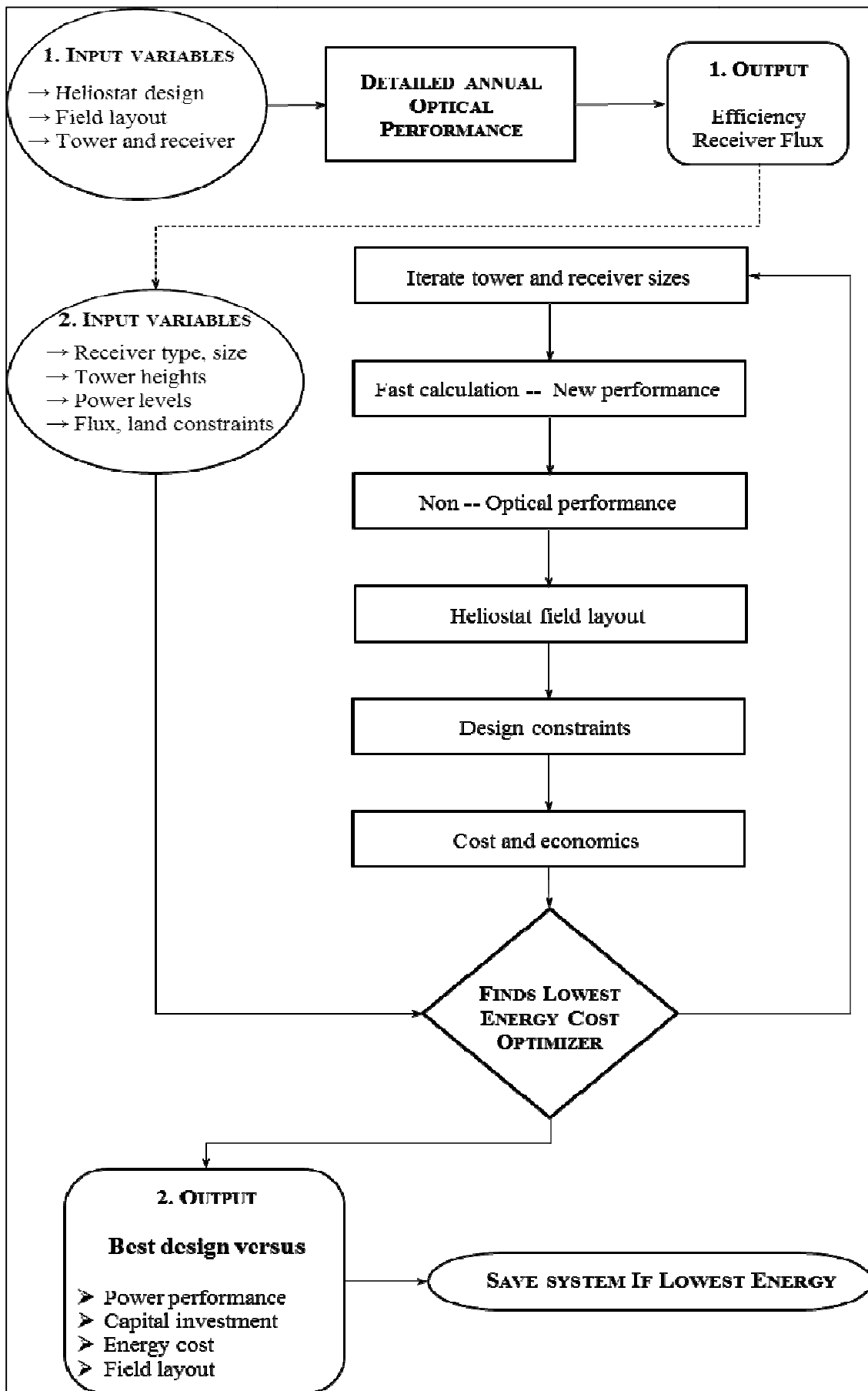
FIGURE 2.5: DELSOL ALGORITHM PRINCIPAL USED IN THE PRESENT SIMULATION. [34, 35]
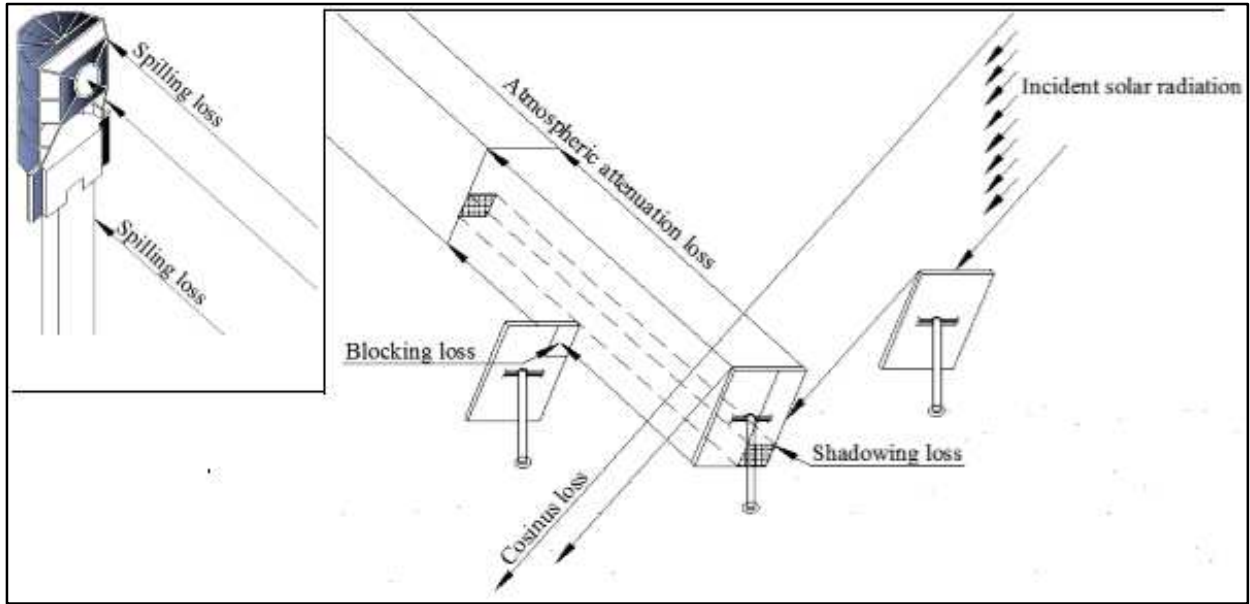
FIGURE 2.6: DIFFERENT TYPE OF LOSSES FOR CENTRAL RECEIVER TOWER PLANT.

DELSOL 3 provides options for a single-point aiming technique (where the complete flux is focused on a central point of the receiver panels) and a smart aiming technique (where the flux is vertically and horizontally spread out along the absorbing surface).

During optimization, DELSOL 3 works with the field defined by the minimum and maximum field dimensions and the heliostat densities in each zone, for which performances were calculated during an initial performance calculation.

Each zone is rated by a performance/cost ratio PCR, and zones are packed with heliostats, starting with that zone having the best PCR, until a requested power is reached.

$$\text{PCR} = \frac{\eta_{field}}{C_{field}} \dots\dots\dots\dots\dots\dots\dots\dots\dots\dots\dots\dots\dots\dots\dots\dots\dots\dots \text{(2.14)}$$

Where:

$$\eta_{field} = \eta_{cos} \cdot \eta_{shad} \cdot \eta_{block} \cdot \eta_{atm} \cdot \eta_{intr} \dots\dots\dots\dots\dots\dots\dots\dots\dots\dots \text{(2.15)}$$

The different terms of losses are defined as:

η_{cos}: cosine efficiency = 1- cosine losses…………………………………………….……. (2.16)

η_{shad}: shadowing efficiency = 1- shadowing losses ………..………………..……………… (2.15)

η_{block}: blocking efficiency = 1- blocking losses …..……………………………………… (2.16)

η_{atm}: atmospheric transmittance efficiency= 1- atmospheric attenuation ……..……….... (2.17)

The cost of each element of the heliostat field represented by the term C_{field} is comprised of three parts:

$$C_{field} = \frac{C_{hel}+C_{land}+C_{wire}}{C_{hel-R}+C_{land-R}+C_{wire-R}} \dots\dots\dots\dots\dots\dots\dots\dots\dots\dots\dots\dots\dots\dots\dots (2.18)$$

Where:

$$C_{hel} = \frac{cost\ of\ the\ heliostat\ structure\ [\$]}{surface\ of\ mirror\ area\ [m^2]} \text{ for all heliostat in the field ;} \dots\dots\dots\dots\dots (2.19)$$

$$C_{land} = \frac{cost\ of\ the\ land\ [\$]}{surface\ of\ land\ [m^2]} \times \frac{1}{mirror\ density} ; \dots\dots\dots\dots\dots\dots\dots\dots\dots\dots (2.20)$$

$$C_{land} = \frac{wire\ cost\ [\$]}{heliostat} \times \frac{1}{glass\ area / _{heliostat}} ; \dots\dots\dots\dots\dots\dots\dots\dots\dots\dots (2.21)$$

A PCR is calculated for each zone, and the zones are selected from best to worst PCR before optimization starts. As each zone is quantified, the design point thermal power to the receiver, the annual energy production from the field, and the total field costs (heliostats, land, and wiring) are updated.

However, the thermal output power from the receiver and piping radiation and convection losses are recalculated to determine the net electrical power production.
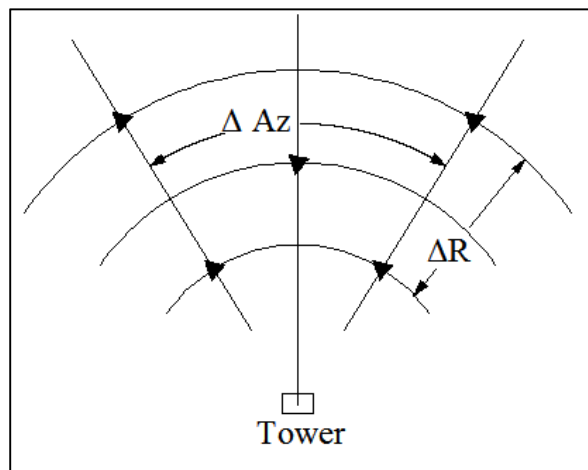
FIGURE 2.7: RADIAL STAGGERED ARRANGEMENT OF THE OPTIMIZED HELIOSTAT FIELD. [36, 37, 40]

The heliostat field layout could be carried out by determining the optimal values of the radial spacing ΔR, and azimuth spacing ΔA$_z$. There are various optimization procedures to

establish these two geometric position parameters. One of the most effective procedures is the radial staggered layout which is shown in figure 2.7.

For a power plant with a north-south configuration and cavity receiver, the empirical relations, given by equation2.22 and equation 2.23, can be used to calculate the radial and azimuth spacing.

As represented in figure2.8, these relations depend also on the loft angle (α) between the heliostat, the ground and the tower. They are determined using curve fits method [03, 04].

$$^{\Delta R}/_{H_h} = [62.32 + 0.63 * E + (0.84 + 0.16 * E) * \cos\alpha] * \theta^{-1} - [0.53 + 0.08 * E +$$

$$(0.19 + 0.06 * E) * \cos\alpha] + [2.25 + 0.21 * E + (0.84 + 0.16 * E) * \cos\alpha] * \left(\frac{\theta}{100}\right) \dots\dots$$

…………..……………………………………….…………………………. (2.22)

$$^{\Delta A_z}/_{W_h} = (2.16 - 0.01 * E - 0.10 * \cos\alpha) + (0.49 + 3.32 * \cos\alpha) * \left(\frac{\theta}{100}\right) - (3.38 +$$

11.18∗cosα∗θ1002…………………………….………………..……… (2.23)

The combination of all the above factors affecting the performance of the solar field should be optimized to determine an efficient layout. Since a large area of land is required to install big central receiver CRS power plant, complex optimization algorithms are used to optimize the annual energy produced by unit of land.

DELSOL3 algorithm includes an analytical Hermite polynomial expansion-convolution method which is used to predict flux images from the heliostats field.

This algorithm implemented under SAM advisor software is used to assess the power plant optical performance. In this work, a simulation has been carried out to determine the optimum layout giving a trade-off between performance, costs and energy flux absorbed by the receiver.
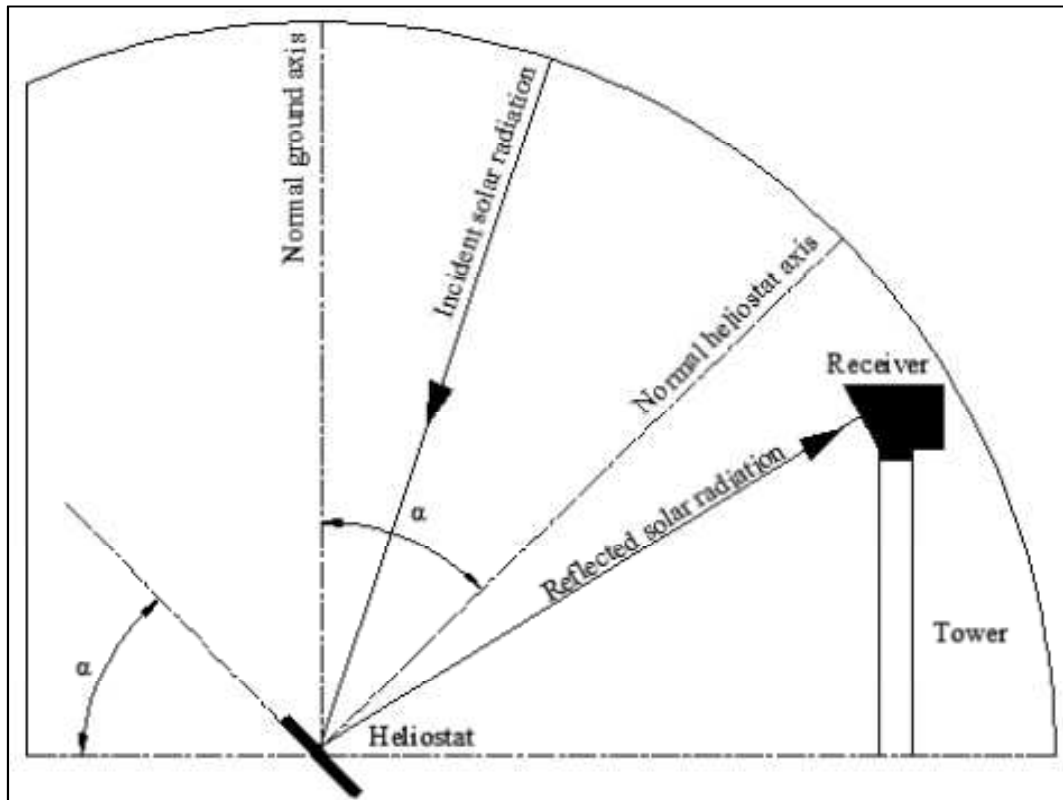
FIGURE 2.8: CONCEPTION OF THE OFF-AXIS OPTICS OF HELIOSTATS REPRESENTING THE LOFT ANGLE A.

II.5. Heat transfer fluid system

Two types of coolants or heat transfer fluids are used in today's solar power towers: water in a latent energy change configuration and single phase sensible energy change molten salts.

As molten salt has a high energy storage capacity per volume (500–700 kWh/m^3), they are excellent candidates for solar thermal power plants with large capacity factors. Even though nitrate salt has a lower specific heat capacity per volume than carbonates, they still store 250 kWh/m^3. The average heat conductivity of nitrates is0.52 W/mK and their heat capacity is about 1.6 kJ/kgK.

A widely used salt composition of 60% $NaNO_3$ and 40% KNO_3canwithstand relatively high operating temperatures (up to 866 K) and the high operating temperatures potentially permit greater turbine thermal efficiencies in the power cycles.

II.6. Energy storage with two tank model

For high annual capacity factors, solar-only power plants must have an integrated cost-effective thermal storage system. One such thermal storage system employs molten nitrate salt as the receiver HTF and thermal storage media. To be usable, the operating range of the

molten nitrate salt, a mixture of 60% sodium nitrate and 40% potassium nitrate, must match the operating temperatures of modern Rankine cycle turbines.

In a molten-salt power tower plant, cold salt at 290 °C (550°F) is pumped from a tank at ground level to the receiver mounted atop of a tower where it is heated by concentrated sunlight to 565°C(1050°F) (Figure 2.9). The salt flows back to ground level into another tank.

To generate electricity, hot salt is pumped from the hot tank through a steam generator to make superheated steam. The superheated steam powers a Rankine-cycle turbine.
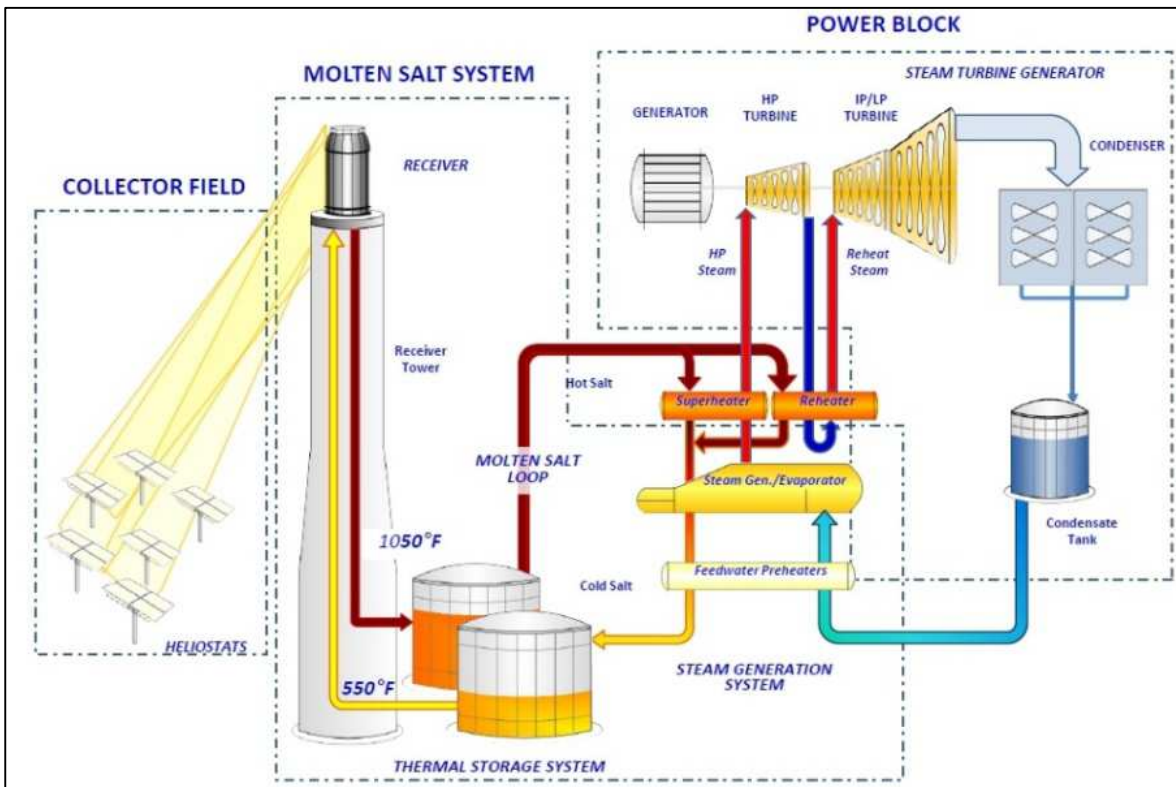
FIGURE 2.9: SOLAR TOWER PLANT CONFIGURATION WITH HEAT STORAGE SYSTEM [38].

The collector field can be sized to collect more power than is demanded by the steam generator system, and the excess salt is accumulated in the hot storage tank. With this type of storage system, solar power tower plants can be built with annual capacity factors up to 70%.

As molten salt has a high energy storage capacity per volume (up to 500–700 kWh/m^3), they are excellent candidates for solar thermal power plants with large capacity factors. Even though nitrate salt has a lower specific heat capacity per volume than carbonates, they still store 250 kWh/m^3.

The average heat conductivity of nitrates is 0.52 W/mK and their heat capacity is about 1.6 kJ/kg K. Nitrates are a cheap solution for large storage systems.

Thermal storage offers the ability to uncoupled energy production of the solar plant from the incident solar energy. This capability can be used to avoid the highly variable energy production that is characteristic for other renewable energy technologies.

In the present study, there are two tanks, one hot tank and one cold tank. The boiler is always fed from the hot tank and once the molten nitrate salt has transferred heat to the water in the unfired boiler, it goes to the cold tank. This tank supplies the solar field, which at the same time feeds the hot tank with the salt heated by the collectors.

In the SAM advisor model, we have considered two main parameters. The maximum power to storage and maximum power from storage variables. They are related to the design turbine thermal input variable on the power block tool box, which also appears on the storage box. The value of these variables is often close to or equal to the design turbine thermal input

value. Solar advisor calculates these values based on the heat exchanger duty, the storage size and the turbine design.

Using rock as a primary material and sand as a secondary material can replace 75% of the tank volume. The Thermocline temperature degradation value is typically 25% of the difference between the hot and cold storage medium temperatures.

II.7.Thermal storage dispatch control

The thermal storage dispatch controls are coefficients for a set of equations that model the timing of releases of energy from the thermal energy storage system to the power block. When the system includes thermal energy storage, Solar Advisor can use a different dispatch strategy for up to six different time-of-use periods.

Solar Advisor decides whether or not to operate the power block based on how much energy is stored in the TES and the values of the thermal storage dispatch controls parameters. You can define when the power block operates for each of the six periods.

For each time-of-use period, there are two targets for starting the power block: one for periods of sunshine, and one for period of no sunshine.

The turbine output fraction for each time-of-use period determines at what load level the power block runs using energy from storage during that period. The load level is a function of the turbine output fraction and design turbine thermal input.

For each time-of-use period, during periods of sunshine, the power block at the load level for that period only when the available storage is equal to or greater than the product of the storage dispatch fraction (with solar) and maximum energy in storage. Similarly, during periods of no sunshine, the power block only runs when the available storage is equal to or greater than the product of storage dispatch fraction (without solar) and maximum energy in storage.

II.8.SAM advisor model description.

System Advisor Model (SAM) was developed by the National Renewable Energy Laboratory (NREL). It allows users to examine and to compare solar and other renewable technologies on economic, technological and operational bases. SAM is based on the transient Systems Simulation (TRNSYS) program, maintained and distributed by (Klein, S.A. et al., 2007). TRNSYS provides a software platform to model thermodynamic systems on a modular basis in dependence on hourly weather data. It is widely used to simulate renewable energy systems.

Any process in a thermodynamic system simulated in TRNSYS can be represented as a separate module that interacts with other modules in the system. TRNSYS offers an extensive library of existing modules for various applications; modules can also be developed by the user, coded according to a TRNSYS template in FORTRAN and complied in the TRNSYS dynamic Link Library. SAM provides a graphical interface to specify and run a predefined TRNSYS simulation and to analyze the outputs. It provides detailed modules in TRNSYS to simulate complex energy systems such as concentrated solar power (CSP), photo-voltaic systems and solar heating systems.

SAM is a comprehensive model developed to perform techno-economic evaluations of various solar technologies, and can develop plant designs and LCOE based on climate data for a specified location. SAM models an entire CSP plant from the collector field through to the power block, and allows the user to specify key parameters such as the per unit capital cost of different plant areas(e.g., \$/kW$_e$), the amount of thermal storage and whether the plant uses wet or dry cooling.

II.8.1. Solar only mode parameter definition.

II.8.1.1.Solar multiple

The duration of solar operation is intrinsically linked to the size of the solar collector field. Larger fields can collect larger amounts of energy, and thus provide nominal output with lower

levels of solar radiation input. Over sizing the solar collector field is thus one means of extending the duration of nominal operation, at a relatively high cost.

The size of the solar collector field can be expressed in terms of the solar multiple SM, defined using equation 2.24, as the ratio of the nominal thermal power delivered by the field Q_{field} to the nominal power demanded by the receiver Q_{rec}. The nominal output from the heliostat field is typically defined considering a direct normal irradiation of 850 W/m^2 at solar noon on the Equinox (21st of March or 22nd September) [47].

$$SM = \frac{Q_{field}}{Q_{rec}} \dots\dots\dots\dots\dots\dots\dots\dots\dots\dots\dots\dots\dots\dots\dots\dots\dots\dots\dots\dots (2.24)$$

The cost of the solar field is roughly proportional to the solar multiple and, as such, the marginal cost of increasing the duration of nominal receiver operation rises exponentially as the solar multiple is increased above a value of SM 1.0. These limitations can be overcome by the integration of thermal energy storage, which avoids the need to spill excess solar heat from the system by storing it for later use.

II.8.1.2.Capacity factor

The capacity factor of a power plant is the ratio of average output power to peak power that the station could deliver. Due to fluctuations in the availability of the primary energy source and outages due to maintenance of the equipment, the capacity factor is never 100%.

In fact, for renewable energy sources, it is mostly below 50%.

It is therefore given by

$$CF = \frac{Se}{P_{rated}} \cdot \frac{\lambda}{\tau} \dots\dots\dots\dots\dots\dots\dots\dots\dots\dots\dots\dots\dots\dots\dots\dots\dots\dots\dots\dots (2.25)$$

'Se' being the electricity generated in a whole year with solar energy, λ being the conversion factor from kWh to J, and τ is being the time (seconds) in one year. The 'Se' aspects bringing to the technical and economic studies of CSP added dimensions that are not present in other renewable energy production technologies.

II.8.2. Hybrid mode parameter definition.

SAM's CSP models calculate the energy required to supplement solar energy in order to maintain the solar field outlet temperature at its design point. The financial model accounts for

the cost of using natural gas to meet that energy requirement based on the LHV (lower heating value) efficiency you specify on the power cycle tool box, and the fuel cost you specify on the O&M page [48].

II.8.2.1.Fossil fuel fraction (FFF)

For systems with fossil-fuel backup, fossil fuel fraction defines the solar output level at which the fossil backup will run during each hour of a specific time-of-use period. For example, a fossil fuel fraction of 1.0 would require that the fossil backup operate to fill in every hour during a specified time-of-use period to 100% of design output. In that case, during periods when solar is providing 100% output, no fossil energy would be used. When solar is providing less than 100% output, the fossil backup operates to fill in the remaining energy so that the system achieves 100% output.

II.9. Economic parameter definition.
II.9.1. Levelized cost of electricity.

The levelized cost of electricity (LCOE) is the price (per kWh) for generated electricity that makes the net present value (NPV) of the installation zero. Nonetheless, if the sales price is lower than the LCOE, the plant does not provide the required return [41].

$$LCOE = \frac{\sum_{i=0}^{N}\left[\frac{I_i + O_i + F_i + ITC_i + PTC_i}{(1+r)^i}\right]}{\sum_{i=0}^{N}\left[\frac{E_i}{(1+r)^i}\right]} \dots\dots\dots\dots\dots\dots\dots\dots\dots\dots\dots\dots\dots (2.26)$$

Where:
- o I_i investment costs in year i
- o O_i operating and maintenance costs in year i
- o F_i fuel costs in year i
- o ITC_i investment tax credits in year i
- o PTC_i production tax credits in year i
- o E_i energy generated at year i
- o r   weighted average cost of capital (WACC)
- o N   lifetime of the project (years)

II.9.2.The weighted average cost of capital (WACC).

The weighted average cost of capital (WACC) is a measure of how much money the plant has to pay banks and investors in order to provide them with their expected return on the assets. The returns are shared by debt providers (banks) and investors.

This expected return also reflects the risk associated with this type of business.

The WACC is impacted by level of maturity of technology, predictability of the energy yield, fuel supply risk and also policy risk. The expectation of rising carbon prices could increase the cost of capital for coal-fired power plants in future.

II.9.3. The net present value (NPV).

If the investment in the power plant is to be profitable, enough revenue must be generated during the operation phase to pay for construction and decommissioning, as well as to cover the operational expenses. The most commonly used measure to determine how much value an investment accrues to an investor is the net present value (or NPV).

The net present value can be calculated using equation 2.27, based on the discounted sum of the cash flows over the life-time of the power plant. Only configurations with a positive net present value should be considered as viable investments, as a negative value indicates that construction and operation of the power plant would subtract value from the firm making the investment [50].

$$NPV = \sum_{n=0}^{N} \frac{C_n}{(1+d_{nom})^n} \dots\dots\dots\dots\dots\dots\dots\dots\dots\dots\dots\dots\dots\dots (2.27)$$

Where:

C_n: after tax cash flow discounted to year ($)

n :analysis period

t : total analysis period (year)

d_{nom}: nominal discount rate in ($)

The revenue that can be generated by selling electricity is strongly dependent on the price at which the electricity is sold. In a liberalized electricity market electricity prices can vary

significantly, both over the course of the day and throughout the year [51], due to shifting patterns of supply and demand.

The interest of the designer is the minimum electricity sale price which, over the lifetime of the power plant, generates enough revenue to pay back the initial loan, cover the operating costs and accumulate reserves to pay for decommissioning once operation has ceased; in other words, it is the electricity sale price which gives a net present value of zero.

This minimum electricity sale price is known as the levelized cost of electricity (or LCOE), and is possibly the most important indicator of the economic comparison between different competitive technologies.

III.1.Introduction

CSP plants convert solar radiation to heat before using the heat to generate electricity. This makes it possible to pair a CSP plant in a hybrid configuration with another plant that either generates or consumes large quantities of heat. Furthermore, the power cycle used in CSP systems is similar to that used by traditional power generation facilities, such as coal or natural gas plants. As a result it is possible to integrate the two types of plants in a solar–fossil hybrid system.

Although adding natural gas generation to a CSP system does not, amount to adding storage, hybrid solar–gas systems can provide backup power when the sun is not shining while also enabling more efficient plant utilization, thus lowering costs per kWh. The simplest form of hybrid design is illustrated in figure 3.1, which shows an additional backup boiler that can be fired by fossil fuel generally natural gas when steam is needed, that cannot be generated from the solar field.
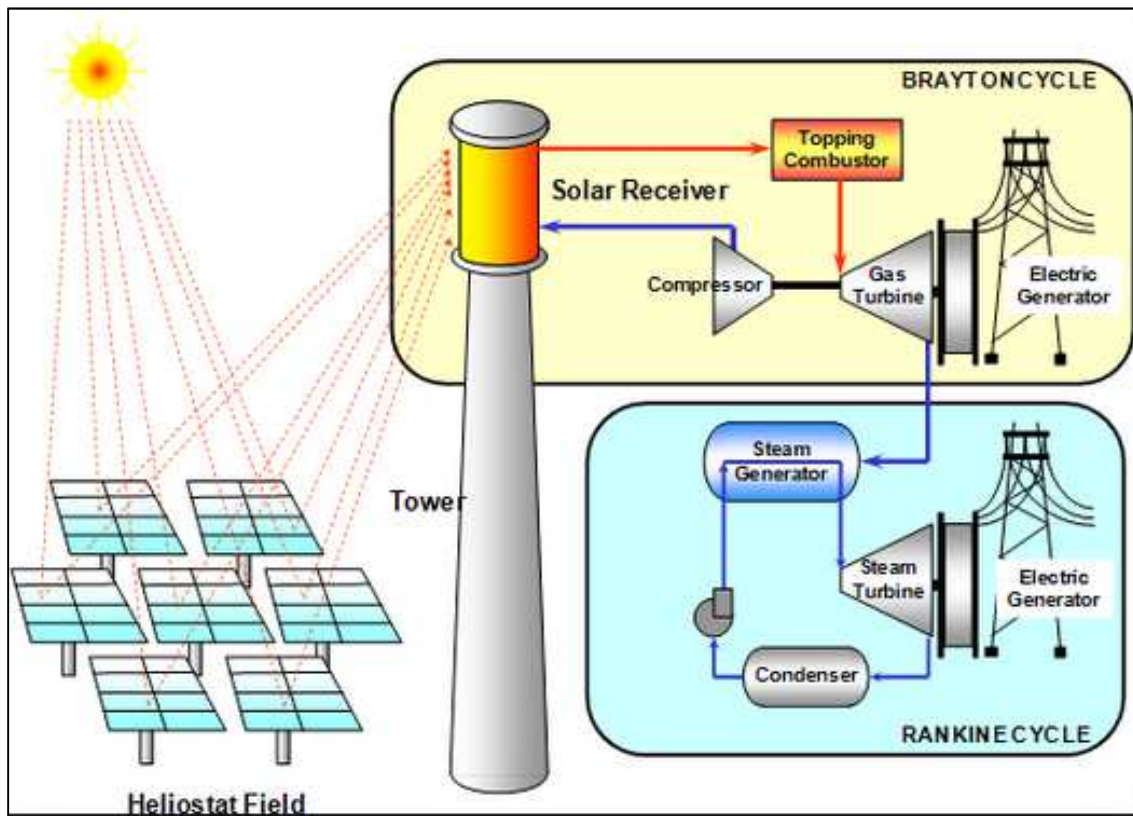
FIGURE 3.1:HYBRID CENTRAL RECEIVER BASIC CONCEPT [52].

The incremental costs for this approach, including the additional boiler and fuel, are relatively modest; such gas-fired backup systems have been used in eight of the nine SEGS plants currently in operation on a base-load fossil-fuel-fired power plant over the world [53].

In this configuration, power is produced from the gas turbine (fossil fuel only) as well as from the steam turbine, which uses steam generated from the lower temperature heat sources.

The boiler must be oversized relative to the fossil-only plant to accommodate the steam produced by the solar field.

The scale of the over sizing is determined by a techno-economic optimization since the use of a larger boiler leads to higher capital cost compared with a fossil-fuel-only plant. A specific form of this type of hybridization is the integrated solar combined cycle system (ISCCS), which combines solar with a natural gas combined cycle power plant. A process flow diagram for an ISCCS is shown in figure 3.2.

The other option for hybridization is to use the thermal energy from CSP plants as process heat for integrated applications.
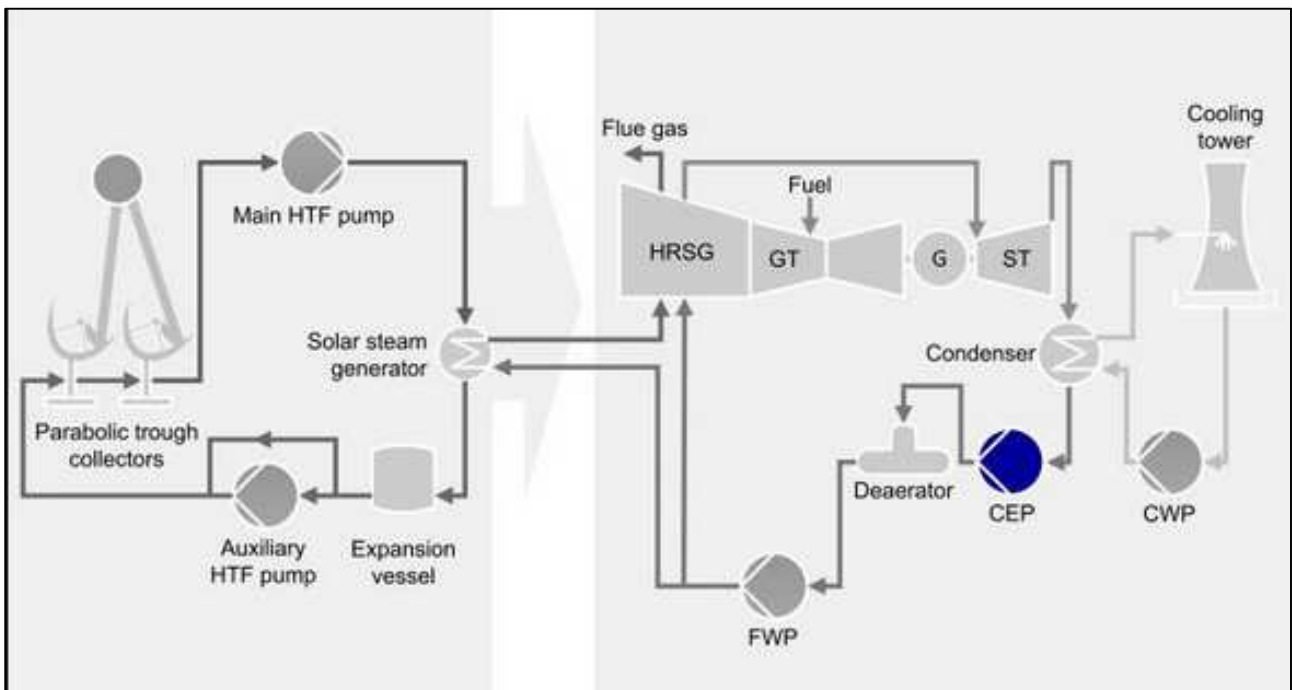
FIGURE 3.2: FLOW DIAGRAM OF AN ISCCS [54].

Hybridization of CSP plants with thermal desalination facilities is a good example of this approach. This hybridization scheme may be especially interesting given the good overlap between regions of the world with abundant direct solar irradiance and water stress.

In such hybridizations, the low-temperature heat from the turbine can be used for evaporating water in the desalination process. This also helps reduce the size of the condenser system (either wet or dry)

III.2.Fossil buck up methodology in CSP plant

The solar electricity generating systems (SEGS) plants built in California between 1984 and 1991 have used natural gas to boost production.

In the summer, SEGS operators use backup in the late afternoon and run the turbine alone after sunset, corresponding to the time period (up to 22:00) when mid-peak pricing applies.

During the winter mid-peak pricing time (12:00 to 18:00), SEGS uses natural gas to achieve rated capacity by supplementing low solar irradiance. By law, the plant is limited to using gas to produce 25% of primary energy.

CSP plants in Spain similarly used natural gas as a backup, limited to 12% or 15% of annual energy depending on the owner's choice of support system, until the support system was modified for all existing plants, and generation from natural gas stopped receiving any premium.

Solar-fossil hybridization can also consist in adding a small solar field to a fossil-fired thermal power plant, either a gas-fired combined cycle or a coal-fired plant. On integrated solar combined cycle (ISCC) plants, the solar field provides steam (preferably high-pressure steam) to the plant's steam cycle. Since the supplementary cost of the turbine (corresponding to its extra capacity) is only marginal, ISCCS plants provide cheap solar thermal electricity.

III.3.Thermal storage with fossil back up dispatch control under SAM advisor tool

The storage dispatch system control gives decision whether or not to operate the power block in each hour of the working day on based load regime, and how much energy is stored in the TES, how much energy is provided by the solar field, and the values of the thermal storage dispatch controls parameters.

You can define when the power block operates for each of the six dispatch periods under SAM advisor simulation tool. For each hour in the simulation, if the power block is not already operating, SAM looks at the amount of energy that is in thermal energy storage at the beginning of the hour and decides whether it should start the power block.

For each period, there are two targets for starting the power block: one for periods of sunshine (with solar), and one for period of no sunshine (without solar).

The turbine output fraction for each dispatch period determines at what load level the power block runs using energy from storage during that period.

The load level is a function of the turbine output fraction, design turbine thermal input, and the five turbine part load electric to thermal factors.

For each dispatch period during periods of sunshine, thermal storage is dispatched to meet the power block load level for that period only when the thermal power from the solar field is insufficient, and available storage is equal to or greater than the product of the storage dispatch fraction, (with solar) and maximum energy in storage.

Similarly, during periods of no sunshine when no thermal power is produced by the solar field, the power block will not run except when the energy available in storage is equal to or greater than the product of storage dispatch fraction (without solar) and maximum energy in storage.

By setting the thermal storage dispatch controls parameters, you can simulate the effect of a clear day, when the operator may need to start the plant earlier in the day to make sure that the storage is not filled to capacity and solar energy is dumped, or of a cloudy day when the operator may want to store energy for later use in a higher value period.

III.4.Minimum backup level

In the minimum backup level mode, whenever the fossil fuel fraction is greater than zero for any dispatch period, the system is considered to include a fossil burner that heats the HTF before it is delivered to the power cycle.

In this mode, the fossil fuel fraction defines the fossil backup as a function of the thermal energy from the solar field (and storage, if applicable) in a given hour and the power cycle design gross output.

For an hour with a fossil fuel fraction of 1.0, when solar energy delivered to the power cycle is less than that needed to run at the power cycle design gross output, the backup heater would supply enough energy to fill the missing heat, and the power cycle would operate at the design gross output. If, in that scenario, solar energy (from either the solar field or storage system) is driving the power cycle at full load, the fossil backup would not operate.

For a fossil fuel fraction of 0.75, the heater would only be fired when solar output drops below 75% of the power cycle's design gross output.

III.5.Hybrid concept integration to solar power plant

From a functional point of view, there are two basics approaches to hybridizing a solar power tower to a base-load fossil plant: fuel saver and power booster [55].

In a power booster mode, fuel input to the plant is constant and additional electricity is produced when the radiation heat source is available. This typical configuration needs oversizing the steam turbine in about 25% to 50% contained within the bottoming portion of the combined cycle base load power plant.

Over sizing the turbine leads to the degradation of the thermal to electric conversion efficiency. This configuration is not recommended in real market introduction.

In power saver alternative configuration, fuel input to the plant is reduced when solar is available and electricity output is constant. In a Rankine cycle application, the solar steam generator can be sized to provide the entire input to the steam turbine or a fractional amount.

However, when hybridizing with a base-load fossil plant, it is perhaps preferred to contribute a fractional amount of heat from solar.

This keeps the fossil boiler hot all the time and prevents daily startup losses and thermal cycles. In a combined-cycle application, solar heat is added by preheating the inlet air to the gas turbine via a salt-to-air heat exchanger.

In general, hybrid power towers were shown to be economically superior to solar only plants with the same field size. Furthermore, the **power-booster hybrid approach** was generally **preferred** over the fuel-saver hybrid approach. The hybrid cases that showed the most promising economic potential are a power boost to a coal plant and a power boost to a combined cycle plant. However, in order for the latter case to be attractive, the solar boost must offset the construction of a new gas-turbine plant.

An advantage of a fuel-saver over a power booster plant is that a given amount of solar energy can be added to the grid for less cost because additional steam turbine capacity does not have to be built. In addition, when performing the fuel saving at the entrance to the gas turbine within a combined cycle [47, 48], the solar energy is converted at a higher efficiency than when adding a power boost to a pure Rankine cycle
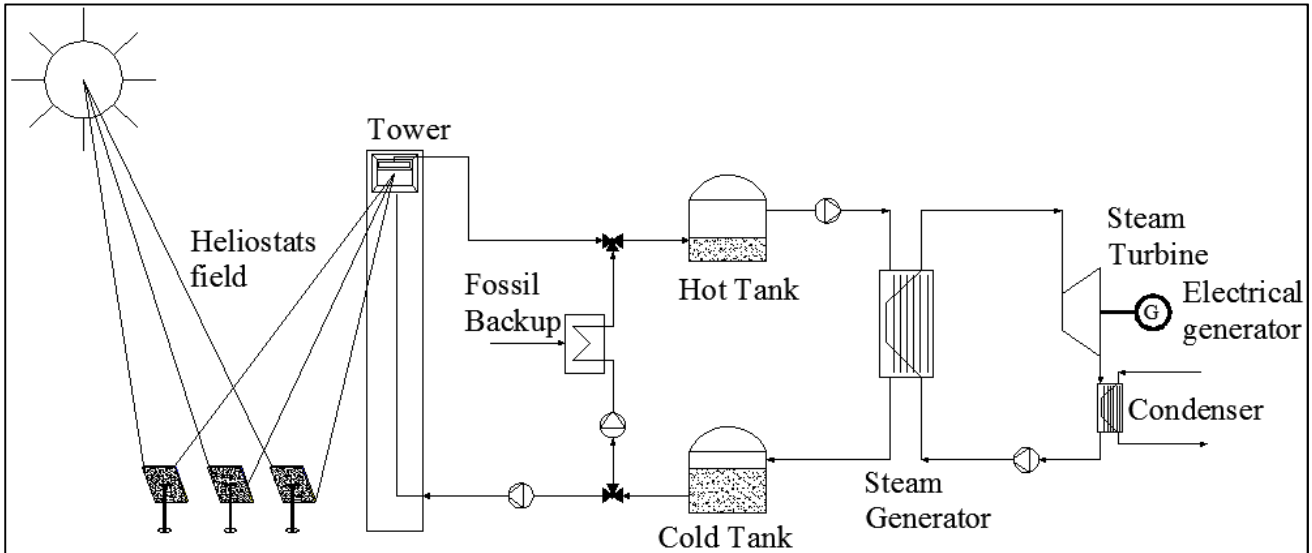
FIGURE 3.3: FOSSIL BACK UP INTEGRATION TO SOLAR POWER PLANT.

III.6. CO2 avoidance indicator evaluation

In the context of climate change, the most commonly used environmental indicator for a power plant is the specific carbon dioxide emissions f_{CO2} per unit of electrical output, typically given in kg_{CO2}/MWh_e. Lower specific emissions are indicative of a less carbon-intensive electricity production technology.

Specific carbon dioxide emissions can be calculated using equation 3.1, based on the fuel mass flow M_f in the combustion chamber and the carbon content C_c of the fuel [56].

$$f_{CO_2} = \frac{44}{12} \cdot \frac{\int_{year} \dot{M}_f c_C^f \, dt}{E_{net}^-}$$

………………………………………………………..…………….. (3.1)

When comparing different options for reducing carbon dioxide emissions from power production, an interesting performance indicator is the cost of avoided carbon emissions, typically given in in USD/tonneCO2, which measures the increase in electricity cost that is necessary to avoid a given amount of emissions.

The cost of avoided carbon emissions C_{co2} (can be calculated using equation 3.2, where Δ LCOE is the increase in levelized cost of electricity and Δf_{CO2} the reduction in specific carbon dioxide emissions, measured relative to a reference power plant [48,49].

$$c_{CO_2} = \frac{\Delta \text{LCOE}}{\Delta f_{CO_2}}$$

………………………………………………………………………….. (3.2)

Chapter IV. Heat Transfer and Fluid Flow In the Open Volumetric air Receiver Under Homogenous Irradiation

IV.1. Introduction

Solar tower technology is a promising way to generate large amounts of electricity from concentrated solar power in countries with high solar resources such as North Africa and the Middle East, India, Australia or parts of North and South America, countries known to belong to the so-called "sun-belt" of the Earth.

The world's first solar tower power plant based on the open-volumetric-receiver technology has been built in Jülich, North-Rhine-Westphalia, Germany and is in operation as demonstration and research plant since December 2008.

The plant, which has been built by Kraftanlagen München GmbH (KAM) is owned and operated by the German Aerospace Center (DLR). All partners, including the Solar-Institut Jülich (SIJ) of the Aachen University of Applied Sciences are doing research and development of this technology.

The most recent application of the HITREC Technology figure4.1 (a) is in the Solar Tower of Jülich, a power plant of 1.5 MW electrical power erected in West Germany.
It was launched in June 2009 and since then it has been delivering electrical power into the German electricity grid. It was erected by the company Kraftanlagen München with financial and scientific support of DLR. It is currently operated by Stadtwerke Jülich, the local utility.

It works according to the principle shown in figure 4.2. The total number of heliostats needed is more than 2000 and they comprise a mirror surface area of more than 20000 m².

The receiver consists of 1080 HITREC receiver elements figure4.1 (c) and covers a total area of 20 m². The main technical characteristics of the power plant are given in table 4.1.

<div align="center">(a)   (b)   (c)</div>
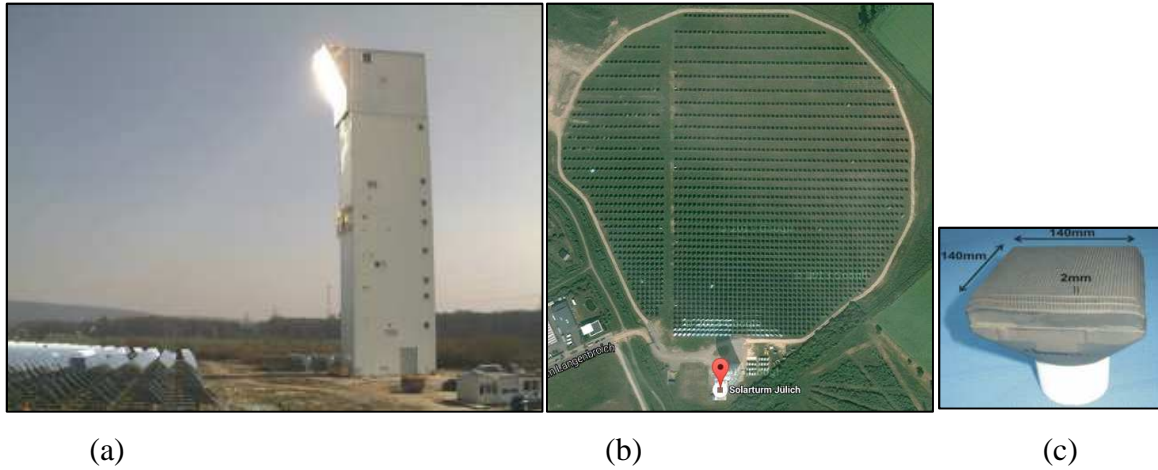
FIGURE 4.1: THE SOLAR TOWER IN JÜLICH IN OPERATION, (A) LATERAL VIEW OF THE TOWER WITH RECEIVER, (B) SATELLITE VIEW OF THE PLATFORM, (C) HITREC RECEIVER ELEMENT. [42]

TABLE 4.1: MAIN TECHNICAL CHARACTERISTICS OF THE SOLAR POWER PILOT PLANT [44]

	Value	Unit
Operational concept	GT-hybrid parallel	-
Heliostat field	25,000	m²
Tower height	60	m
Solid bed thermal energy storage capacity	20	MWh
Hot air Temperature	680	°C
GT exhaust gas temperature	515	°C
Gas turbine design power	4.6	MW
Steam turbine power	2.5	MW
Cooling concept	Dry air cooling	-

At the Solar Tower of Jülich, a field of sun-tracking mirrors, reflects and concentrates the direct solar irradiation onto the open volumetric air receiver. This receiver consists of porous ceramic absorber modules. Incident sun rays enter the porous receiver, are absorbed inside and heat it up. To remove the heat, ambient air is continuously sucked through the porous receiver and is heated up to almost 700°C.

The hot air is passed through a heat recovery steam generator (HRSG) in which it passes its heat to a water-steam cycle. The steam is expanded in a steam turbine and the rotation of the turbine's shaft drives a generator to produce electricity.

Using the air as heat transfer fluid (HTF) gives a high plant efficiency due to the fact that air can be heated to very high temperatures, which in turn enables higher steam temperatures in the Rankine cycle and thus a better thermal efficiency. Moreover, it allows afast start-up to operating conditions; it is not toxic and is available at no costs in unlimited amounts.

In order to increase the operational hours of a solar tower power plant, a heat storage system and/ or hybridization is considered.
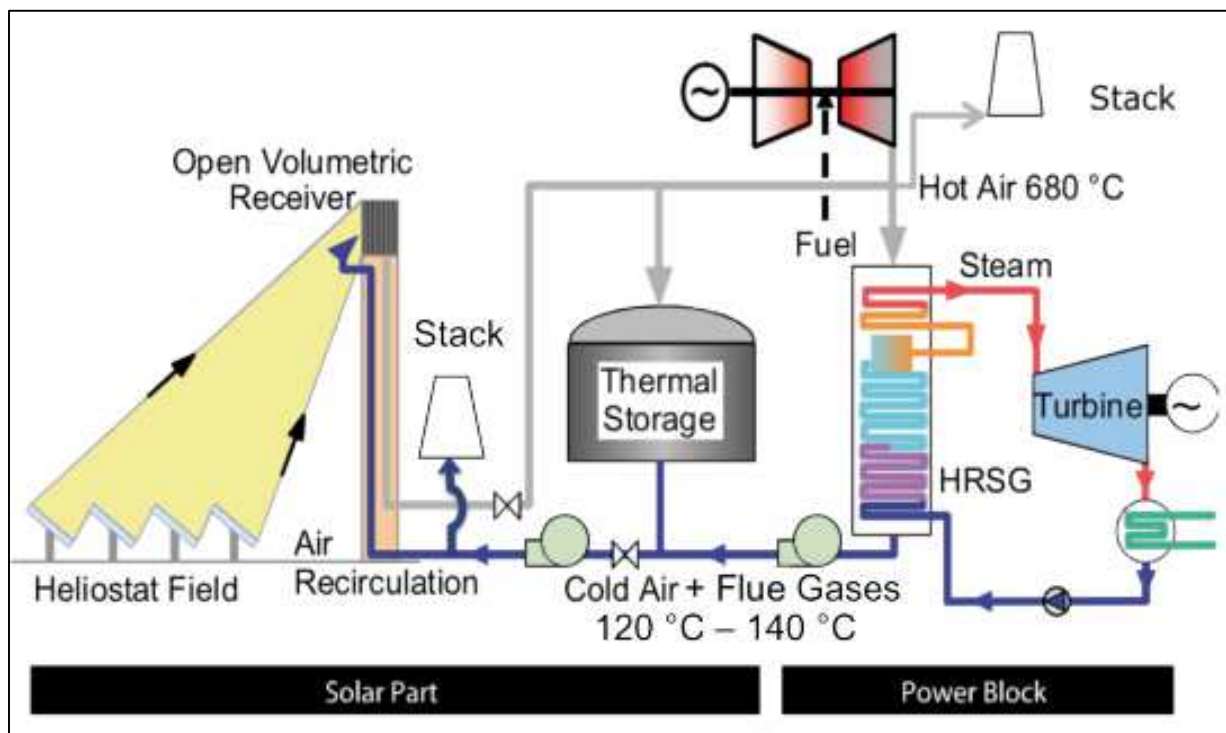
FIGURE 4.2: SCHEME OF THE HYBRID OPEN VOLUMETRIC AIR RECEIVER SOLAR TOWER [45]

The objective of the power tower project in Jülich is to demonstrate the entire system in commercial-like operation over a longer period of time, to develop control and plant management strategies and to further improve performance and reliability of the key components.

Jülich was chosen as the favored location because it is situated close to the involved research institutions and due to its fluctuating direct solar irradiation conditions. The latter reason has the advantage that it allows and requires the investigation into the system operation strategy under transient conditions, especially with regard to optimizing the charging and discharging process of the thermal storage.

IV.2. Fluid flow and heat transfer throw porous structure of the volumetric absorber.

Investigating fluid flow and heat transfer either by radiation, convection and conduction, within the porous structure in the open volumetric air receiver is extremely related to a relationship between solar flux and air flow rate value [41].

Higher flux densities must not lead to higher average outlet temperature, if the local mass flow is not adapted well to the local flow density or if the porosity and heat transfer is too low [40, 42, 44].

During the 1995 to 1996, experiments in the solar furnace at DLR cologne have been conducted to show the performance and flow stability of the Hitrec-I receiver, for high porous absorber materials, it show an unstable air flow through the absorber structure under a high solar flux which leads to the destruction of the structure due to overheating [40, 42, 43].

Hitrec-II (200 kW) project has started in later of 2000, the goal was to demonstrate the cooling of the stainless steel construction operated with the air return from the heat exchanger of the Sulzer test bed. Thermal efficiency was at 8% lower than the Hitrec-I receiver model due mainly to overheating of the side area of the absorber module [41, 43, 45].

The increase in outlet air temperature can be achieved at a given flux level by reducing the mass flow rate, which is in general linked to lower pressure loss over the porous media [40, 41, 46].

Instabilities of air flow through the porous structure depend on the pressure loss characteristics of the material. Previous studies have demonstrated that, when characterizing the flow in a particulate volume of the porous structure by a linear dependency of the pressure loss on the flow velocity (Darcy law) instabilities appears, with a pure quadratic dependency (Dupuit, Forchheimer) model these do not occur [40].

Chapter IV. Heat Transfer and Fluid Flow In the Open Volumetric air Receiver Under Homogenous Irradiation

Recently, an extruded honeycomb volumetric air receiver structure made out of silicon carbide material is investigated using tow numerical models, (single channel model) and (porous continuum). These approaches present a correspondence between experimental and numerical results such as average air outlet temperatures, the temperature distribution and the solar-to-thermal efficiency.

Both models confirm the capability of the two methods for further investigation [43]. In the present work, due to the symmetry of the single absorber module constituting the volumetric air receiver designed by DLR research group figure 4.4, a quarter geometry is used to model the physical phenomenon (concentrated radiation heat transfer applied to the absorber which transfer energy to the air flow) in order to compute the outlet air temperature, the solid body temperature, the relative pressure losses and the thermal efficiency of the receiver.
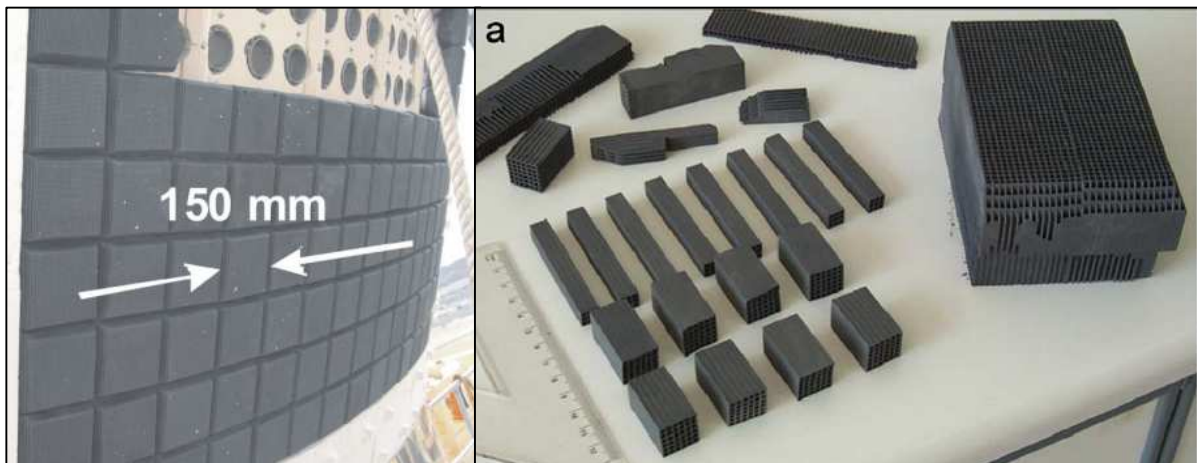
FIGURE 4.3: SOLAR AIR RECEIVER TEST POWER PLANT. EACH HITREC MODULE OF 150 MM ABSORBS 15-20 KW THERMAL RADIATION. [43]

These parameters then are compared to the experimental ones to establish the reliability of the physical model. The numerical calculations are performed using the present model which is the homogenous approach.

This considers the receiver as a solid porous continuum with effective permeability and volumetric air thermal conductivity of the absorber. Using the mathematical model describing the physical phenomenon undergoing in the volumetric air receiver, the fully coupled radiation, convection and conduction heat transfer model is applied to the silicon carbide porous structure.

Chapter IV. Heat Transfer and Fluid Flow In the Open Volumetric air Receiver Under Homogenous Irradiation

The laminar air flow, through the channels constituting the honeycomb receiver geometry is modeled by the weakly compressible 3 dimensional Navier-Stokes equations with variable density, and resolved using numerical finite element method.

The stationary segregated solver with adaptive mesh refinement strategy is implemented. For stabilization algorithm issue and convergence criteria, we have adopted the Petrov-Galerkin/Compensated streamline artificial diffusion parameter applied to the advection term in the Navier-Stokes energy equation.

The Brinkman equations modifying slightly the continuity and the momentum Navier-stokes equations are used to model the fluid flow and heat transfer in the porous structure using empirical value of the volumetric effective thermal conductivity, porosity, permeability, extinction coefficient and the emissivity of the receiver material.

As an assumption, constant thermal radiation flux condition is applied at the inlet boundary of the receiver, and the absorbed concentrated solar radiation was considered in this model as volumetric heat source.

FIGURE 4.4: 3D QUARTER GEOMETRY OF THE VOLUMETRIC AIR RECEIVER. [43]

IV.3. Numerical simulation of the heat transfer and fluid flow on the absorber

In the present work, Porous ceramic channel are used to achieve high performance in solar heat recovery systems. Understanding the convective heat transfer between the air flow

and the ceramic absorber channels is of great importance when optimizing the volumetric air receiver.

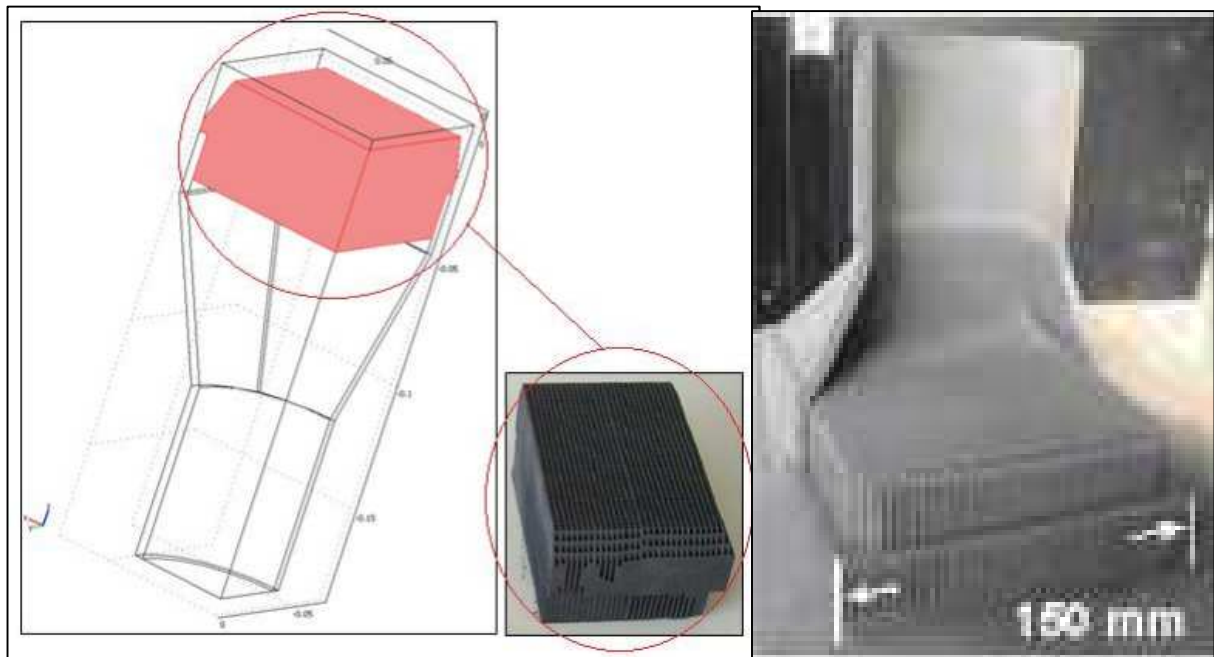In this work, the convective heat transfer coupled to air flow was numerically studied. The present approach was designed to compute the local convective heat transfer coefficient between the air flow and the porous structure. For that purpose, the energy balance and the flow inside the porous ceramic were solved. In addition, a detailed geometry of the porous ceramic structure was considered.

The numerical simulations were based on the three dimensional Reynolds-averaged Navier–Stokes (RANS) equations. Based on the numerical simulation results, a correlation for the volumetric local convective heat transfer coefficient between air and ceramic foams was developed. The resulting correlation covers a wide range of porosities, velocities, cell sizes and temperatures.

The correlation results were compared with experimental data from the literature.

IV.3.1.ComsolMultiphysics Software description

COMSOL Multiphysics is a general-purpose software platform, based on advanced numerical methods, for modeling and simulating physics-based problems. With Comsol, we can account for coupled phenomena.

With more than 30 add-on products to choose from, we can further expand the simulation platform with dedicated physics interfaces and tools for electrical, mechanical, fluid flow, and chemical applications. Additional interfacing products connect your Comsol simulations with technical computing, CAD software.

Comsol desktop is a powerful integrated environment designed for cross-disciplinary product development with a unified workflow, regardless of the application area.

The add-on modules blend in seamlessly with Comsol, and the way you operate the software remains the same no matter which add-on products are engaged.

The model tree in the model builder gives you a full overview of the model and access to all functionality – geometry, mesh, physics settings, boundary conditions, studies, solvers, post processing, and visualizations. With Comsol you can easily extend conventional models for one type of physics into multi-disciplinary models that solve coupled physics phenomena – simultaneously. What's more, accessing this power does not require in-depth knowledge of mathematics or numerical analysis.

It includes a set of core physics interfaces for common physics application areas such as structural analysis, laminar flow, pressure acoustics, transport of diluted species, electrostatics, electric currents, heat transfer, and Joule heating.

It assembles and solves models using state-of-the-art numerical analysis methods. Several different methods are used in the add-on modules, including finite element analysis, the finite volume method, the boundary element method, and particle tracing methods, but the emphasis of COMSOL Multiphysics is on the finite element method.

IV.3.2. Heat transfer by conduction in the absorber [43]

Heat transfer properties of the absorber materials are presented as the product of volumetric heat transfer coefficient k_p and specific surface αA_v.

$$-\nabla(k_p.\nabla T_2) = q_o \tag{4.1}$$

$$q_o = I_0 \epsilon \xi . \exp(-\xi.z).\cos a + \alpha A_v(T - T_2) \tag{4.2}$$

$$k = (1 - \epsilon) * 280.7 * \exp(-0.0021.T_2) \tag{4.3}$$

$$\alpha A_v = \frac{\overline{Nu}}{\delta}.A_v.k \tag{4.4}$$

Here, k_p, ϵ, I_0, T_2, T, α, ξ, q_o, z, αA_v, $A_v k$, δ, $\overline{Nu}$, denotes respectively as effective thermal conductivity of the porous structure [W/m.K], porosity [-], radiation flux [W/m²], temperature of the solid, temperature of the air, geometric angle, extinction coefficient [m^{-1}], the heat source [W/m²], coordinate in flow direction [m], volumetric heat transfer coefficient [W/m^3.K], specific surface [m²/m^3], thermal conductivity of the air [W/m.K], characteristic length of the porous structure [m] and the average Nusselt adimensionel number [-];

IV.3.3. Weakly compressible Navier –Stokes equations for the air flow

$$\nabla.\rho u = 0 \tag{4.5}$$

$$\rho.(u.\nabla)u = -\nabla p + \mu\left[\nabla^2 u + \frac{1}{3}\nabla(\nabla.u)\right] + \rho f \tag{4.6}$$

$$p = \rho\frac{R}{M}T \tag{4.7}$$

Where: f, R, M denotes the volume forces [N/m^3], ideal gas constant [J/mol.K], molar mass of the air [g/mole] respectively.

Within the porous media, the boundary conditions between the porous structure and the air are modeled using the Brinkman equation formulation:

$$\left(\frac{1}{\epsilon}\right).\mu.\nabla(\nabla u + (\nabla u)^T) = \frac{\mu}{K}u \qquad \dots\dots\dots\dots\dots\dots\dots\dots\dots\dots\dots\dots\dots\dots\dots\dots\dots\dots \text{(4.8)}$$

Here, ϵ, μ, K represents the porosity [-], dynamic viscosity [kg/m.s], and the permeability [m²] of the porous structure respectively.

IV.3.4. Heat transfer by conduction and convection of the air flow model

In the air region, the convection and conduction heat transfer is given by the relations:

$$\nabla(-k.\nabla T + \rho c_p u T) = q_o \qquad \dots\dots\dots\dots\dots\dots\dots\dots\dots\dots\dots\dots\dots\dots\dots\dots\dots \text{(4.9)}$$

$$q_o = \alpha A_v(T_2 - T) \qquad \dots\dots\dots\dots\dots\dots\dots\dots\dots\dots\dots\dots\dots\dots\dots\dots\dots\dots \text{(4.10)}$$

IV.3.5. Boundary conditions specifications

IV.3.5.1.Inlet conditions

Velocity : $u = u_0$ $\dots\dots\dots\dots\dots\dots\dots\dots\dots\dots\dots\dots\dots\dots\dots\dots\dots\dots\dots$ (4.11)

Temperature : T=T_0 $\dots\dots\dots\dots\dots\dots\dots\dots\dots\dots\dots\dots\dots\dots\dots\dots\dots\dots\dots$ (4.12)

IV.3.5.1. Heat flow radiation [43]:

$$k.\nabla T_2 = q_0 + C.(T_{amb}^4 - T_2^4) \qquad \dots\dots\dots\dots\dots\dots\dots\dots\dots\dots\dots\dots\dots\dots\dots \text{(4.13)}$$

$$q_0 = I_0 cos\varphi(1 - \epsilon) - (1 - \epsilon).F.(T_2 - T_0) \dots\dots\dots\dots\dots\dots\dots\dots\dots\dots\dots \text{(4.14)}$$

$$C = \varepsilon_m 5.67 e^{-8} \qquad \dots\dots\dots\dots\dots\dots\dots\dots\dots\dots\dots\dots\dots\dots\dots\dots\dots\dots \text{(4.15)}$$

Here C, ε_m, F denotes respectively the emissive constant [W/m².K⁴], emissivity of the porous material [-] and the convection heat transfer coefficient [W/m.K], which describe the convective heat losses at the front of the receiver.

IV.3.5.1. Outlet conditions

Pressure without viscous stress: $p = p_0$ $\dots\dots\dots\dots\dots\dots\dots\dots\dots\dots\dots\dots\dots$ (4.16)

Convection flow: $n.(-k.\nabla T) = 0$ $\dots\dots\dots\dots\dots\dots\dots\dots\dots\dots\dots\dots\dots\dots$ (4.17)

Temperature: $T_2 = T$ $\dots\dots\dots\dots\dots\dots\dots\dots\dots\dots\dots\dots\dots\dots\dots\dots\dots\dots$ (4.18)

Chapter V. Technical and Economic Pre-feasibility Study

To correctly predict the technical and economic performance of a system CSP, it is essential to have appropriate methodology analysis. A good estimate of performance reduces industrial risk and optimizes the design and pipe installation.

In addition to environmental and other benefits, renewables have a long-term economic advantage over non-renewable energy carriers.
Embracing the benefits and deploying renewables requires the adoption of appropriate policies at the national level.

Algeria is very rich in solar energy resources. It possesses large unpopulated and unproductive land in the Sahara which represents 80% of the total country area. This makes the country an ideal place for the implementation of the concentrating Solar Thermal Power Plant technologies (STPP). Algeria has expressed a high interest in developing its solar energy resources. To this end, it has introduced a program where solar thermal energy plays a central role.

In order to study the viability of the molten salt central receiver power plant under Algerian climate, we present here a techno economic assessment under different weather conditions.

V.1. Economic and Environmental aspects for the deployment of CSP technology in Algeria

The estimate of the plant investment costs is required to identify the main cost drivers and thus the potential improvements to bring them down. By breaking down the plant equipment into distinct cost categories, a detailed parameter of prefeasibility study is given in this chapter, whose share is expected to be the highest.

However, in the present analysis, the costs involved by the planning, the construction and the operation of a solar tower thermal plant are investigated in order to estimate its economic performance.

First, the investment costs are broken down into distinct categories of equipment, with an emphasis on the level of detail for the heliostat field, and an expression of the corresponding expenses is presented.

Based on the reference cases from the literature, the cost breakdown and the investment costs of the Gemasolar power plant are estimated as an example. Second, specific financial

indicators are proposed to set up the project funding, and assess its financial viability and the cumulated incomes over the entire plant lifetime.

V.1.1. Site selection

For a solar central receiver power plant, the primary criteria used for site selection include insolation, land, meteorological conditions, water, transportation, transmission lines, and aircraft interference.

However, key plant characteristics must first be defined; among the more important plant specifications are its rated electrical output, type of service, configuration and energy storage strategy.

V.1.2. Land availability

CSP plants need a high land area compared to conventional power plants. The specific surface area for a solar tower power plant is about 0.02 km² to 0.025 km² per MW_{The} slightly high comparing to parabolic trough power plant which is in the range of about 0.015 to 0.02 km² per MW_{The}. The availability of land to build large CSP collector fields is therefore an important site criterion.

In the case of Algeria, we have more wasted land at the south which is very suitable to CSP plant implementation as subsidy, poorly dense in population and low agriculture usage but less economic activities which is not compatible with other criteria like existence of roads and electrical network in the north side, the main strain is the land ownership with a dense population and agriculture activities.

V.1.3. Water availability

Water requirements for the solar thermal power station would be similar to a conventional thermal power station of similar output plus additional water that would be used for solar reflector cleaning. For a wet cooled system the total water consumption would be around 276 ML/a, while if dry cooling was introduced this could fall to around 36 ML/a.[06].

In one hand, There is a dense hydraulic network linked to several big dam in the north of Algeria, and in another hand, in the region of highland and south of Algeria, a great water table exist which is important to feed-in water all economical investment such as new power plants far from urban cities.

V.1.4. Naturel hazard potential

Natural risks comprise phenomena like earthquakes, storms, and others. These risks can affect the operating safety of a CSP plant. In order to resist the impacts of these phenomena, the design of the solar field and of the power block must be adapted, which may imply higher construction costs. Additionally, insurance costs may rise at sites with higher damage risks.

V.1.5. Infrastructure convenience

CSP plants need certain infrastructure for their operation. Existing infrastructure is, hence, an important site criterion. Missing infrastructure requires higher investment. A power plant needs access to roads or other transportation ways (navigable waterways), to high or medium voltage power grids and to water resources if wet cooling is planned. Additionally, pipelines may be favorable for water transport or fuel transport for hybrid plant operation.

In the context of our country, the government has invested a big highway all over the territory such as the named est-ouest and another in project phase which link the north regions to the south ones.

V.1.6. Political and economic frameworks

Political and economic conditions in a country represent important site criteria. Promotion measures for renewable energies are especially decisive. There are different promotion strategies. The most important strategies are special feed-in tariffs or premiums for electricity generated on the basis of renewable energy sources, quotas for the renewable energy share and tax incentives.

The politically controlled promotion of CSP is still necessary because of the currently higher levelized electricity cost of CSP plants in comparison to fossil fired power plants and some other competitors.

Political promotion has the aim to make CSP plants economically competitive until they get competitive on their own.

Incentive premiums for CSP projects are granted within the framework of Algeria's new Decree 04-92 of March 25th, 2004 relating to the costs of diversification of the electricity production. The incentive premiums of this decree shall attract private investors to implement integrated solar combined cycle plants in Algeria.

According to the current power expansion planning of the Ministry for Energy and Mines, the capacity targets for CSP power implementation in Algeria are 500 MW of new ISCCS plants until 2020. With these CSP targets and the new Decree 04-92, Algeria has established the necessary GMI commitment on national solar thermal power market implementation. As the next GMI step to be agreed at the Renewables 2004 Conference in Bonn, the Government of Algeria pledges to develop a framework for solar thermal electricity export from North-Africa to the European Union.

V.2. Pre-feasibility study for CSP project installation

V.2.1. Management schedules

The main objective should be to obtain a first approach on the profitability of predefined alternatives.

To this end, we present in this section the following methodology:

- Define and estimate the different investment costs;
- The different Changes in fees and revenue in the period of construction.

The criteria that will be used to compare different management alternatives will be, without limitation, profitability, risk distribution between the public and private agents, the cost of funding for participating agents and financial needs.

V.2.2. Schema and financial profitability analysis

Based on the results obtained in previous studies, it will realize an economic and financial feasibility study of the planned actions, from the prediction of loads and predictable revenue and investment needs, as well those from private initiative and public authority.

For all this, it will be useful to study the following items:

- Investment Plan: In this point, we analyses the investment plan that reaffirms the actions proposed, with their corresponding budget, distinguishing between public and private investment and between infrastructure and empowerment, equipment and facilities.
- Operation costs: This will be essentially those related to personnel, gas, water, depreciation, amortization to the immobilized body expenses, etc.
- Maintenance costs: these refers to costs of the works which will be counted as annual percentages of their original cost, that is to say, as regular maintenance costs.

- Estimation of water and electricity revenues: Financial estimates will be for a sale price that ensures an IRR of 6% for funding and 8% for financing by the bank. Also include a study to evaluate the different formulas prices for water and electricity.

- Assessment of other financial resources: A basic aspect of this study should be the analysis of possible alternative sources of financing for the construction of structures. We will have to investigate possible financial resources, debt, etc.

- Analysis of the financial profitability.

V.2.3.Financial profitability analysis

In the financial evaluation, a comparison of the monetary differential input and output flows (cash flow) is carried out. As the indicators of profitability, we consider the following parameters:

- Net present value (NPV), based indicator among others that incorporates in its calculation the concept of the time value of resources. It's the most important disadvantage is the implicit subjectivity in the election "a priori" discount rate or discount, the value of which significantly affects the result (although the brand theory as the cost of appropriate value appropriateness of resources, in practice this is not a simple question, at least in the economic evaluation);

- Internal Rate of Return (IRR), defined as the discount rate that makes NPV equal to zero, of great simplicity and solidity, but presupposes that the generated funds flow throughout the investment and are immediately reinvested that in certain circumstances, it can offer more than one value, which must be appropriately interpreted.

- Profit over cost ratio (PCR). It establishes the relationship between the overall costs and benefits generated by actions throughout the time period.

- Payback period (PR), defined as the time required to recover the amount of the initial investment, widely used in the financial analysis, due to its conceptual and practical simplicity.

However, the greatest difficulty lies not in the calculation of the project profitability for assumptions determined, but in the establishment of consistent assumptions and estimates their impact on the indicators (NPV, IRR, etc.).

This is why a substantial part of the analysis should aim to achieve this aspect, by linking the sensitivity calculation that would detect the most critical elements for the assessment and its respective individual impact on results.

V.3. Cost reductions and potential drivers

In many countries, research and industry are committed to improve CSP performance and reduce its costs. Important drivers for cost reduction include:

- Technology advances of components and systems;
- Increased plant size and economies of scale;
- Industrial learning in component production;
- Lithium-based molten salts with high operation temperatures and lower freezing points;
- Concrete or refractory materials at 400–500ºC with modular storage capacity and low cost;
- Phase-change systems based on Na- or K-nitrates to be used in combination with DSG;

  Cheaper storage tanks (e.g. single thermocline tanks), with reduced (30%) volume and cost in comparison with the current two-tank systems.

An increased plant size reduces the costs associated with conventional components and systems, such as power block and balance of plant rather than the cost of the solar field, which depends primarily on industrial learning and large-scale production of components.

The learning rate for CSP systems and components is highly uncertain given the early stage of deployment of CSP technology. Estimates of 8-10% based on other technologies (IEA 2010b; Trieb, 2009) are considered conservatively realistic.

V.4. Principal barriers for CSP deployment

Despite the environmental, social, health and economic (in some applications) benefits of utilizing renewable energy technologies, their utilization in high insolated countries is nearly negligible until now.

They are facing many barriers and constrains to their large deployment in this region. These include financial, economic, institutional, political, technical and information barriers.

V.4.1. Technical barriers

The considerable international investment made in renewable energy R&D during the previous three decades has demonstrated the potential and technical availability of some of these technologies.

Even though renewable energy technologies are technically proven, additional development is still required to become fully mature. Among the barriers in this field are:

- In case of central receiver systems the promising technologies such as the molten salt-in-tube receiver technology with energy storage system needs more experience to be put for large-scale application;

- Lack of technical standard and inappropriate technical designs. This gives renewable energy
technologies a bad reputation, impeding their future dissemination;

- Some of renewable energy technologies and component (e.g. solar thermal power plant and large scale thermal storage) are not yet commercially tested. This increases the investment cost and financial risk for plant operators;

- Lack of qualified personnel. Problems in technical implementation, maintenance and financial
arrangements hinder renewable energy technology market development in general;

- Insufficient resources for data collections and information transfer. This may lead to no, or wrong decisions by project developers, investors etc. -Inadequate and insufficient education of consumers and renewable energy systems user. This brings technological mistrust in case of system breakdown.

V.4.2. Economic barriers

The most important issue is the economic performance of renewable energy technologies compared to the energy sources that presently dominate the energy market. The barriers in this area include:

- High upfront cost coupled with lengthy payback periods and small revenue streams raises creditworthiness risks;

- Financing is a critical barrier. Financial institutions consider solar energy technologies to have unusually high risks while assessing their creditworthiness;

- High specific cost of renewable energy technologies versus subsidized low fuel prices and electricity tariffs. This will cause a lack of willingness and/or ability to finance expensive investments in renewable energy technology because of high risk premiums;

- Taxes and customs on imported equipment. This will lead to increase the initial cost of renewable energy equipment;

- High transaction costs due to the small-scale and decentralized nature of some renewable energy technology applications. This will discourage the implementation of renewable energy projects;

V.4.3. Institutional and regulatory barriers

Most of countries which have highly insolated areas are lack of an adapted and stable institutional and regulatory frame work for renewable energy utilization.

These include: -Conflicting objectives and interests among policy-makers. This will shift power to fossil fuel lobbyists, hinder objective policy formulation, and lack of policy coherence.

- The limited capability to train adequate number of technicians to effectively work in a new solar energy infrastructure;
- Limited understanding among key national and local institutions of basic system and finance;
- Barriers limiting entry of distributed technology platforms into the grid, including potential for access restrictions by conventional utilities;
- Institutions for renewable energy technology promotion are relatively powerless compared to institutions of fossil fuels. This will lead to government concentration on fossil energy;
- Unclear Ministerial responsibilities and insufficient coordination between government agencies responsible for renewable energy technology. This will lead to weak promotion of renewable energy technologies;

- Monopolistic energy market. This will lead to no guaranteed grid access and no fair feed-in tariffs for independent renewable energy power producers which lead to keep renewable energy technologies out of the market and competitiveness;
- Lack of awareness of potentials and benefits of renewable energy technology utilization among decision makers at different political and administrative level.

V.5. Potential policy instruments to increase solar energy development

In spite of the high potential of renewable energy resources availability (solar, wind, biomass and hydro) in highly insolated region, small portions of these resources are exploited at present. This is due to many barriers and constrains which affect the renewable energy utilizing processes.

To remove the barriers toward the utilization of renewable energy resources, the following are several suggestions and practical measures which can help in the adaption of renewable energy technologies in these countries.

V.5.1. Feed-in-tariff

It refers to a premium payment to new and renewable energy technologies which are relatively expensive or thus not competitive with conventional technologies for electricity generation.

The tariff is based on the cost of electricity produced, including a reasonable return on investment for the producer. It thus reduces the risk to potential investors for long-term investments in new and innovative technologies.

In the context of the diversification of source to electricity production, and aware of the increasing interest in renewable energies and their stakes, Algeria has integrated their development into its energy policy by adopting a legal framework favorable to their promotion and to the development of the concerned infrastructures.

Incentives measures and encouragement are mentioned in the law relative to the energy control (financial, fiscal advantages and customs duties) for the actions and the projects which contribute to the energy efficiency improvement and to the renewable energies promotion.

A National fund for energy efficiency (NFEE) was also established to finance these projects and grant loans unpaid and guarantees for the loans made with banks and financial institutions, for the energy efficiency investments.

The objective of these measures is to encourage the local products and to provide good conditions especially in fiscal terms, to the investors willing to get involved indifferent sectors of renewable energies.

V.5.2. Tax incentives

Tax incentives help individuals and corporations justify purchasing, installation and manufacturing
renewables energy technologies. Because renewables have high initial capital and installation costs, tax policies compensate investors with tax credits, deductions and all allowances.

The tax incentives could include income, property and sales tax incentives. The policy should remain until the new technologies have increased their economy of scale and are cost competitive with alternatives in the sector.

Once cost for renewable technologies decline, the tax credit level should decline. Additional examples of tax incentive are:

- Production Tax Credit: production tax credit is a policy driver to promote the development of electricity generated from renewable sources. A production tax credit provide the generator or owner of the renewable energy facility an annual tax credit based on the amount of energy that particular facility produced. The credit is ideally set at a level that makes it more cost effective to produce electricity from renewable resources than from fossil fuel;
- Emission (Carbon) Tax Credit: emission taxes can internationalize the costs caused by emissions into the price of energy. Essentially they make polluters pay for the damage (in the health, safety, security and environment) caused to society from their polluting activities. Carbon taxes have the same effect changing a tax on the quantity of carbon
- in the energy recourse. Renewables are cleaner because they are not carbon based. So the effect is that producers have the intensive of switch to renewable energy resources.

V.5.3.The clean development mechanism

The clean development mechanism (CDM) is a flexibility mechanism established under the Kyoto Protocol. It allows governments or private entities in industrialized countries to implement emission reduction projects in developing countries and receive credit in the form of certified emission reductions.

The purpose of the CDM shall be to assist developing countries in achieving sustainable development and to assist developed countries to achieve compliance with their quantified emission limitation and reduction commitments.

V.5.4. Research and development

R&D is critical for maintaining the pipeline of innovative energy supply and end-use technologies. Industrial countries governments funded R&D has helped to advance a number of energy efficiency and renewable technologies during the past twenty years (examples are: wind turbine innovators, electronic lighting ballasts, high efficiency appliances, new window technologies …. etc).

Including renewable energy subjects in the university curricula, supporting R&D activities in the universities and research centers and encouraging the collaboration among renewable energy organizations and research centers in MENA region and between these centers and international centers could have a wide range of benefits.

These include cost and risk sharing, faster learning, increase access to global market, and better prospects for rapid deployment of innovative technologies.

V.5.5. Codes and standards

Maximum greenhouse gases emission rules and minimum equipment efficiency standards are of a great help to energy sustainability. The minimum equipment efficiency standard could be set by either the remove of the least efficient products from the market place, leaving consumers to choose from an array of more efficient products with other desired options and features, or require that all new products meet a certain efficiency level on average.

These standards have been successfully adopted in a number of countries for mass produced goods such as domestic appliances, air-conditioning equipment, motors, and lighting products. This should also include renewable energy equipment.

V.5.6. Regulatory and legislative framework

To promote the renewable energy deployment, national policies, strategies and laws should be adopted. These includes: issuing laws and regulations for inclusion of renewable energy technologies in energy budget, demand side management law, allocate budget for institutions working in the field and encouraging R&D in various renewable energy technologies.

V.5.7. Technology transfer

Renewable energy technology and information transfer was recognized as a barrier to the market penetration of renewable energy technologies and products. The governmental and private sectors in MENA countries should continue efforts to eliminate the information transfer barrier by corporation with industrial world especially Germany and other European countries in organizing educational programs, printing product literature and other initiatives.

Chapter V. Results, Discussions and Conclusions

In the present study, we have carried out simulations using SAM advisor software. It deals with two scenarios, Solar only mode and hybrid with fossil fuel back up mode. Using radiometric and economic variables, thermal performance and economic evaluation of each configuration of solar power tower plant have been derived.

VI.1.Simulation data

TABLE 6.1: SIMULATION DATA FOR SOLAR ONLY MODE. SCENARIO1.

Parameter	Design parameter	Value
Location and resources		
	DNI [kWh/m².year]	1907.30
	Latitude [°]	35.55
	Longitude [°]	6.18
Heliostat field		
	Annual average wind speed [m/s]	4.50
	heliostat mirror area [m²]	120
	Number of heliostats	1298
	Total land area [ha]	280
Tower and receiver		
	Heliostat stow deploy angle [°]	8
	Maximum distance from tower [m]	905
	Cavity aperture high [m]	13.00
	Tube outer diameter [mm]	60
	Tube wall thickness [mm]	1.25
	Tower height [m]	120
	Maximum receiver flux [kW_t/m²]	1000
	Receiver design thermal power [MW_t]	91.76
Heat transfer fluid		
	HTF type (60% NANO3 , 40% KNO3)	Molten salt
	Material tube type (Stainless steel)	AISI 316
	HTF outlet temperature [°C]	565
	Minimum required temperature [°C]	290
Power block		
	Design turbine output (Nameplate) [MW_e]	20
	Thermodynamic cycle efficiency [%]	31.8
	Boiler operating pressure [bar]	27

	Maximum flow rate to receiver [kg/s]	656
	Condenser type cooling medium	Air
Thermal storage dispatch control		
	Storage type	Two tank
	Full load hours of storage [h]	[0-12h]
	Fossil fuel fraction	[0-1]
Tower system costs*		
	Specific investment cost for solar field [$/m²]	300
	Specific investment cost for land improvement [$/m²]	130
	Specific investment cost for power block [$/kW$_e$]	550
	Specific investment cost for balance of plant [$/kW$_e$]	
	Specific investment cost for tower with receiver [$/m²]	420
		754.3
	Specific investment cost for storage [$/kWh$_{th}$]	30
	Construction ,engineering and contingencies [%]	20
	O&M costs by capacity and by year [$/kW.year]	65
	Annual inflation rate [%]	2.5
	Annual nominal discount rate [%]	10.9
	Life time analysis [year]	30

* Reference [12].

TABLE 6.2: SIMULATION DATA FOR HYBRID MODE. SCENARIO 2.

Design parameter		Value
Direct normal irradiation	(Tamanrasset) [kWh/m²]	2759,4
	(Batna) [kWh/m²]	1907.3
	(Algiers) [kWh/m²]	1446,4
Nominal design output	[MW]	20
Thermal energy storage	[h]	8
Solar multiple		1.5
Fossil backup cost reference	[$/kW$_e$]	25
Fossil fuel fraction value	[%]	0-1

VI.2. Model validation

As suggested by SAM designers, a 1.05 turbine output fraction during the highest irradiation conditions is considered in (summer time and daytime) corresponding to period 1. This allows the plant to produce a power output higher than the design specifications in these periods.

From April to September (period 2), the FFF has been set to zero during the central hours of the day (from noon to 4 pm), supposing that a hybridization is not needed during this period.

At night and from october to march (period 3), FFF has been set to 0.85 in order to guarantee a correct turbine operation [36].

The power block cannot operate properly when it is operated in partial load lower than 25% of the design point parameters.

Taking into account these operating conditions; and using the parameters given in table 6.1 and table 6.2, the net annual power electrical output of 18.15 GWh for solar only mode and 44.40 GWh for hybrid mode have been obtained. These results agree well with the experiments at PS20 cavity type receiver datasheet. Note that the hybrid mode of the PS20

could provide about 48 GWh[37]. As shown in table 5.3, this confirms the accuracy of the present model.

TABLE 6.3: MODEL VALIDATION PARAMETER

Type of parameter	Planta Solar 20 (PS20) [37]	Simulated case. Scenario 1	Simulated case. Scenario 2
Annual DNI [kWh/m²]	1944	1907.30	1907.30
Hybridization [%]	15	0	15
Net energy production [GWh/year]	48	18.15	44.40
Net energy production difference [%]		7.5 (scenario 2 and PS20)	
Annual capacity factor [%]	27	10.6	26

VI.3. Radiation measurements

Solar power systems need reliable local radiation data for the project site. There are different possibilities to get such data. Radiation can be measured by ground measuring or by satellite measuring. The direct normal irradiance (DNI) is defined as the radiant flux density in the solar spectrum (0.3–3 lm) incident at the earth's surface perpendicular to the direction to the sun integrated over a small contracting the sun.

The need for more precise DNI-data values will increase strongly as solar-thermal electrical power generation stands on the threshold of economic profitability.

For all concentrating solar technologies knowledge of DNI at ground for each potential site is one of the most important parameters, because it strongly affects the performance of such systems.

The areas of interest for solar-thermal power stations are located in the so-called Sun Belt countries between latitudes around 10–40 (North and South), where only few measurements of DNI are available today.

Chapter V. Results, Discussions and Conclusions

Several hundreds of ground stations would be necessary to map the spatial variability of the solar irradiance for a larger region. This is practically impossible, because ground measurements suffer from high costs for purchasing of equipment, adequate maintenance and time-consuming data screening ground and satellite measurements have different functional characteristics. Ground measurements are local satellite measurements which cover large regions and allow the comparison of many possible sites.

In the present study, the annual weather database, known asthe test reference year (TRY) ortypical meteorological year(TMY), is used. It consists of monthly measured values that are statistically selected from individual yearly measured values over a long period, and averaged to obtain a typical year for the givenlocation. In the present work, the measured values obtained from1986 to 1999 have been used to determine the typical year [08, 13]. Figure 6.1 shows the obtained average DNI values over this fourteen year period for three different sites in Algeria.
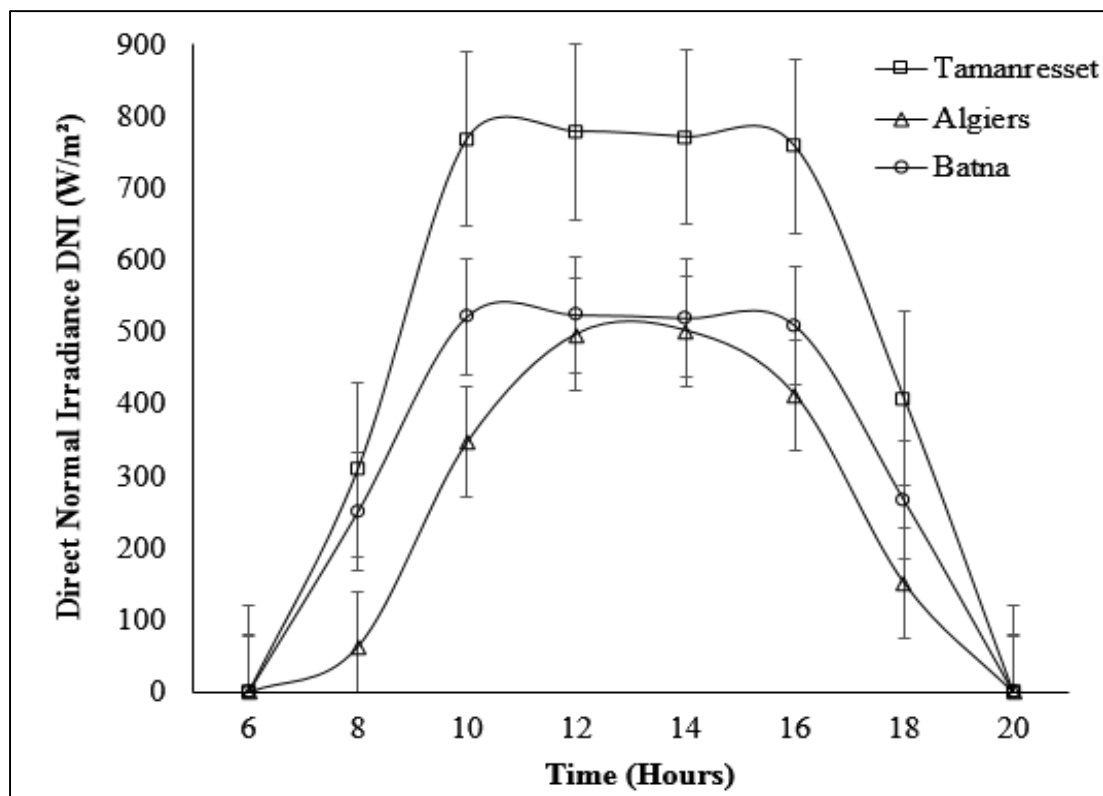

FIGURE 6.1: DIRECT NORMAL RADIATION DATA ILLUSTRATION FOR THREE SITES IN ALGERIA.

VI.4.Site selection

Defining the mission of solar thermal power plant is a critical prerequisite to establishing the key characteristics of the plant. Many of these key characteristics have a significant impact on site selection.

The first criteria for designing and selection of the type of solar power plant for a dedicated site are his rated electrical output for utility scale setting.

For actual plant rated electrical output, the size range for solar thermal power plant is between 10 to 100MW.

It may be useful and cost effective to use modular approach to solar plant construction; this allows the generating capacity of the plant to increase over the time similar to the growth in energy demand.

The choice of the type of plant depends not only on the rated electrical capacity, but also of the type of the services which will be provided to costumers.

However, the utility plant might be used as peaking, intermediate or base load unit, and the time on the day during which the plant energy is dispatched

The three categories of unit loading relate to the plant's capacity factor. The typically peaking services have a capacity factor around 0.15, while for intermediate unit plants is nominally in the range of 0.20 to 0.40. For base load units typically have a capacity factor between 0.60 to 0.70.

In the designing of solar power plant for specific sites, appropriate thermal energy storage and solar multiple are important in the determining the total land area required.

As a case study, the instantaneous effect of direct normal irradiation on the capacity factor for Tamanraset site is shown in figure 6.2. The main conclusion depicted on this simulation is that the central receiver power plant doesn't begin working (steam production and electricity generation on the turbine) for lower value of DNI than 825 W/m².
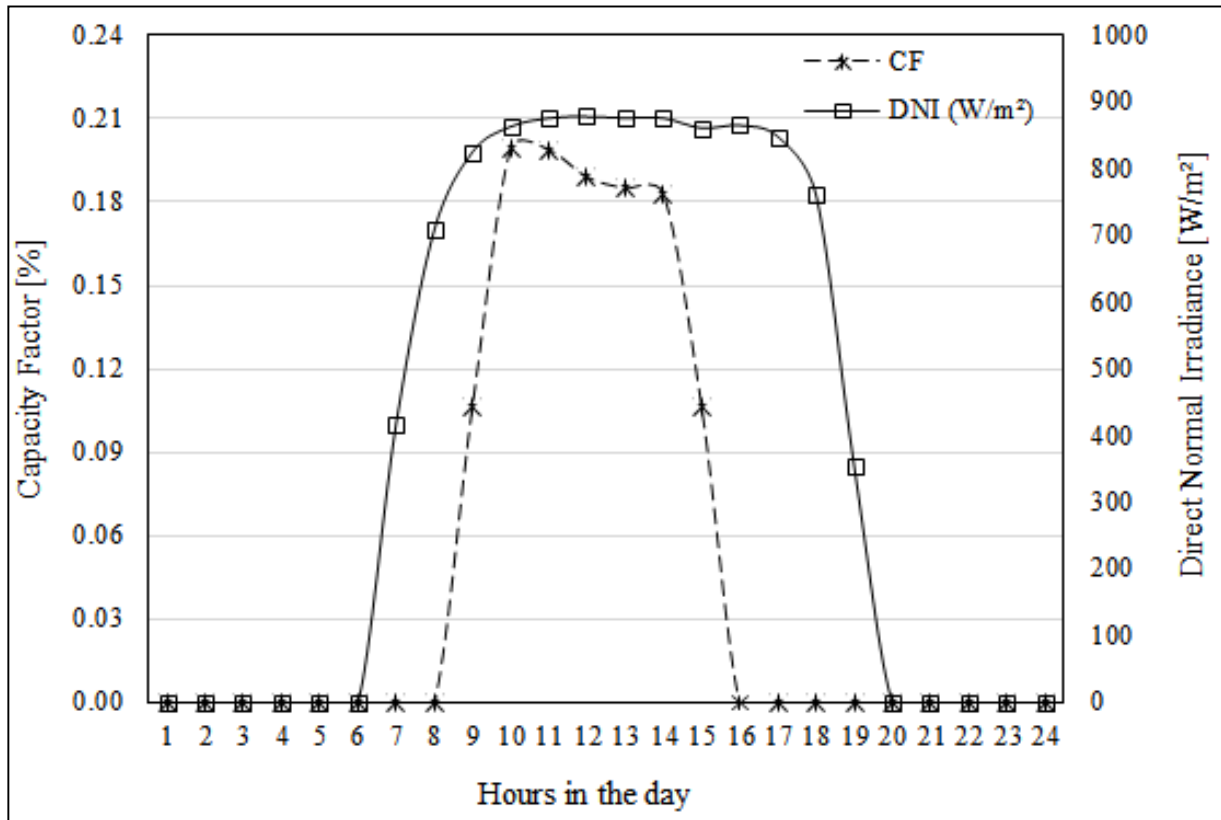
VI.5. Instantaneous performance of the selected power plant (20 MW$_e$ molten salt cavity receiver solar power tower) at design point

In order to evaluate the instantaneous performance of the solar field, it is necessary to estimate the solar radiation intensity from sunrise to sunset. The DNI, of course, depends on the local weather conditions at the site where the power plant is built.

In the operation strategy, the inlet and outlet temperatures of the heat transfer fluid remained constant and equal 290, 560 °C respectively. The following figures 6.3 shows the solar field performance for the representative day in summer. This month is chosen to illustrate the solar field performance at different hours of the day. The selected day is 21stJune.

The HTF mass flow rate, the thermal efficiency and solar field output increase according to the increase in solar radiation from sunrise till sunset of each day, where the operation duration varies for each day. The amount of solar field output during the summer is greater due to the higher solar radiation intensity and longer sunshine duration. The period of Peak

solar field output generally occurs between 10a.m to 16p.m. In summer, the solar thermal
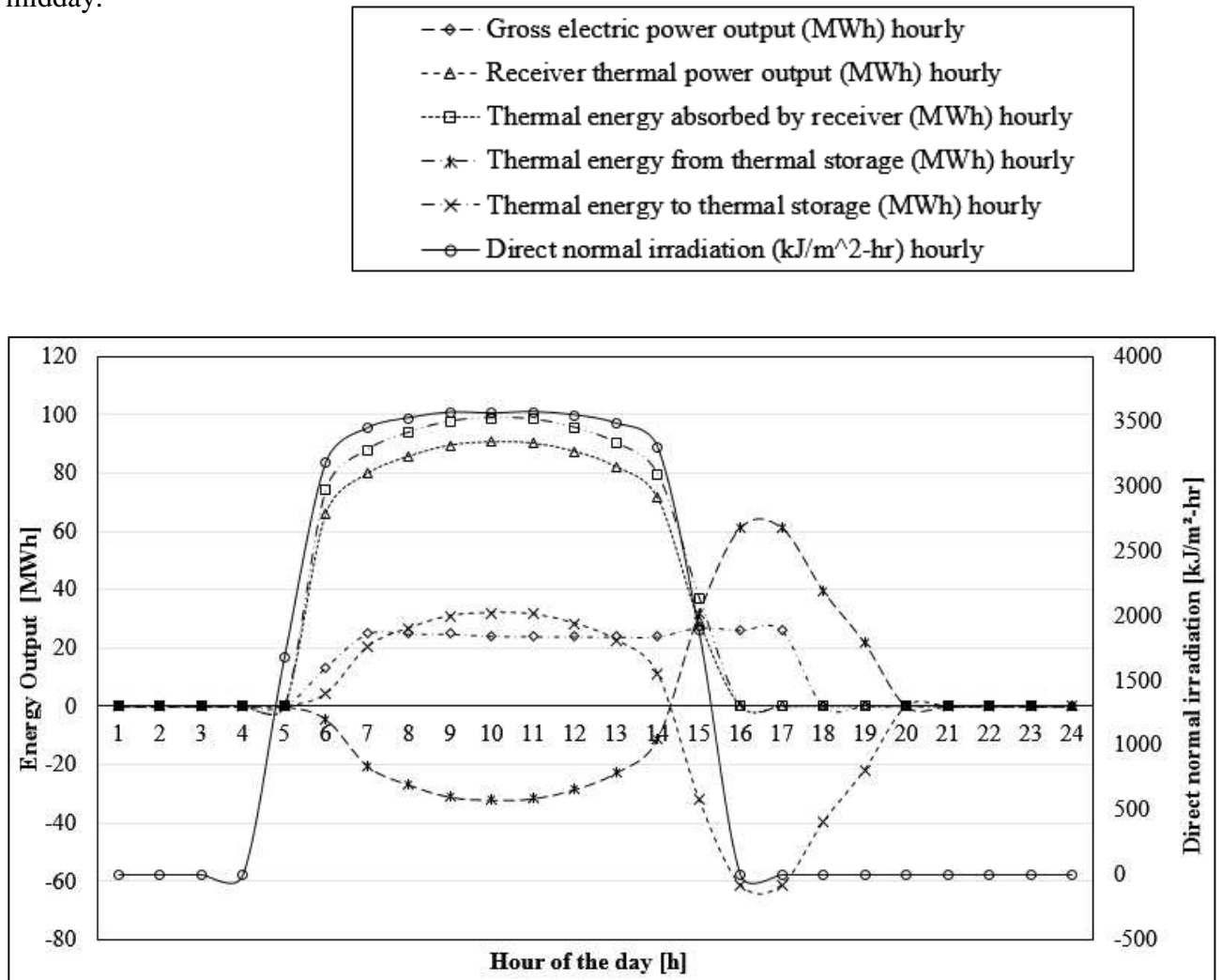
energy is about 22 MW at

midday.

FIGURE 6.3: INSTANTANEOUS SOLAR FIELD PERFORMANCE FOR THE REPRESENTATIVE DAY IN SUMMER FOR TAMANRASSET SITE.

VI.6.Effect of storage capacity

The storage capacity represents about 3% of the total power plant costs [12]. Figure 6.4shows the influence of solar multiple on the capacity factor for different thermal storage capacities. A higher solar multiple leads to a larger storage system and a higher plant capacity factor.

Figure 6.5 indicates that for a TES equal to 8 hours, corresponding to a CF of 0.26, and a LEC of about 0.65 $/kWh$_e$,$ the capacity factor for solar only mode (scenario 1) is maximum. The analysis has also pointed out that for a higher solar multiple, there is higher LEC value.
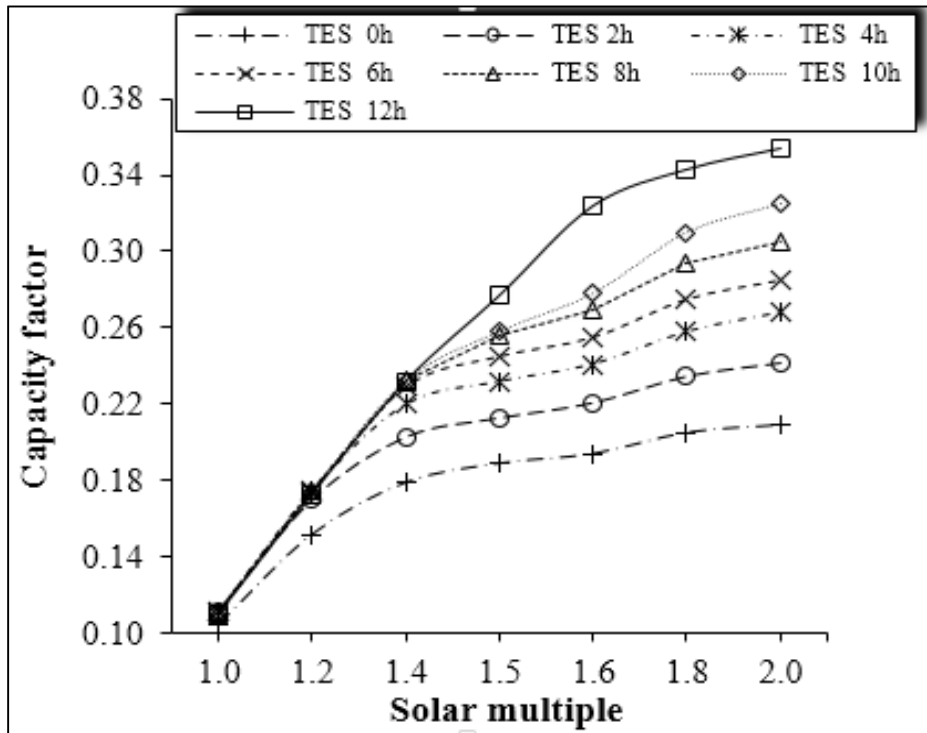
FIGURE 6.4: EFFECT OF SM ON THE CF UNDER DIFFERENT TES VALUES.

Moreover, the CF increases with increase in both TES and SM. For SM of 1.6 and TES equals to 8 h, the plant operates at optimal conditions.

The present study has indicated that the higher the solar radiation the more attractive the solar only mode.
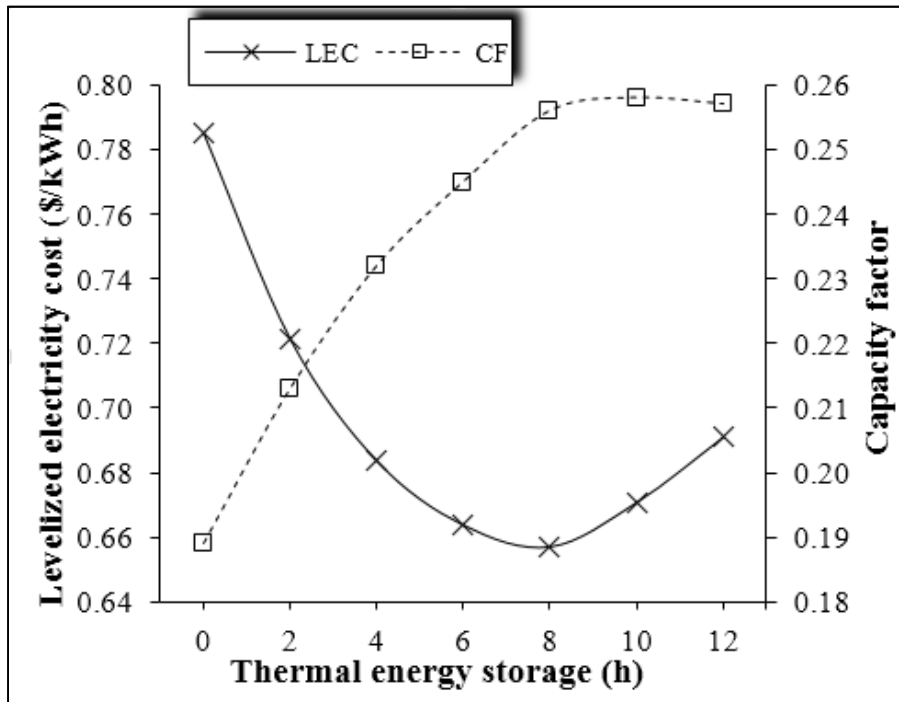

FIGURE 6.5: EFFECT OF TES ON THE LEC AND THE CF WITH RESPECT TO OPTIMAL SM VALUE.

We have also estimated the annual solar electricity generated per unit area of land. Figure 6.6 shows that the larger the solar field the lower the performance due to the poor optical and thermal performance of solar components. Thus the lower is the solar electricity generated per unit area of land.

We have found that for lower value of TES (0 to 4h) and SM ranging from 1.1 to 1.3, the maximum annual solar electricity generation is about 15.9 kWh/m²/year. As can be seen from figure 6.6, for a solar multiple ranging from 1.4 to 1.6, a 17.6 kWh/m^2/year power output can be achieved in the case of a TES value in the interval of 6 hours to 12 hours. This is valid in the case of very high capacity factor.
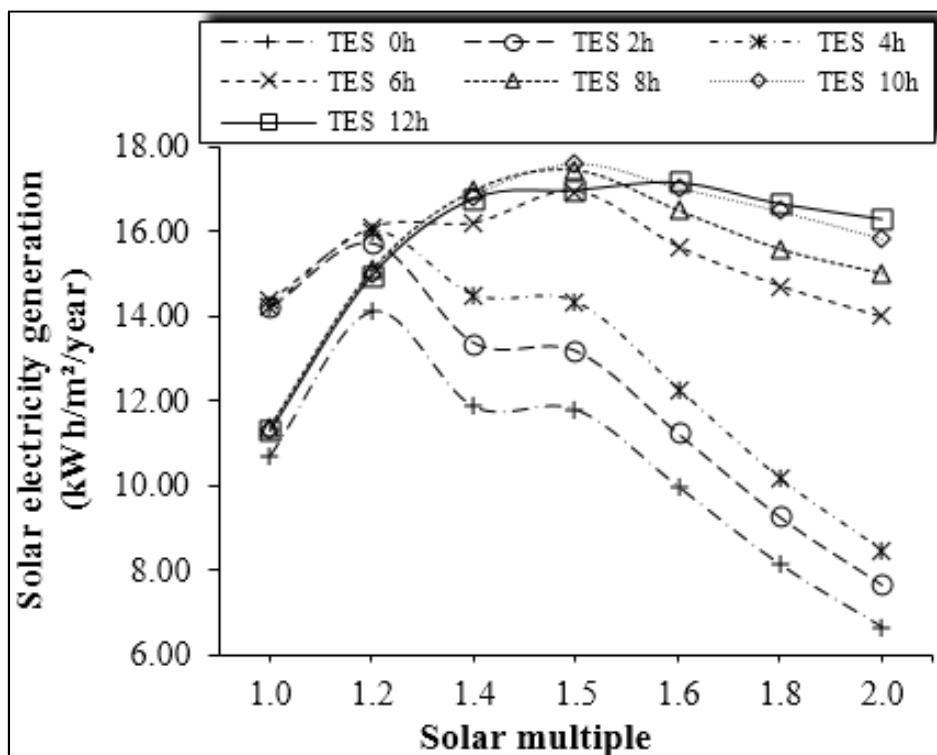

FIGURE 6.6: EFFECT OF SM ON THE SOLAR ELECTRICITY GENERATION FOR VARIOUS TES.

As illustrated in figure 5.6, the maximum annual electricity generation per unit area reaches 17.6 kWh/m²/year for TES = 8 hours and for solar multiple optimal value SM = 1.5. This configuration corresponds to the optimal design of the solar field and the storage capacity.

From figure 6.7, it can clearly be seen that the annual electricity generation per unit area is maximal (17.6 kWh/m²/year) for TES = 8 hours and for solar multiple optimal value SM = 1.5. This configuration gives an optimal design of the solar field, the storage capacity and the

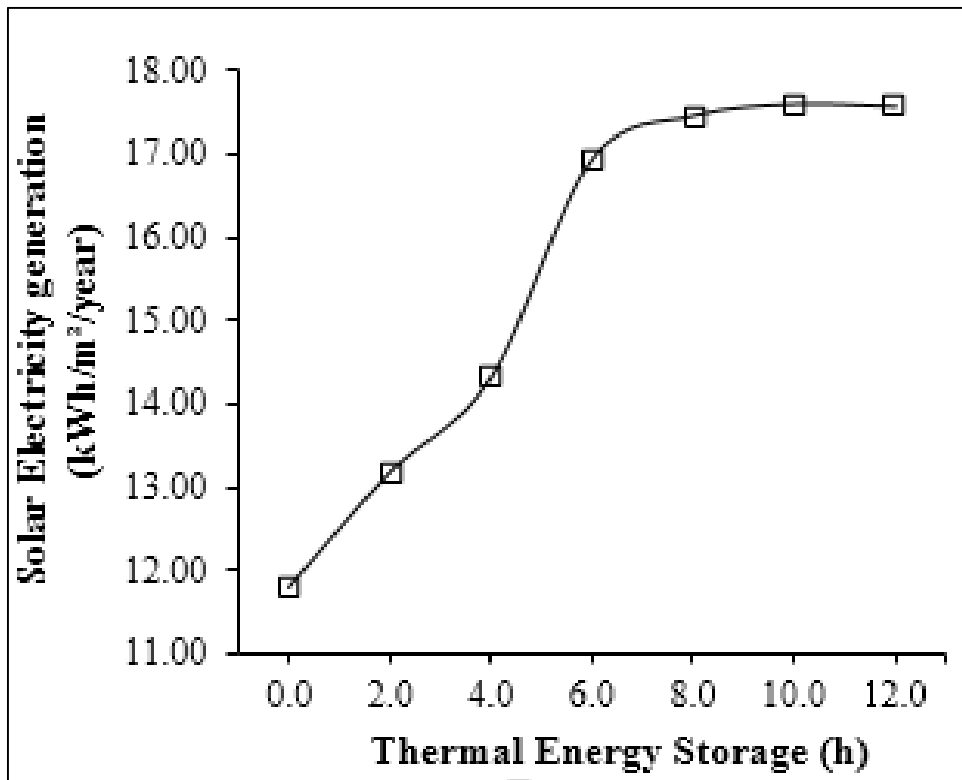maximum solar electricity generation. There is however a need to look at the cost benefit of such issue.

FIGURE 6.7: EFFECT OF TES ON THE SEG FOR OPTIMAL SM = 1.5.

In order to determine the Levelized electricity cost LEC for the case of scenario 1 with and without thermal storage option, we have carried out a sensitivity analysis to get the optimal solar field multiple. In figure 6.5, the cost per unit of electricity generation is compared for different values of storage capacity.

Figure 6.5and figure 6.7 indicate that for a thermal energy storage capacity of 8 hours and for a solar multiple SM = 1.6, the value of LEC is minimum (LEC= 0.66 $/kWh) but, it is still higher than that of a fossil power plant (LEC = 0.07 $/kWh) [14].

It is important to note that the higher the solar radiation, the higher the storage capacity for the same SM and therefore the lower the LEC value.
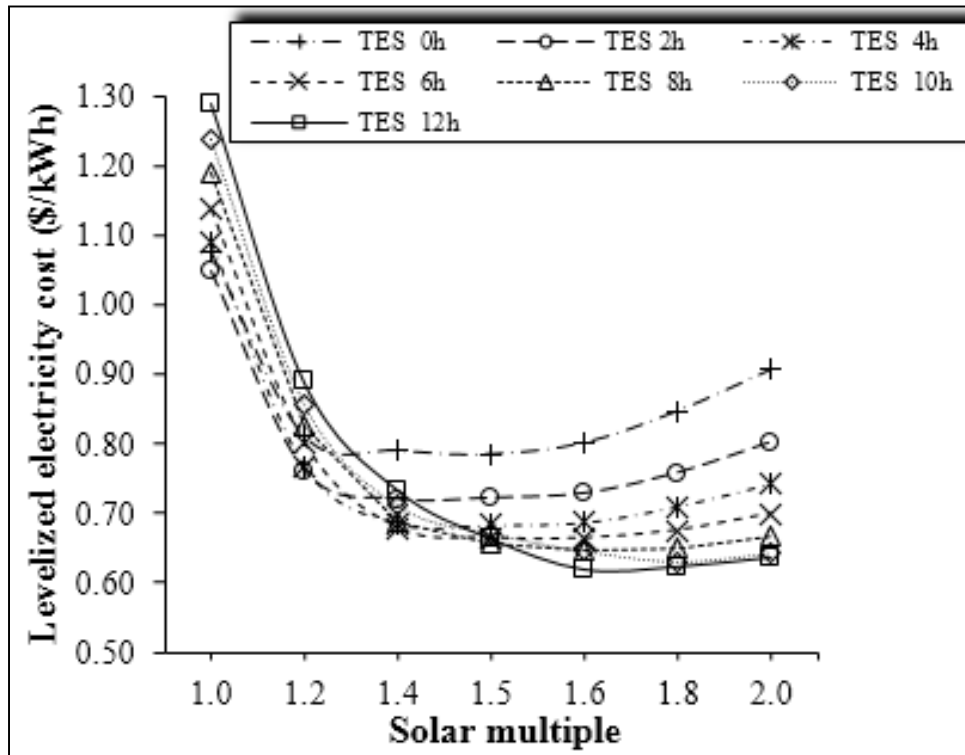
FIGURE 6.8: EFFECT OF SM ON THE LEC FOR DIFFERENT VALUE OF TES.

VI.7.Effect of the DNI on the performance of CSP

The performance of the CSP plant depends significantly on the incident solar radiation, which depends on the geographical position and the climatic conditions. To investigate the effect of incident solar radiation on the LEC, the specific investment cost and the performance of the CRS, three regions sites, namely, Tamanrasset, Batna and Algiers have been selected.

These sites, located in three different geographical regions, are characterized by different climatic conditions. These regions are the coastal zone, the high plateaus and the Sahara desert. The results are reported in figure 6.9.
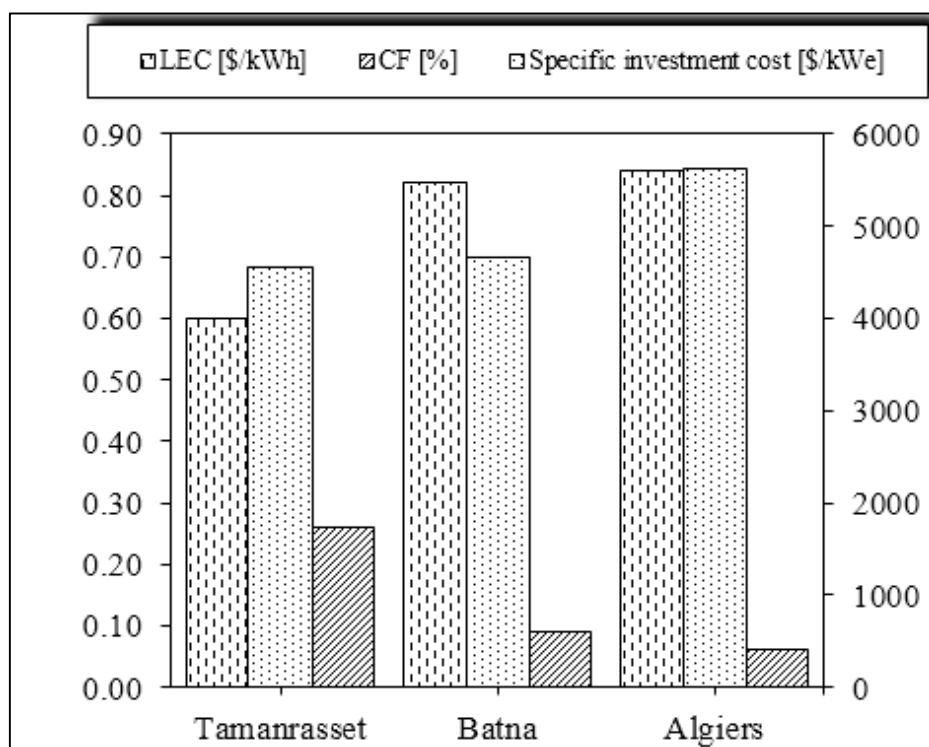
FIGURE 6.9: EFFECT OF DNI ON THE CAPACITY FACTOR, LEC AND SPECIFIC INVESTMENT COST.

Figure 6.9 shows that as the DNI increases, the capacity factor goes up and the LEC goes down. The LEC is nearly the same for Algiers and Batna site which is about 0.85$/kWh.

This is significantly higher than that of a fossil power plant (0.07$/kWh), while the specific investment cost is similar for Tamanrasset and Batna, about **4600 $/kW_e**. This value is not so much far from the costs given in the literature, indicating a good agreement[32].

The results indicate that for optimal working parameters and for a given size of the solar field, Sahara regions (Tamanrasset site) are more suitable for the implementation of large scale solar CRS power plants.

VI.8. Hybridization effect and fossil fuel fraction optimization parameter

As outlined in table6.10, for each hour in the simulation, the amount of energy in storage is evaluated. For each period, there are two dispatch targets for starting or continuing to run the power cycle; one for periods of sunshine, and one for periods of no sunshine.

- During periods of sunshine when there is insufficient energy from the solar field (cloudy days) to drive the power cycle at its load requirement, the system dispatches energy from storage only when energy in storage is greater than or equal to the dispatch target.

- During periods of no sunshine, the power cycle will not run unless energy in storage is greater than or equal to the dispatch target.

The turbine output for each dispatch period determines the power cycle output required for hours that fall within the dispatch period. During the period when the solar field energy is insufficient to drive the power cycle at the output requirement, the power cycle runs on energy from both the solar field and storage system.

The effect of the fossil fuel fraction on both Levelized electricity cost and capacity factor is illustrated in figure 5.10,we get an optimum value of FFF in the range of 0.8 to 1 where we have a trade-off between cost and performance of the plant operation in hybrid mode.
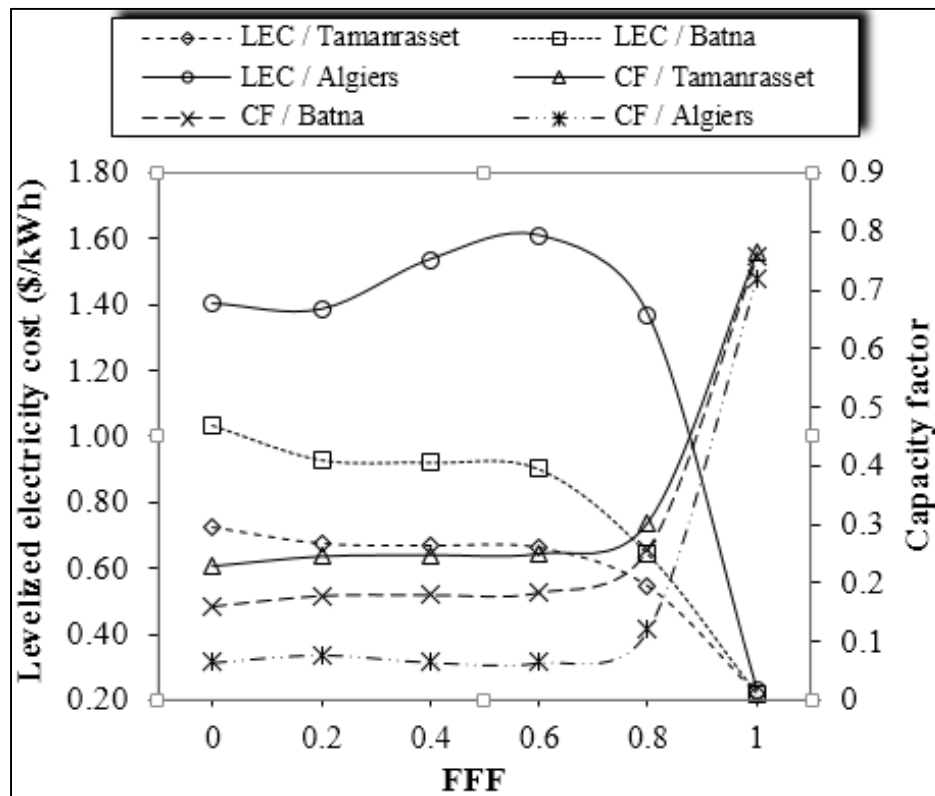
FIGURE 6.10: EFFECT OF FOSSIL FUEL FRACTION ON THE LEVELIZED ELECTRICITY COST AND CAPACITY FACTOR.

The sensitivity of both LEC and CF is less important for lower values of fossil fuel fraction parameter (less than 0.8) in the three regions. This due to the low quantity of energy added from the solar part. In the solar only mode, the energy conversion efficiency is lower than in the case of hybrid mode. The need to develop more suitable components, such as turbines and heat exchangers, is necessary in order to increase the competitiveness of solar only mode.

VI.9. Capital cost estimates simulation for solar central receiver power plant

VI.9.1. Methodology

Component costs for 1MWe, 20MWe, 50MWe and 100 MWe net electrical output plant have been estimated using SAM advisor utility software.

To achieve this, each plant was divided into 4 main areas:

− Solar Field

− Receiver and Tower

− Storage and molten salt system

− Power Block

Within each area, approximately 10 equipment items or systems were identified for detailed costing. Depending on the particular equipment, the following method was used to estimate installation cost.

In most cases an alternative method was used for verification. The methods include:

Cost scaled from pilot plant actual cost: For certain plant areas where the only known data is pilot plant cost information, the pilot plant values were scaled to full size.

A risk associated with this approach is that benefits due to economies of scale and technology learning are not considered. The solar field was costed using this method, table 6.4.

VI.9.2. Plant specifications

TABLE 6.4: SIMULATION RESULTS FOR EACH PLANT DESIGN COMPONENTS

	without storage	with storage	with storage	with storage
Plant capacity [Mwe]	1	20	50	100
Plant location	Tamanresset			
Solar Field Heliostats: number, each 12.2 m x 12.2 m	92	1680	4550	8697
Total heliostat field area [m²]	13282	242550	656761	1255483
Working fluid HTF	Molten salt (60% NaNO3, 40% KNO3)			
Hot temperature [°C]	574			
Cold temperature [°C]	290			
Receiver Cylindrical, n panels.	20	20	20	20
Height [m]	3.56	6.85	10.16	21.83
Diameter [m]	5.93	16.64	17.34	18.59
Tower high [m]	143.25	129.78	161.44	202
Turbine steam conditions	539 °C / 16.5 MPa			
Cooling System	Dry cooled			
Storage [h]	8			
Condenser	Air cooled			
Land area [acres]	56	286	879	1780

Chapter V. Results, Discussions and Conclusions

➜ Solar Field: The cost estimation for a 20MW CSP plant was based on solar fields of 242550 m²with storage, which will require 1680 heliostats. Each heliostat has a reflecting surface just over 144 m². The heliostat mirrorsdesign consists of glass mirrors and steel structure supported on concrete foundations. Eachheliostat will require motors and tracking systems and field wiring to control and track the sunand concentrating the solar radiation on the receiver.

Costing was based on a combination of literature review. Receiverwere reviewed for heliostat pricing in $/m² and material quantities perheliostat. Materials included kilograms of glass, steel and concrete as well as actuators andfield wiring. The review approach concluded that $170/m²(Table 5.5)is an appropriateestimate of heliostat fabrication and erection cost.

➜ Receiver: The receiver is assumed to be of cavity design with 20 adjacent panels arranged around the perimeter of a 12.44 m diameter tower structure. Each panel is 6.85 m high and

comprises of 40 individual 0.04 m tube joining to a common header at either end. Several flow arrangements have been proposed. Costing the receiver assumed two pipe sizes, 40 mm for the parallel panel runs and 150 m mat the headers and inter-panel connections to maintain the flow rate. All components are to be fashioned from commercially available schedule 5, 316L Stainless Steel tubing.

➜ Tower: A set of civil and structural conceptual designs were developed to enable accurate solar tower cost estimates. This cost is based on a concrete tower shell design with a total height of 130 m with storage option. Included are all associated civil/structural requirements

such as piling, footing, excavation and refill. A steel platform floor was assumed to support receiver rather than a concrete slab to reduce weight. Also a lift, ladders and landing were all included in the price estimate.

➜ Molten Salt and Storage Systems: Depending on the specific storage and operational requirements, a concentrated solar power plant requires at least one Heat Transfer Fluid (HTF) tank for cold molten salt and a second hot tank should storage be required. For this study the variation in tank requirements for each case forms the basis for the difference in capital cost. In the no storage case, HTF is pumped up the tower where it is heated before descending the tower to the steam generator and

returned to the cold storage tank. When storage is required, an amount of the descending hot HTF is directed into a hot storage tank for later use.

➔ Power Block: The power block design consists of a conventional steam cycle. Steam is raised and superheated by the heat transfer fluid (HTF) via a number of shell and tube heat exchangers. The steam drives a single reheat turbine with air cooled condenser (ACC). The turbine consists of two cylinders with single flow high pressure turbine (HPT) and combined opposed single flow intermediate pressure (IPT) and low pressure turbines (LPT). A single bled steam open feed water heater is employed as well as a HTF feed water pre-heater. The feed water pre-heater is again a shell and tube type.

The analysis of each equipment and its contribution in the estimated cost of the central receiver power plant shown in the different figure 6.11, 6.12, 6.13, 6.14 and 6.15 have been in concordance to the literature review[34], however the main conclusion to the issue of the overall capital cost reduction to CSP power plant is the increase in the plant size and the economies of scale procedures.

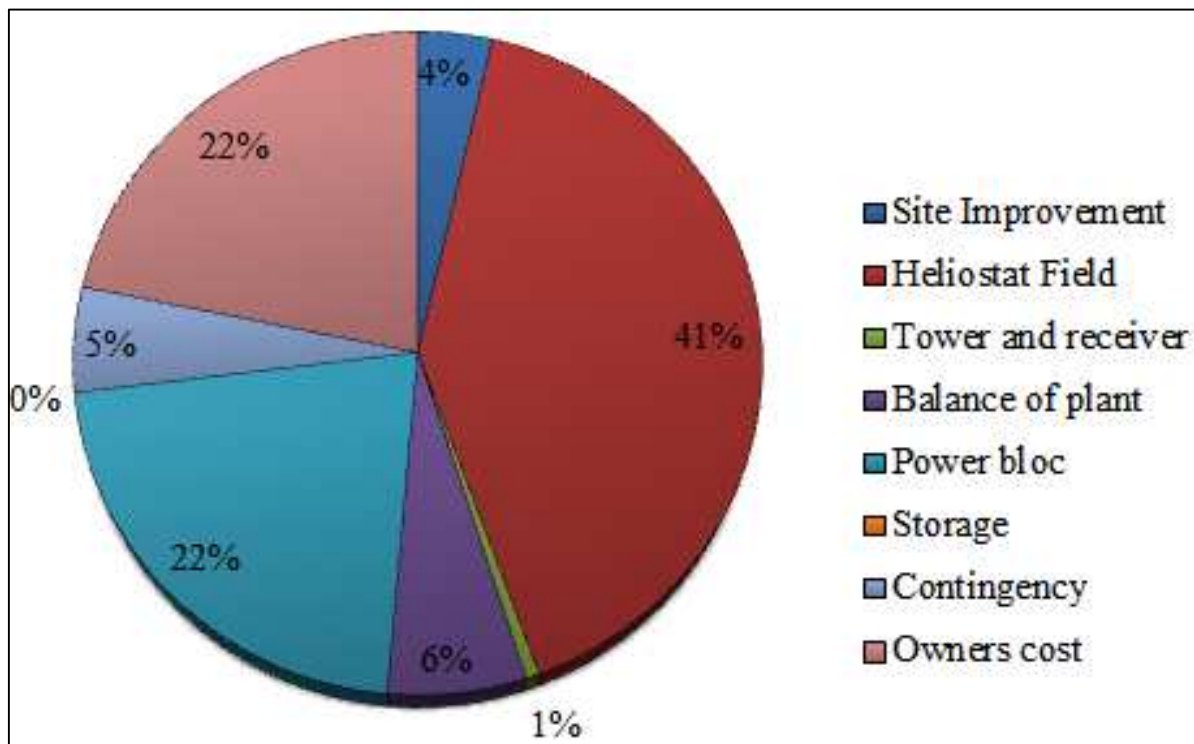
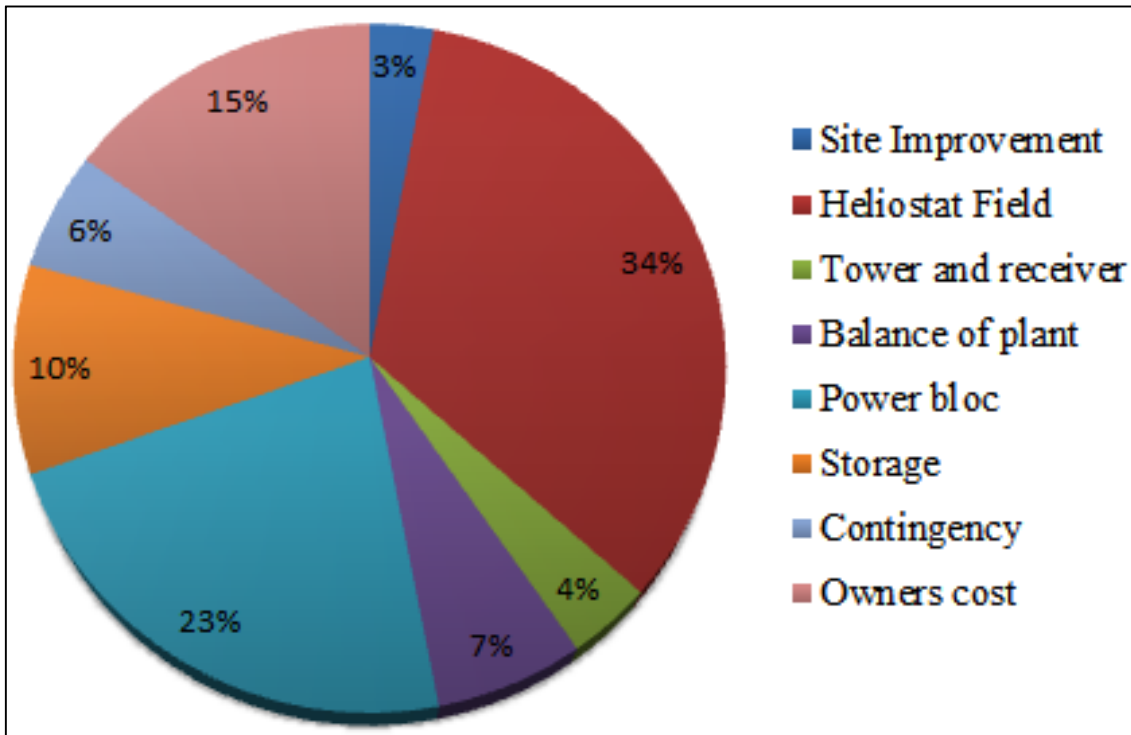FIGURE 6.11: CAPITAL COST ESTIMATED FOR EACH COMPONENT OF THE 1MWE POWER PLANT

FIGURE 6.12: CAPITAL COST ESTIMATED FOR EACH COMPONENT OF 20 MWE POWER PLANT.
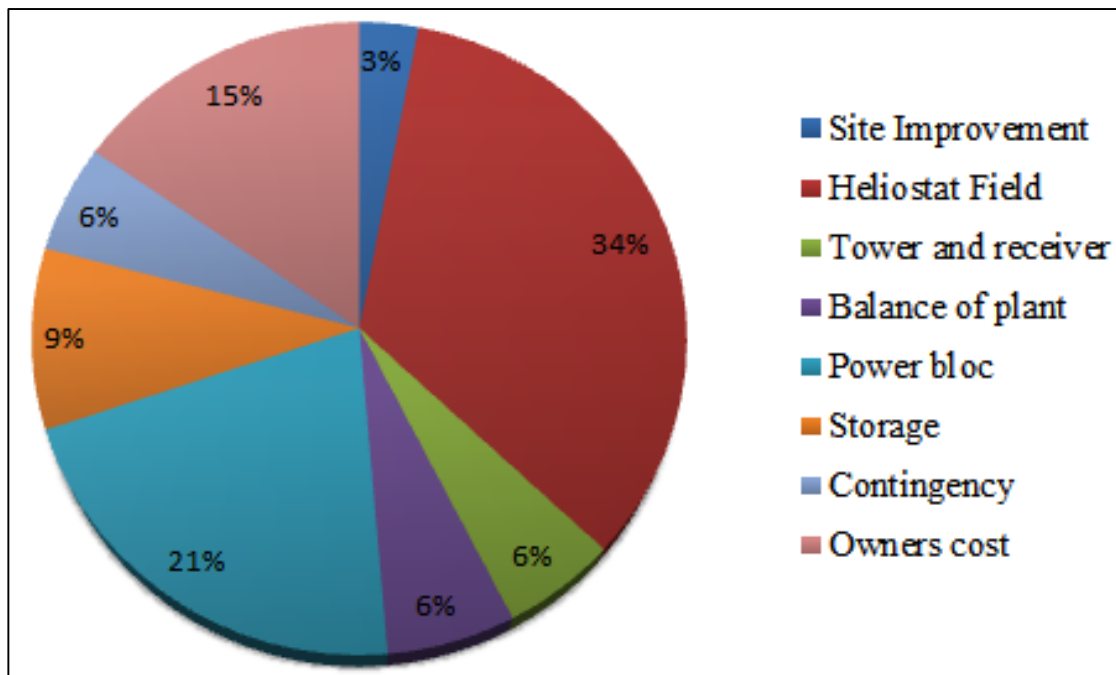

FIGURE 6.13: CAPITAL COST ESTIMATED FOR EACH COMPONENT OF 50 MWE POWER PLANT.
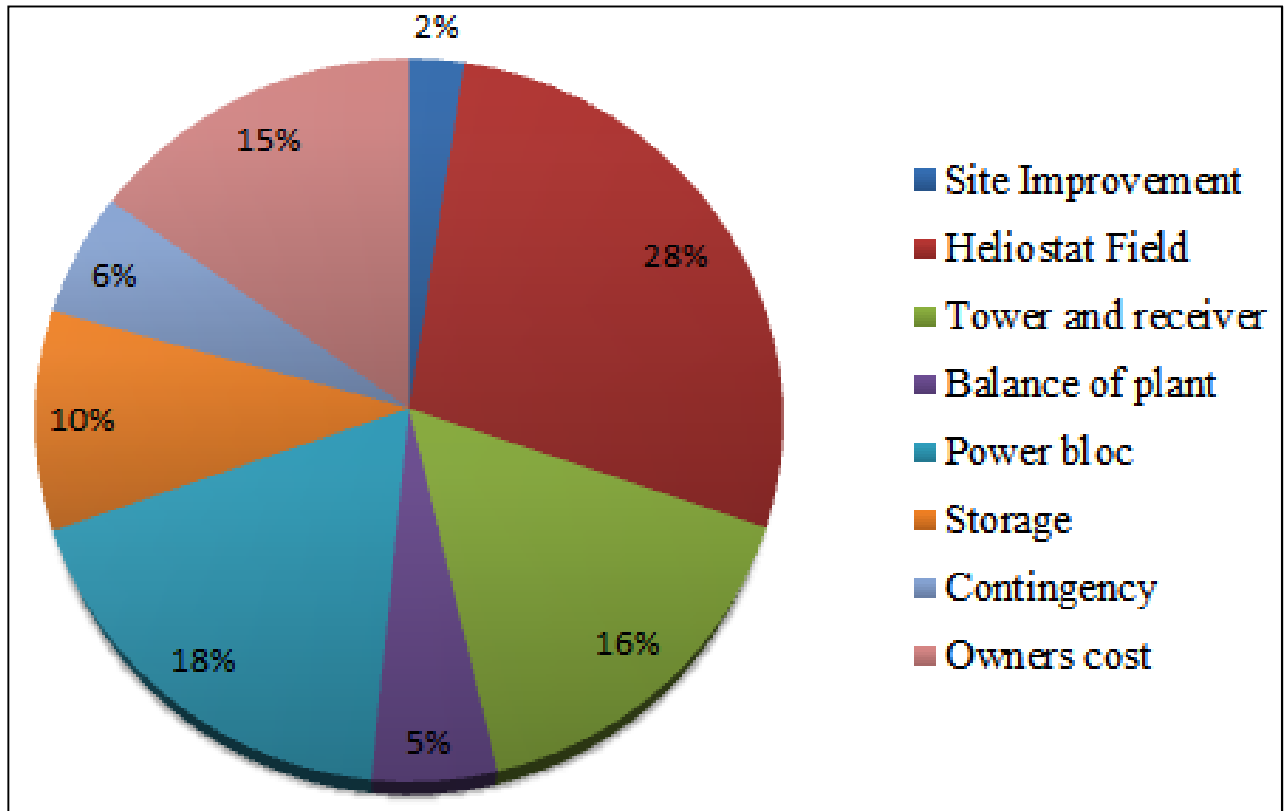
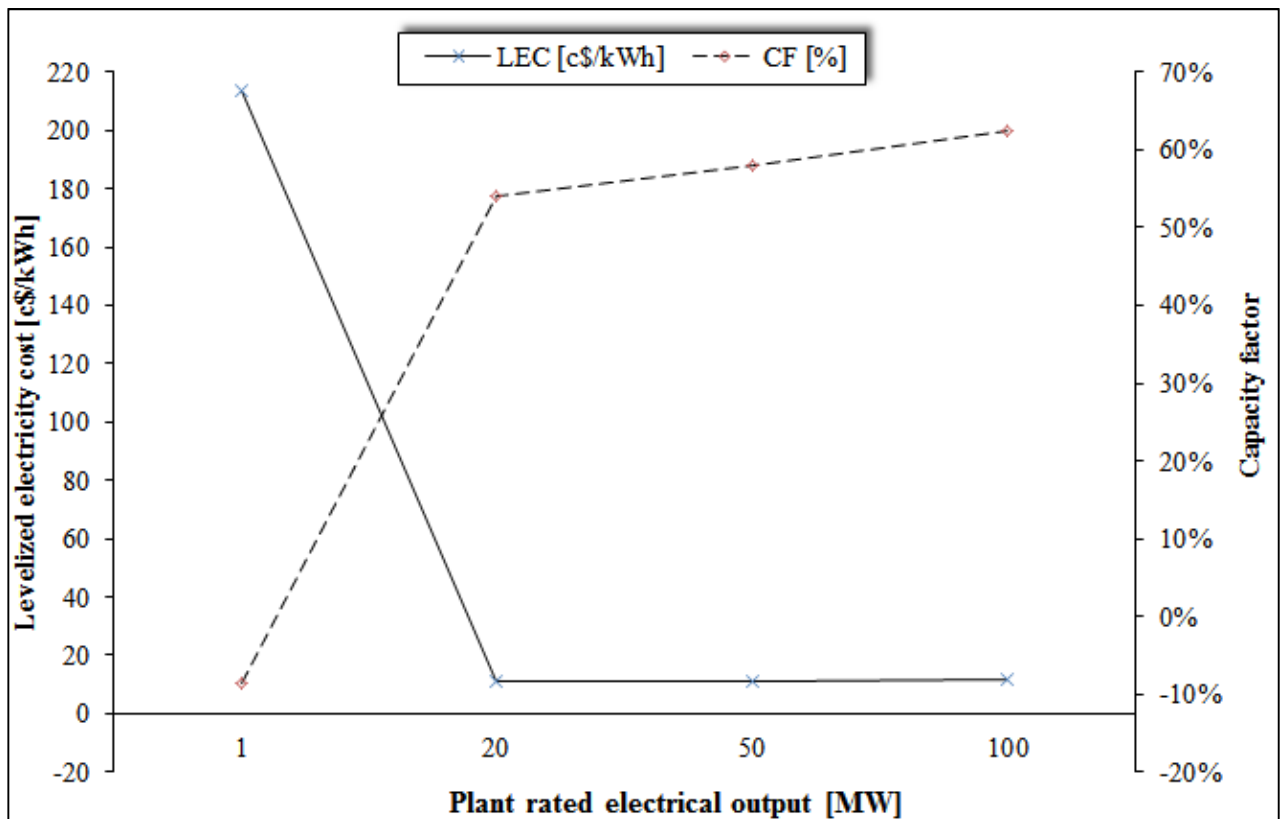FIGURE 6.14: CAPITAL COST ESTIMATED FOR EACH COMPONENT OF 100 MWE POWER PLANT.

FIGURE 6.15: SENSITIVITY OF THE LEC AND CF TO THE RATED ELECTRICAL OUTPUT.

VI.9.3. Overall estimated capital cost

The methodology described above was used to determine the overall cost of the 20 MW plant with storage. A summary of the major plant area costs is provided in table6.5.

TABLE 6.5: CAPITAL COST ESTIMATES FOR 20 MWE NET ELECTRICAL OUTPUT PLANT (2014).

	Unit cost	Estimated cost Million $
Site preparation & civils	$15 /kW,net	15
Solar Field	$170 /m²	170
Tower	$29 /kWth	14.5
Receiver	$19 /kWth	23.4
Molten Salt and Storage Systems	$12 /kWhth	20.8
Turbine systems (inc generator)	$464 /kWe,gross	48.6
Steam generation	$187 /kWe,gross	20.6
Controls	$350 /kWe,net	10
Spares		17.9
Owner & contractor costs		112
	Total	452.8

VI.10. Open volumetric air receiver analysis and simulation

As the results discussed of the previous work about the single channel flow [46], further analysis about the air flow and heat transfer inside the continuum homogenous model are assumed in the present approach.

The main objective is to investigate all parameters such as the radiation model applied at the surface of the absorber, the Brinkman model applied to the fluid flow through the porous structure affecting the physical model. The air temperature distribution in figure 6.16 is homogenous along the receiver geometry with frustum version. The gap between the air temperatures is about 7.5% at the outlet of the porous structure. Nevertheless, the proposed model predicts better the radiation, convection and conduction heat transfer in the absorber with the air flow, comparing to the experimental ones;

Table 6.6 indicates the measured values and simulations in terms of thermal to fluid efficiency and the outlet temperature. Figure 6.16 shows the correspondence between experimentally and numerically determined air outlet temperature values, the measured thermal efficiency is higher at about 6.1 % more than the simulated one.

TABLE 6.6: COMPARISON BETWEEN THE EXPERIMENTAL AND NUMERIC RESULTS OF THE CONTINUUM MODEL

Tests N°	Inlet mass flow [kg/s]	T_{in} [°C]	Experimental values		Numerical values	
			T_{out} [°C]	η [%]	T_{out} [°C]	η [%]
1	1*0.6*0.026=0.0156	44.85	717.71	82	676.53	77

Analyzing the figure 6.17, figure 6.18 and figure 6.19 and comparing with the previous results given in the study done by Elona, the present model is more realistic in predicting (calculating) the air temperature, the solid temperature and the air velocity respectively along the receiver.
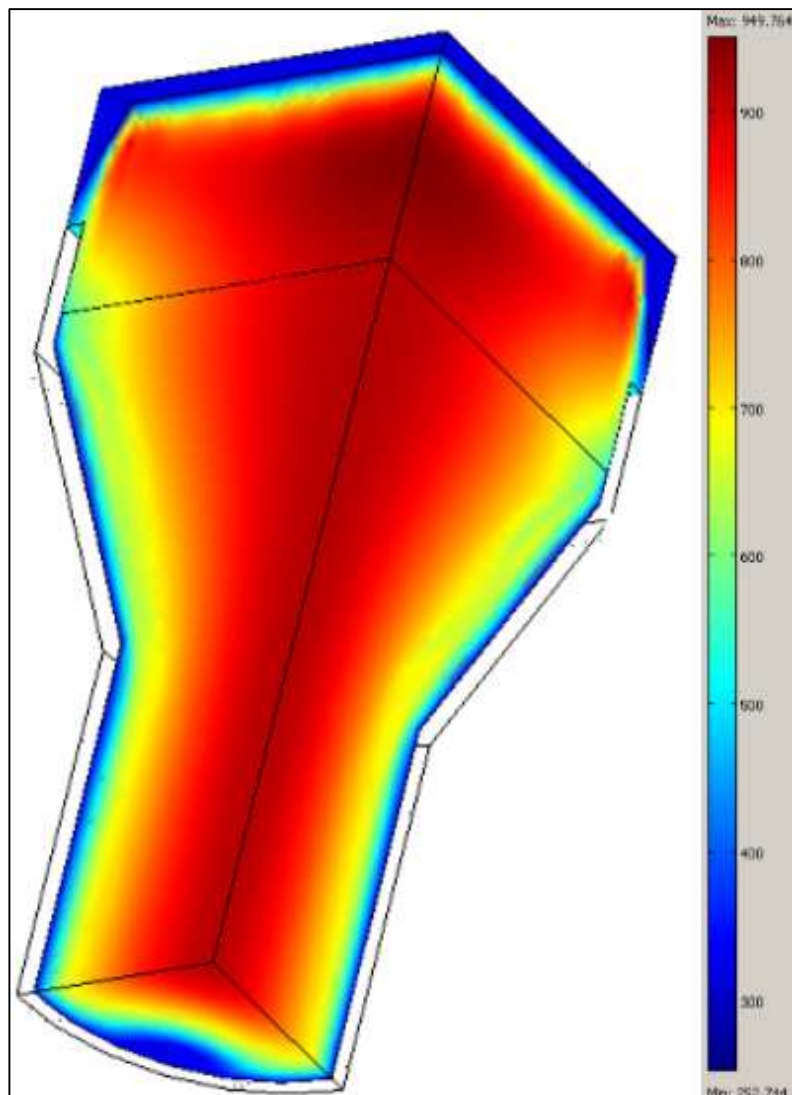
FIGURE 6.16: THE RECEIVER AIR TEMPERATURE DISTRIBUTION

Chapter V. Results, Discussions and Conclusions

Thus, coupling dynamic effects and thermal heat transfer along the absorber and the air area gives more scope to further optimize the receiver optimal working conditions such that air mass flow inlet, radiation flux energy absorbed by the porous structure, the channels dimensions and air return ratio for cooling purpose of the absorber structure.

FIGURE 6.17: NUMERICALLY DETERMINED TEMPERATURE DISTRIBUTION IN THE CENTER OF THE AIR RECEIVER VOLUME IN FLOW DIRECTION. PRESENT MODEL UP, ELONA'S MODEL AT THE DOWN [43].

FIGURE 6.18: THE SOLID TEMPERATURE DISTRIBUTION. PRESENT MODEL AT THE TOP, ELONAS'S MODEL AT DOWN [43]

FIGURE 6.19: NUMERICALLY DETERMINED FLOW VELOCITY DISTRIBUTION. PRESENT MODEL AT THE TOP SIDE, ELON'AS MODEL [43] AT THE DOWN SIDE.

VI.11.Conclusions

In the present study, the thermal performance and economicanalysis of a future 20 MW$_e$ molten salt cavity receiver solar 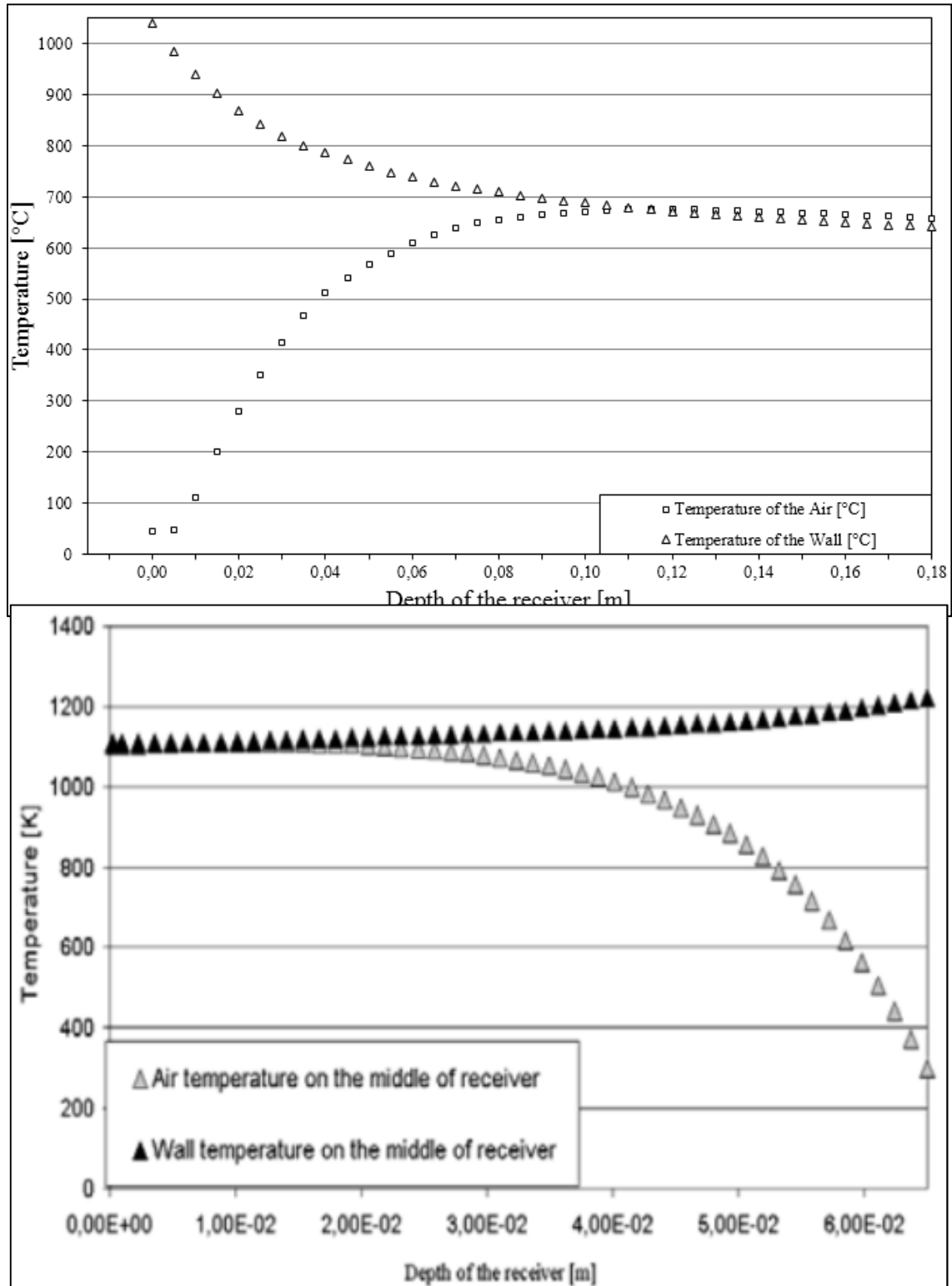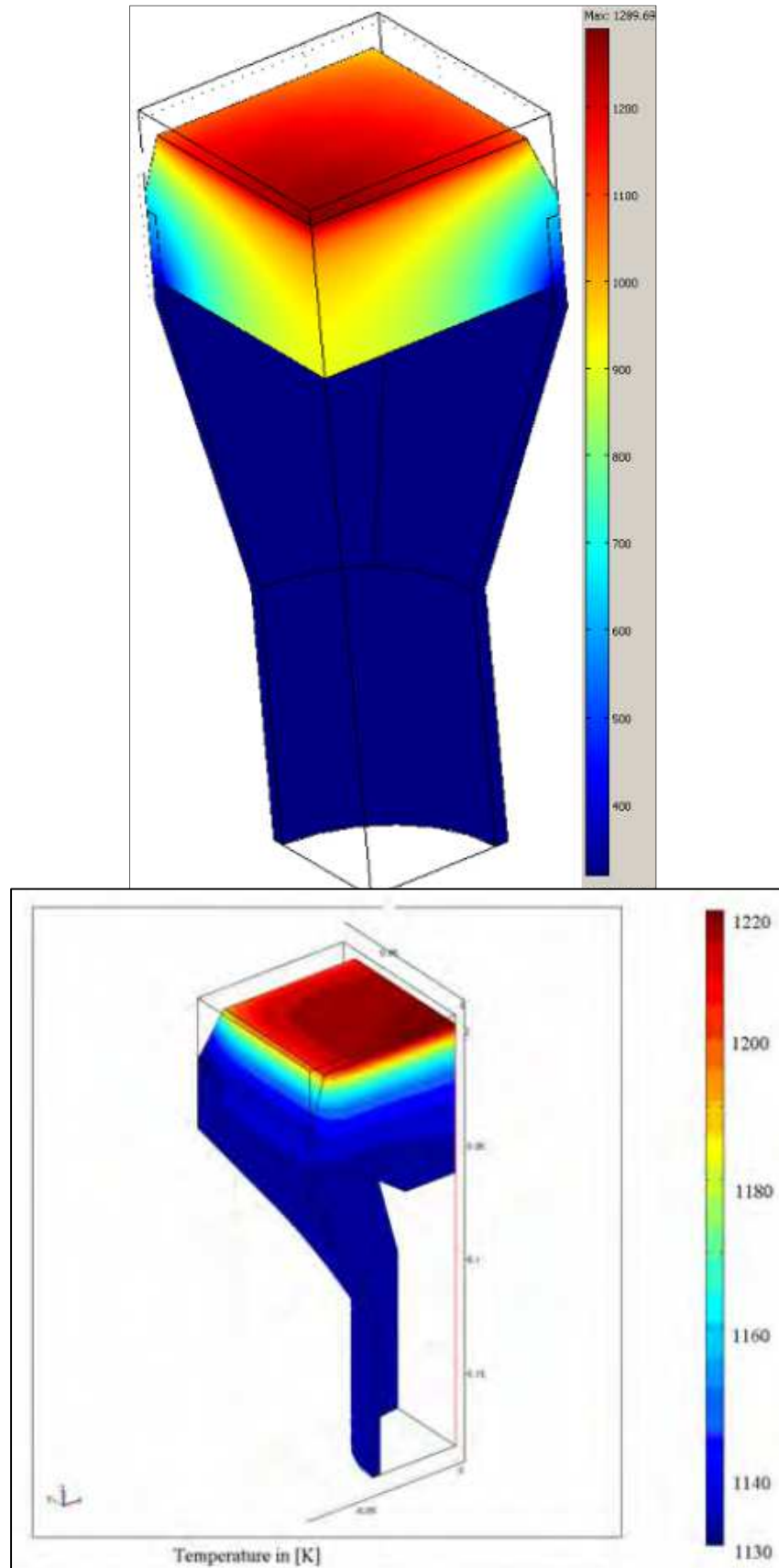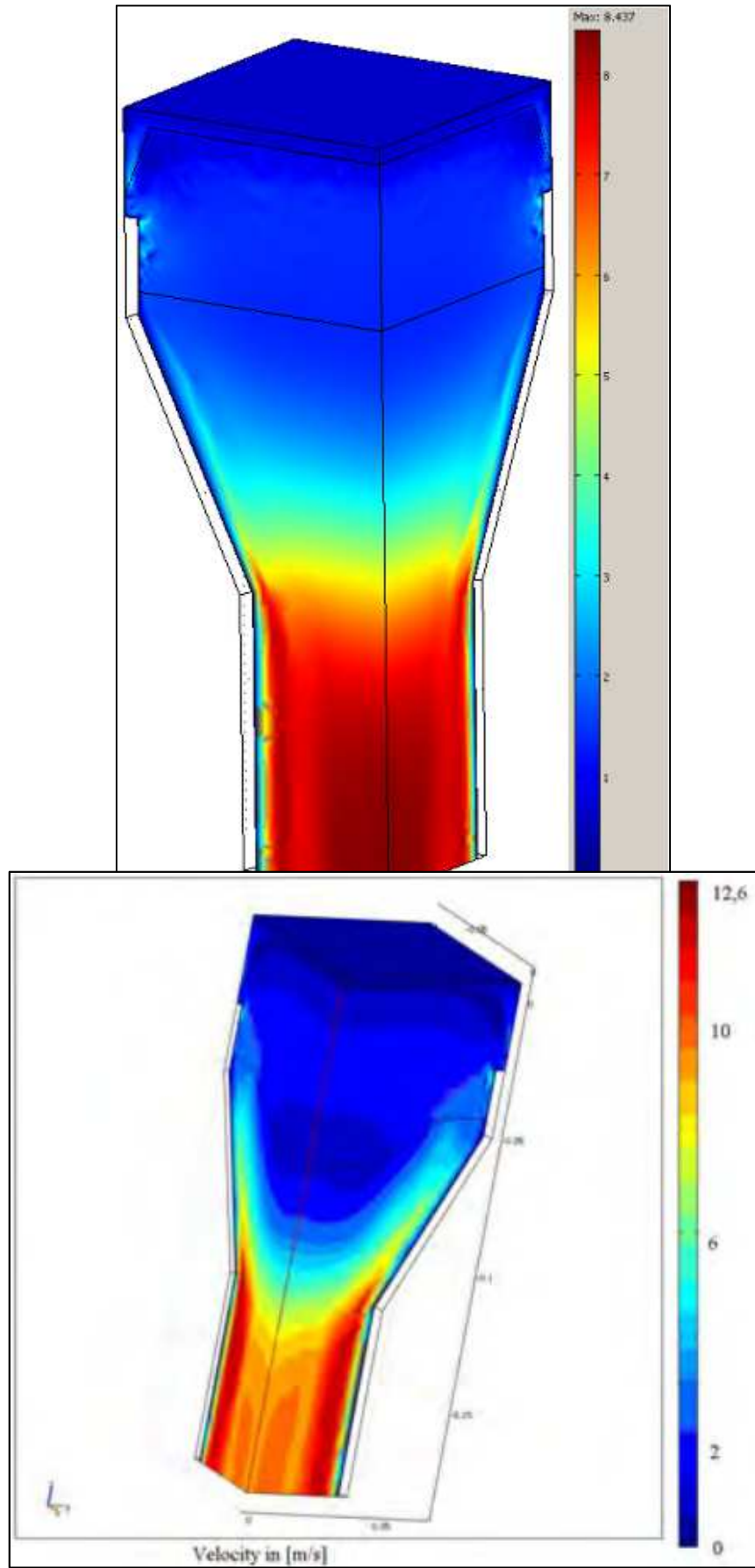power plant has been carried out. Two scenarios, namely the solar only mode and the hybrid mode have been investigated. The comparison of the simulated results to those of PS20 has shown good agreement. A comparative study with earlier simulation work carried out by Izquierdo et al. [20] has been undertaken. However, critical parameters are missing for a meaningful comparison.
Nonetheless, there is a qualitative agreement between the present results and those reported by Izquierdo et al.

The analysis has pointed out to the fact that the larger the storage capacity, the larger the solar multiple and the lower is the LEC since the storage system has the lowest investment costs.

A strong relation between the capacity factor, solar multiple, and the TES have also been found. In solar only mode, it is shown that the higher the DNI the higher the storage capacity, thus the higher the plant capacity factor considering the same solar multiple. This is the case of Tamanrasset that has the highest solar radiation intensity compared with Batna and Algiers. The hybridization is an attractive option that enhances the efficiency and increase the capacity factor. It decrease the LEC compared with the solar only mode.

The fully coupled heat transfer and fluid flow exhibits more advantage to model the physical phenomenon experiencing the honeycomb structure of the absorber. Furthermore, the homogenous continuum model can be used to determine the effect of volumetric convective heat transfer coefficient exposed to nonhomogeneous thermal radiation with further adapting the irradiative inlet boundary conditions of the honeycomb material investigated.
This is a useful quantity, which can be used for reduced numerical models such as the continuum model.
The present model can be used to predict temperatures and velocity distributions in the volumetric solar air receiver. However, more investigation need to be assumed in future work to assume the non-homogenous irradiative heat transfer model, (using ray tracing monte-carlo or P1 gray diffusion model) to assess accurately the energy transferred to the porous structure. Thus, we could choose the best optimal model to be applied with up scaled version of the volumetric air receiver.

Finally, analysis of such model given by the present study can be used as a tool to further optimize the receiver geometry which could be used in solar commercial plant, and further introduction in international market trading.

The application of this technology (high efficient storage systems and hybridization option) to solar towers, requires however more in-depth R&D activities. For the solar subsystems, the Micro Tower Configuration (MTC) appears to be one of the most promising options to reduce investments costs induced by higher tower and enhance optical efficiency as it is recently confirmed by simulation tools.

To meets these targets, increase in research funding and a stronger integration of fundamental and applied research, together with demonstration programs and market incentives are required to speed up the innovation stage. Fundamental research on solar radiation assessment, solar subsystems, heat transfer fluids and storage technology are needed for taking some advanced CRS concepts from laboratory-scale prototype systems out to commercial scale applications.

Therefore, with the continuous progression in solar power conversion cycles technology, the development of the central receiver solar plant could be the best choice in the future, and it might become competitive with fossil fuel power technologies in the coming decades.

VI.12. General Conclusions and forthcoming insights

The present work deals with the technical feasibility of central receiver system using solar tower technology. This technology is based on solar concentration ratio of up to 1000 suns that can supply solar process heat at higher temperatures of about800°C.
This technology has been under development since 1980s after the pioneering experience of Solar I and Solar II in USA and the Plata forma de Almeria in Spain during the period of 2000-2010.
It has reached the commercial maturity and is full expansion. Algeria is very rich in solar energy resources. It possesses large unpopulated and unproductive land in the Sahara which represents80% of the total country area. This makes the country an ideal place for the implementation of the concentrating solar thermal power plant technologies. Algeria has expressed a high interest in developing its solar energy resources.

Chapter V. Results, Discussions and Conclusions

To this end, it has introduced a program where solar thermal energy plays a central role. In order to study the viability of solar tower power plant, we present here a technical and economic assessment of a hybrid molten salt central cavity receiver under Algerian climate. Using the economical, technical, meteorological and radiometric data, we have carried-out a simulation under SAM advisor tool.

However, we have done further analysis (fluid flow and heat transfer simulation) for the solar power tower element which is the open volumetric air receiver (porous ceramic absorber) taken from a pilot plant of Jûlich, Germany.

VI.12.1.General Conclusions

- In this type of concentrating solar plant, the biggest investment is critical in the heliostat field and all associated operating and Maintenance costs during the life time cycle;
- The levelized cost of electricity is inversely proportional to the capacity of the plant, more high the capacity factor of the power plant less the LEC value;
- The need for more precise DNI-data values will increase strongly as solar-thermal electrical power generation stands on the threshold of economic profitability.
- The choice of the type of plant depends not only on the rated electrical capacity, but also of the type of the services which will be provided to costumers.
- However, the utility plant might be used as peaking, intermediate or base load unit, and the time on the day during which the plant energy is dispatched
- In general, hybrid power towers were shown to be economically superior to solar only plants with the same field size. Furthermore, the power-booster hybrid approach was generally preferred over the fuel-saver hybrid approach;
- The HTF mass flow rate, the thermal efficiency and solar field output increase according to the increase in solar radiation from sunrise till sunset of each day, where the operation duration varies for each day.
- The amount of solar field output during the summer is greater due to the higher solar radiation intensity and longer sunshine duration. The period of Peak solar field output generally occurs between 10a.m to 16p.m. In summer, the solar thermal energy is about 22 MW at midday;
- The main conclusion depicted on this study is that the central receiver power plant doesn't begin working (steam production and electricity generation on the turbine) for lower value of DNI than 825 W/m².

- The fully coupled heat transfer and fluid flow exhibits more advantage to model the physical phenomenon experiencing the honeycomb structure of the absorber.

- Furthermore, the homogenous continuum model can be used to determine the effect of volumetric convective heat transfer coefficient exposed to nonhomogeneous thermal radiation with further adapting the irradiative inlet boundary conditions of the honeycomb material investigated.

VII.12.2. Forthcoming insights

Several remaining items that should be addressed in future work might be considered as a detailed model is developed, but have a significant impact on the accuracy of the system model.

However, the need to evaluate the viability of the technology is a thorough economic and costing analysis to determine the actual capital, operation, and maintenance costs associated with the plant. Further development of the costing parameters and system economics is expected as the model presented in this research is integrated into the Solar Advisor Model.

Fundamental research on solar radiation assessment, solar subsystems, heat transfer fluids and storage technology are needed for taking some advanced in central receiver system concepts from laboratory-scale prototype out to commercial scale applications.

REFERENCES

[01] Y. Himri et al.Review and use of the Algerian renewable energy for sustainable development.Renewable and sustainable energy reviews 13 (2009) 1584–1591

[02] A.B. Stambouli.Promotion of renewable energies in Algeria: Strategies and perspectives. Renewable and sustainable energy reviews 15 (2011) 1169–1181

[03] A. BoudgheneStambouli et al. A review on the renewable energy development in Algeria: Current perspective, energy scenario and sustainability issues. Renewable and sustainable energy reviews 16 (2012) 4445–4460.

[04] A.B. Stambouli, H. Koinuma A primary study on a long-term vision and strategy for the realization and thedevelopment of the Sahara Solar Breeder project inAlgeria.Renewable and sustainable energy reviews 16 (2012) 591– 598.

[05] A. Tsikalakis et al.Review of best practices of solar electricity resources applications in selected Middle East and North Africa (MENA) countries. Renewable and sustainable energy reviews 15 (2011) 2838– 2849.

[06] A.B. Stambouli.Algerian renewable energy assessment: The challenge of sustainability Energy Policy 39 (2011) 4507–4519.

[07] Boukelia.T.e., M.-S.Mecibah.Parabolic trough solar thermal power plant: Potential, and projects development inAlgeria.Renewable and sustainable energy reviews 21 (2013) 288–297.

[08] Renewable energy and energy efficiency program. Ministry of energy and mines.Sonelgaz GroupCompany, March 2011.

[09] B. L. Kistler. A user's manual for Delsol-3: A computer code for calculating the optical performance and optimal system design for solar thermal central receiver plants.

[10] Lukas Feierabend.Thermal model development and simulation of cavity-type solar central receiver systems.A thesis for the degree of Master Science.University of Wisconsin – Madison 2009.

[11] Robert Y. Wind effects on convective heat loss from a cavity receiver for a parabolic concentrating solar collector. Department of Mechanical Engineering California State Polytechnic University Pomona, CA 91768

[12] SoenkeHolgerTeichel. Modeling and calculation of heat transfer relationships for concentrated solar power receivers.A thesis for the degree of Master of Science.University of Wisconsin – Madison 2011

[13] Winter C.J., Sizmann R.L., Vant-Hull L.L. Solar power plants. Springer Verlag, Berlin, ISBN 3-540-18897-5.

[14] Kodama T. High temperature solar chemistry forconverting solar heat to chemical fuels, Progress in energy and combustion science 29 (2009), 567–597.

[15] Kearney A.T. Solar thermal electricity 2025.STE industry roadmap for the European solar thermal electricity Association (ESTELA).

[16] Geyer M. Briefing material on status of major project opportunities. The current situation, issues, barriers and planned solutions. International executive conference on expanding the market for concentrating solar power (CSP).Moving opportunitiesinto Projects; 19 – 20 June 2002; Berlin, Germany.

[17] Herring G. Concentrating solar thermal power gainssteam in Spain, as momentum builds for major projects inthe US, North Africa, the Middle East, Asia and Australia. PhotonInternational, December 2009, 46-52.

[18] P. Garcia, A. Ferriere, J-J Bezian. Codes for solar flux calculations dedicated to central receiver systemapplications: A comparative review. Solar energy (2008), vol. 82, pp. 189-197.

[19] Omar Behar, AbdallahKhellaf, Kamal Mohammedi. A review of studies on central receiver.Solar thermal power plants. Renewable and sustainable energy reviews 23 (2013) 12–39.

[20] Salvador Izquierdo,CarlosMontanes, Cesar Dopazo,NorbertoFueyo. Analysis of CSP plants for the definition of energy policies: The influence on electricity cost of solar multiples, capacity factors and energy storage. Energypolicy 38 (2010) 6215–6221.

[21] Antonio L. Avila-Marin, Jesus Fernandez-Reche, Felix M. Tellez. Evaluation of the potential of central receiver solar power plants: Configuration, optimization and trends. Applied energy 112 (2013) 274–288.

[22] V. SivaReddy, S.C.Kaushik, K.R.Ranjan, S.K.Tyagi.State-of-the-art of solar thermal power plants, a review. Renewableand sustainable energy reviews27(2013)258–273.

Schönhauser, Allee 10-11.10119 Berlin, Germany.

[23] Patricia Kuntz Falcone, A handbook for solar central receiver design. Sandia national laboratories Livermore. SAND 86-8009. December 1986.

[24] Giorgio Simbolotti (ENEA). Concentrating solar power technology brief.IEA-ETSAP and IRENA, January 2013

[25] Ernst & Young etAssociés, Middle East North Africa region assessment of the local manufacturing potential for concentrated solar power projects. January 2011. Fraunhofer Institute for Solar Energy Systems ISE:

[26] Clifford K. Ho. Software and codes for analysis of concentrating solar power technologies.SAND2008-8053. December 2008

[27] Xin Li, Weiqiang Kong, Zhifeng Wang, Chun Chang, FengwuBai, Thermal model and thermodynamic performance of molten salt cavity receiver. Renewable energy 35 (2010) 981–988

[29] Michael J. Wagner.Simulation and predictive performance modeling of utility-scale central receiver system power plants. Master thesis.University of Wisconsin-Madison-2008

[30] Manuel Romero, Alvarezand Eduardo Zarza.Concentrating solar thermal power.Handbook of energy efficiency and renewable energy.Plataforma Solar de Almeria-CIEMAT.

[31] Gregory J. Kolb. Economicevaluationofsolar-onlyand hybridpowertowersusingmolten-salttechnology.Solar energy (1998) Vol. 62, No. 1, pp. 51–61

[32] H.L. Zhang et al. Concentrated solar power plants: Review and design methodology. Renewable and sustainable energy reviews 22 (2013), 466–481

[33] C.K. Ho,B.D.Iverson. Review of high-temperature central receiver designs for concentrating solar power. Renewableand sustainable energy reviews29(2014)835–846.

[34] Robert Pitzpaal, Jürgen Dersch, Barbara Milow. European concentrated solar thermal road mapping. Deutscheszentrum fur luft-und Raumfharte.V, DLR Germany.

[35] Walter Short, Daniel J. Packey, andThomas Holt,A Manual for the economic evaluation of energy efficiency and renewable energy technologies.NREL/TP-462-5173, March 1995.

[36] M. Sanchez, M. Romero.Methodology for generation of heliostat field layoutin central receiver systems based on yearly normalizedenergy surfaces. Solar energy 80 (2006) 861–874.

[37] C.A. Amadei, G. Allesina, P. Tartarini, Wu Yuting. Simulation of GEMASOLAR-based solar tower plants for the Chinese energy market: Influence of plant downsizing and location change. Renewable energy 55 (2013). 366-373

[38] Stefano Giuliano1, Reiner Buck and Santiago Eguiguren, Analysis of solar thermal power plants with thermal energy storage and solar hybrid operation strategy. DLR Report.

[39] Transient Simulation of a Solar-Hybrid Tower Power Plant With Open Volumetric Receiver At The Location Barstow

[40] M. Becker et al. Theoretical and numerical investigation of flow stability in porous materials applied as volumetric solar receivers. Solar Energy 80 (2006) 1241–1248

[41] Antonio L. A'vila-Marı'n. Volumetric receivers in Solar Thermal Power Plants with Central Receiver System technology: A review. SolarEnergy 85 (2011) 891–910

[42] R. Pitz-Paal et al. Experimetal and numerical evaluation of the performance and flow stability of different types of volumetric absorbers under non-homogenous irradiation. Solar Energy Vol. 60, Nos. 3/4, pp. 135-150, 1997

[43] Th. Fend et al. Numerical investigation of flow and heat transfer in a volumetric solar receiver. Renewable Energy 60 (2013) 655-661

[44] Bernhard Hoffschmidt et al. Performance Evaluation of the 200-kWth HiTRec-II Open Volumetric Air Receiver. Journal of Solar Energy Engineering, FEBRUARY 2003, Vol. 125 Õ 87

[45] M.I. Roldán et al. Thermal analysis and design of a volumetric solar absorber depending on the porosity. Renewable Energy 62 (2014) 116e128

[46] T. Fend et al. Porous materials as open volumetric solar receivers: Experimental determination of thermo physical and heat transfer properties. Energy 29 (2004) 823–833

[47] S. Boudaoud et al. Thermal performance prediction and sensitivity analysis for future deployment of molten salt cavity receiver solar power plants in Algeria. Energy Conversion and Management 89 (2015) 655–664

WEBOGRAPHY

[47]   Trynsys. (2012) Trynsys.www.trynsys.com

[48]   Nrel. (2012) Nrel: Concentrating solar power research. http://www.nrel.gov/

[49]   http://www.pressebox.com/pressrelease/novatec-solar-gmbh/

[50]   https://sam.nrel.gov/weather-data

[51]   http://en.wikipedia.org/wiki/Andasol_Solar_Power_Station

[52]   http://social.csptoday.com/technology/world-largest-linear-fresnel-solar-power-station-commences-operation

[53]   http://fr.wikipedia.org/wiki/Centrale_solaire_PS20

[54]   http://en.wikipedia.org/wiki/Stirling_Energy_Systems

[55]   http://en.tutiempo.net/

[56]   http://www.nasa.gov/

APPENDICES

VII.1.Convective heat losses regimes correlation in the cavity receiver

Convective heat losses of a solar central are not negligible; therefore, convective losses need to be considered for the cavity receiver thermal model. The accurate description and modeling of convective losses in cavity receivers is a complex problem due to the complexity of the geometry.

An important parameter to characterize natural convection is the Grashof number. It approximates the ratio of buoyancy to viscous force acting on a flow, and is therefore an indicator if a flow is driven by buoyancy or external effects. The Grashof number is defined in equation A.1, with g the gravitation constant, β the volumetric expansion factor, ν the kinematic viscosity and L the characteristic length of the receiver:

$$Gr = \frac{g\beta(T_W - T_\infty).L^3}{v^2} = \frac{Buoyancy\,effects}{Viscous\,effects} \qquad (A.1)$$

The viscous effects characterized by the Reynolds number is defined in the equation (A.2)

$$Re^2 = \frac{g\beta(T_W - T_\infty).L^3}{v^2} = Gr \qquad (A.2)$$

Consequently, the ratio of the Grashof number to the square of the Reynolds number is a useful indicator of the driving forces of the flow and therefore what kind of convection mechanism has to be considered in the heat transfer model. This ratio is also called the Richardson number that represents the importance of natural convection relative to the forced convection. The Richardson number in this context is defined as:

$$Ri = \frac{Gr}{Re^2} \qquad (A.3)$$

$Ri \ll 1 \rightarrow$ Forced convection is dominant, natural convection can be neglected;

$Ri \approx 1 \rightarrow$ Mixed convection where both natural and forced convection are considered;

$Ri \gg 1 \rightarrow$ Natural convection is dominant, forced convection can be neglected;

Another dimensionless number which characterize the ratio of viscous diffusion rate to thermal diffusion rate, or the importance of convective to conductive heat transfer in a fluid is called the Prandtl number.

$$\text{Pr} = \frac{C_p \mu}{k}$$ ……………………………………………………………….. (A.4)

Many natural convection correlation use the Rayleigh number as the dominating parameter to characterize the fluid proprieties and the heat transfer condition.

$$\text{Ra} = \text{Gr.Pr}$$ ……………………………………………………………………. (A.5)

TABLE A.1:RECEIVER PARAMETER CHARACTERISTICS [17].

Characteristics	Range
Prandtl number : $Pr = \frac{C_p \mu}{k}$	0.7<Pr<0.71
Grashof number : $Gr = \frac{g\beta(T_w - T_\infty).L^3}{v^2}$	$2.8e^{13}< Gr<1.1e^{14}$
Rayleight number : $Ra = Gr.Pr$	$2.8e^{13}<Ra<7.8e^{13}$
Reynolds number : $Re = \frac{\left[\sqrt{g\beta(T_w - T_\infty).L^3}\right]}{v^2}$	$1.5e^{7}<Re< 2.8e^{7}$

VII.2.Radiation heat transfer losses

The radiation is the major heat loss mechanism of a solar central receiver. The radiation loss can be separated in two modes. Thermal radiation losses and wavelength radiation losses. The first type is considered due to the high temperature difference of the receiver surface and the surrounding. The second type of the radiation losses is caused by the imperfect absorptive capabilities of the surface

VII.2.1. Radiosity method

The ratio of radiation leaving an arbitrary surface i falling directly on another surface j, to the total radiation leaving surface i is called view factor.

$$F_{i,j} = \frac{\text{Radiation leaving surface i that falls directly on surface j}}{\text{total radiation leaving surface i}} \dots\dots\dots\dots\dots\dots\dots$$

(A.6)

The radiation view factor calculation algorithm that was developed is a Monte-Carlo type ray-tracing technique that calculates a vector leaving the originating surface at a random location, angle and elevation, and checks to see if it intersects the polygon on the target surface.

Thus the thermal radiation that is emitted by a surface i and directly intercepts surface j is given in the following equation:

$$Q_{i,j} = \varepsilon_i . \sigma . A_i . F_{i,j} . T_i^4 \dots\dots\dots\dots\dots\dots\dots\dots\dots\dots\dots\dots\dots\dots\dots\dots \text{(A.7)}$$

VII.3. DELSOL-3 algorithm principals

As an optical performance calculation tool, DELSOL-3 combines the effect of the different losses occurring in a heliostats filed layout (cosine effect, shadowing effect, blocking effect, atmospheric attenuation, spillage and flux image profile).

DELSOL-3 can analyze system involving flat, focused or canted heliostats with round or rectangular shapes.

As a system design tool, DELSOL-3 defines the best combination of the field layout, heliostat density, tower height, receiver size and tower position. Such arrangement is based on the performance, total plant capital cost and system energy cost.

DELSOL-3 can be used in two ways, to do a detail performance calculation for a system which is completely defined by the user, or to define by optimization a system having a lowest energy cost and then do a detailed performance calculation on that system.
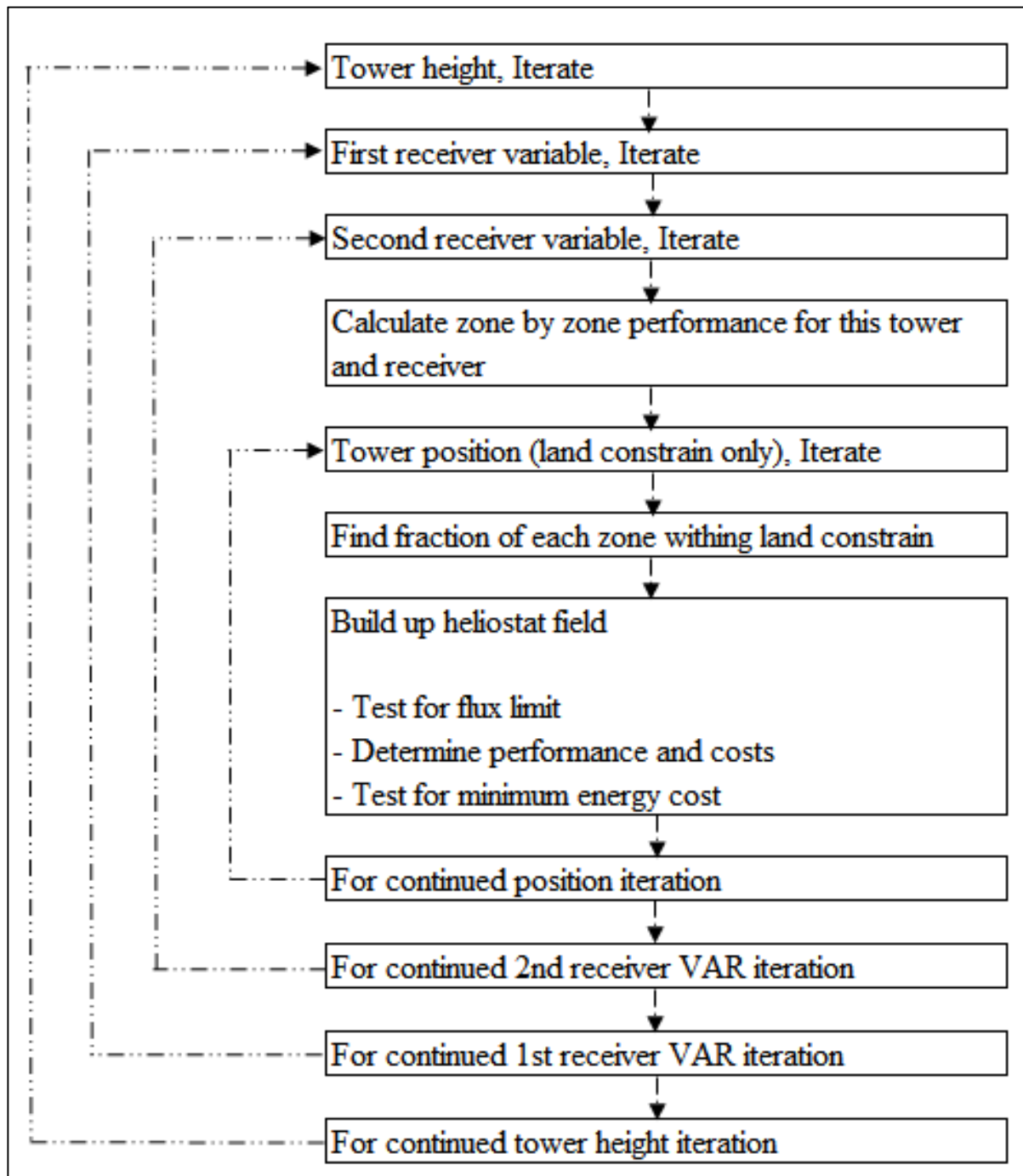
FIGURE B. 1: OPTIMIZATION SEARCH DIAGRAM [18].

VII.3.1.The parameters varying during optimization

In the following item we note that some of variables can have only discrete value (DV) eg.
Tower height, while the other varies continuously (VC).

- Design point power level (DV);
- Tower height (DV);

- Receiver dimensions (DV);
- Tower location for land constrained system (DV);
- Field boundaries (VC);
- Heliostats spacing (VC);
- Storage capacity at a given solar multiple (DV);

VII.3.2.The main parameters held constant during optimization

These parameters can be optimized only by doing several optimization steps, each with a different value for the parameter of interest.

- Site
  - Latitude
  - Insolation
  - Weather
  - Atmospheric attenuation
- Field
  - Type (surround or north configuration)
  - Heliostat patterns
  - Minimum and maximum boundaries
- Heliostat
  - All design parameter
- Receiver
  - Receiver type (external or cavity)
  - Orientation of cavity
  - Ratio of cavity dimensions
- Solar multiple

VII.3.3. Steps in designing a system

1. Define a system

  - Heliostat type, receiver type, flux limit, field boundaries.
  - Non optical performance parameter: receiver loss, EPGS
  - Costs appropriate to technology and application.

2. Initial performance calculation

- Use a guess for optimum tower height

- Save results for other optimization using this heliostat, site, tower height.

3. Coarse optimization

- Limited number of widely spaced optimization variable.

- If optimum value (s) of a design variable (s) is at the minimum or maximum value allowed for search in optimum, increases the ranges of value searched and do another coarse optimization.

4. Fine optimization

- Use a finer grid of optimization variables centered on results of step III.

- Reuse initial performance results from step II, unless tower height is very different.

5. Heliostat density optimization

A. New initial performance calculation

- Use optimum tower height from IV.

- Use default densities or optimized densities from similar system optimization.

B. Optimization (can be done at the same time as VA)

- Do not vary tower height.

- Choose a fine grid of a receiver sizes.

C. Converge density optimization

- If optimum heliostat layout is very different from initial layout used in VA, repeat VA and VB using optimum densities from VB as the input data for VA.

6. Detailed performance calculation for optimum system

- Do a used defined field performance calculation of optimum system.

- Optimize heat storage capacity if desired.

7. Investigate other design concepts

- Repeat I-VI with different heliostat or receiver type, different working fluid.

8. Non-energy cost design consideration

- Energy cost is generally intensive to small perturbation from optimal system.

- If other consideration suggest deviate from DELSOL-3 optimal design, run it to calculate energy cost of modified system.

BIOGRAPHY OF THE AUTHOR

PERSONNEL INFORMATIONS

- Marital status: Married with 2 Children

- Nationality : Algerian

- Date of birth : September, 07th 1980

- Email : sboudaoud@gmail.com

- Téléphone : +213 06 61 87 54 39

- Cleared of all military obligations.

STUDY CURSUS

- 2012-2015: PhD Studies, Research in Solar field Engineering. Modeling Simulation and technical optimization of hybrid solar gaz power plant. "Air and Molten salt Cavity receiver technology". INGM Boumerdes. Algeria.

- 2005-2006: Master II, Professional position. Thermal power plants and energy management facilities. Ecole Nationale Supérieur d'Arts et Métiers de Paris13 'ENSAM'. France.

- 1999-2004: Mechanical engineering and energy management studies. INGM Boumerdes. Algeria.

- 1998-1999 : Mathematical serie Bachelor. Technical school. Tizi-Ouzou Algeria.

PROFESSIONAL EXPERIENCES « 11 YEARS »

From September 2015: (Actual work) ** CSCEC

Client: Ministère de L'habitat, L'agence National De La Réalisation Et La Gestion De Djamaa El-

Djazair (ANARGEMA)

Engineering Procurement and Construction: China State Construction Engineering Corporation
Project: DJAMAA EL DJAZAÏR La Grande Mosquée d'Alger (Algérie)

PMC: Groupement KSP & KUK (KSP Jürgen Engel Architekten, Frankfurt am Main Krebs und Kiefer KSP & KUK)

Project Global Cost: 1150 million Euros

Designation :   Expert Manager HVAC and Fire Extinguishing systems

Missions:

→ Preparation of atelier study (calculation note .drawings) for Smoke Exhaust and fire and water extinguishing systems for all projects to start manufacturing;
→ Coordinate with other disciplines Electrical, plumbing and civil work;
→ Coordinate with client and contractor, subcontractors.

March to August 2015: **EGIS

Client: Ministère de L'habitat, La FAF (Fédération Algérienne de Football)

Engineering Procurement and Construction: China State Construction Engineering Corporation
Project: Rénovation Stade 5 Juillet Complexe Olympique. (Algérie)

PMC: EGIS Bâtiment international.

Project Global Cost: 250 million Euros

Designation: QA and QC Engineering manager (HVAC and Fire and plumbing systems)

Missions:

→ Monitor all quality related activities on the project;
→ Perform all internal and external audits on behalf of the company's management;
→ Verify contractor quality requirements are specified to vendors and contractor documentation submittals;
→ Attend client quality management meetings;
→ The preparation and control of project quality system management documentation prior to project commencement;
→ Monitor the disposition of all issued nonconformance reports;
→ Monitor the progress and effectiveness of the project quality management system. Recommend and implement improvements when required;
→ Coordinate all QA/QC activities with the site QC manager;
→ Coordinate all QA/QC activities with the site QA/QC procurement manager;
→ Coordinate all quality related correspondence with the customer's representatives.

July 2014 to February 2015: **SARL MEGA Contracting

Client: AH Promotion | AH Promotion immobilière
Engineering Procurement and Construction: SARL MEGA Contracting

Project Global Cost: 15 million Euros

Designation : Project Manager HVAC and Fire Extinguishing systems

Missions:

➔ Direct and lead MEP subcontractors to achieve the project milestone dates on the design, installation and testing works;
➔ Direct and lead in-house MEP team for the installation and power lighting works;
➔ Deliver consistent and high quality work utilizing industry standard methodologies and materials;
➔ Coordinate on all sub-contractor scheduling and material ordering.

December 2013 to June 2014 ** Groupement: kouGc-Colas-Rail.

Client: Entreprise Metro d'Alger (EMA)

Engineering Procurement and Construction: Kougc COLAS RAIL Groupement
Project: Metro Alger Extension Ligne B. (Algeria)

PMC: ENSITRANS.

Project Global Cost: 330 million Euros

Designation: Project Coordination Manager (Fire, drain and plumbing systems)

Missions:

➔ Coordinate with General Project Manager on all sub-contractor scheduling and material ordering ;
➔ Monitor and supervise sub-contractors on the site for the installation of Fire extinguishing systems, drain and sewage water and plumbing work ;
➔ Ensure build site has tools and materials needed for day's task ;
➔ Responsible for taking deliveries of materials and supplies; ensures all tools and materials are maintained and safeguarded ;

➔ Review and offer suggestions to the project manager's schedule and implement with little or minimal direction ;
➔ Adhere to safety policy and practices, and create a positive and encouraging work atmosphere.

May 2009 to November 2013 ** CEPI

Client: Direction de la jeunesse et des Sports (DJS)

Engineering Procurement and Construction: ETRHB-FCC Groupement
Project: Olympic Stadium at Tizi-Ouzou. (Algeria)

PMC: Dune Architecture.

Project Global Cost: 450 million Euros

Designation: Sub-Contractor General Manager (Low current and Data Network Communication)

Missions:

➔ Facilitate effective coordination at site between MEP subcontractors and civil subcontractor for acquiring clearance required for MEP installation and testing activities;
➔ Direct and lead MEP subcontractors to achieve the project milestone dates on the design, installation and testing works.

Décembre 2006 – Mai 2009 ** ETS Cunin, SA

Designation: Head of Engineering studies (HVAC, plumbing and fire fighting Works)

 Missions:

➔ Technical study and specifications on HVAC, Plumbing Sanitary Smoke, Fire Protection;
➔ Note sizing calculation with reference to standards;
➔ Quantitative and detailed technical description, CCTP;
➔ Update Schedule studies.

Sites of projects

➔ Construction of IBIS Hotel Algiers, Algeria
➔ Construction of Head quarter of Algiers Metro, Algeria
➔ Construction of ROYAL Hotel, Oran, Algeria

Août 2006 – October 2006 ** Junior Engineer

Tests Implementation Engineer on thermal hydraulic performance of brazed plate heat exchangers. Company : CIAT Culoz France.

February 2006 to July 2006 : Internship

Internship For Master thesis Dissertation: Analysis of evaporation and distribution phenomena of multiphase flows in a brazed plate heat exchanger.

Company: CIAT. France.

March 2005 to July 2005 : Internship

Professional internship on the study of ventilation equipment and calculation of the energy balance in the building.

Company: CSTB. France.

March 2004 to July 2004 : Internship

Engineer Thesis Dissertation: 2D Simulation and optimization of heat transfer and fluid flow in a closed two-phase thermo-syphon

 Energy laboratory of fluid solid mechanics 'LEMS' Boumerdes. Algeria.

LANGAGES

- **Berbère** : Native langage.

- **Arabic**: Current speaking and writing.

- **French**: Current speaking and writing.

- **English**: Current speaking and writing.

HOBBIES:

- Sports: soccer, swimming computers, music, cinema.

OTHER:

- Integrates easily into a team.
- Spirit of research and development.

OBJECTIVE:

- Successful teamwork matching my ambitions and my skills

KEY ACHIVEMENTS :

- Possess sound knowledge in Construction supervision, Quality Inspection
- Worked for special project building and industry projects
- Become familiar with design drawing, specifications and HSE standards through
- Training received with international companies

SCIENTIFIC WORKS :

- Participation in doctoral seminars organized by the laboratory LEMI MSM group Expert intervention came from ENSAM ParisTech;

- Participation in training in renewable energy organized by an expert group Germany (DLR, Julich) and UDES of Bousmail (enermena2012) in October 2012;

- Participation in scientific and technical conferences organized by the Sonatrach group Oran Convention Center from 8 to 10 April 2013;

- Participation in the international seminar on modeling, simulation and optimization Applied organized by TDSA (ICMSAO 2013) in Hammamet, Tunisia from 28 to 30 April 2013;

- Publication of an article in IEEE titled "Solar Tower Plant Implementation in Northern Algeria: Technical and Economic Assessment ";

- Participation in the international seminar on electrical energy conversion systems (EPECS 2013) in Istanbul, Turkey from October 2 to 4, 2013;

- Participation in conferences organized by ERA in 2013 at the convention center in Oran from 28 to October 30, 2013 on the integration of photovoltaic modules for control systems Pipeline integrations and gas transport in isolated sites;

- Redaction of a training summary entitled "Fully Coupled heat transfer and fluid flow in the open volumetric air receiver under homogenous irradiation. ". Jülish, Germany;

- Publication of an article in Energy Conversion and Management newspaper entitled: "Thermal performance prediction and sensitivity analysis for future deployment of molten salt cavity receiver solar power plants in Algeria.";

Table 1.1 : Review of csp technology (advantages and drawbacks).

	Parabolic Trough	Power Tower Central Receiver	Dish / Engine Parabolic Dish	Linear Fresnel Fresnel Linear Reflector
Applications	Grid-connected plants, mid to high-process heat (Highest single unit solar capacity to date: 80 MWe. Total capacity built: over 500 MW and more than 10 GW under construction or proposed)	Grid-connected plants, high temperature process heat (Highest single unit solar capacity to date: 20 MWe under construction, Total capacity ~50MW with at least 100MW under development)	Stand-alone, small off-grid power systems or clustered to larger grid connected dish parks (Highest single unit solar capacity to date: 100 kWe, Proposals for 100MW and 500 MW in Australia and US)	Grid connected plants, or steam generation to be used in conventional thermal power plants. (Highest single unit solar capacity to date is 5MW in US, with 177 MW installation under development)
Advantages	• Commercially available – over 16 billion kWh of operational experience; operating temperature potential up to 500°C (400°C commercially proven) • Commercially proven annual net plant efficiency of 14% (solar radiation to net electric output) • Commercially proven	• Good mid-term prospects for high conversion efficiencies, operating temperature potential beyond 1,000°C (565°C proven at 10 MW scale) • Storage at high temperatures • Hybrid operation possible • Better suited for dry cooling concepts than	• Very high conversion efficiencies – peak solar to net electric conversion over 30% • Modularity • Most effectively integrate thermal storage a large plant • Operational experience of first demonstration projects • Easily manufactured and mass-produced	• Readily available • Flat mirrors can be purchased and bent on site, lower manufacturing costs • Hybrid operation possible • Very high space efficiency around solar noon.

		troughs and Fresnel • Better options to use non-flat sites	from available parts • No water requirements for cooling the cycle	
	investment and operating costs • Modularity • Good land-use factor • Lowest materials demand • Hybrid concept proven • Storage capability			
Disadvantages	• The use of oil-based heat transfer media restricts operating temperatures today to 400°C, resulting in only moderate steam qualities	• Projected annual performance values, investment and operating costs need wider scale proof in commercial operation	• No large-scale commercial examples • Projected cost goals of mass production still to be proven • Lower dispatchability potential for grid integration • Hybrid receivers still an R&D goal	• Recent market entrant, only small projects operating

Source: International Concentrating Solar Power Global Outlook Greenpeace International 2009